A NEW APPROACH TO HIGH-PRESSURE, HIGH-TEMPERATURE HYDROGEN-OXYGEN FUEL-CELL AND ELECTROLYSIS-CELL DESIGN

By

HANSELL JACK ALLISON

Bachelor of Science
Louisiana State University
Baton Rouge, Louisiana
1959

Master of Science
Louisiana State University
Baton Rouge, Louisiana
1961

Submitted to the faculty of the Graduate College
of the Oklahoma State University
in partial fulfillment of the requirements
for the degree of
DOCTOR OF PHILOSOPHY
May, 1967

A NEW APPROACH TO HIGH-PRESSURE, HIGH-TEMPERATURE

HYDROGEN-OXYGEN FUEL-CELL AND

ELECTROLYSIS-CELL DESIGN

Thesis Approved:

Wm J Hughes
Thesis Adviser

C M Summers

Jack B Wiest

N N Durham
Dean of the Graduate College

ACKNOWLEDGMENTS

I wish to express my gratitude to Professor William L. Hughes, Chairman of my advisory committee, for his assistance and guidance during my doctoral studies. The research which led to this thesis was directed by Professor Hughes and Professor C. M. Summers, and many of the concepts introduced in this work were originated by them.

I also wish to thank Professor John B. West for many helpful discussions related to the thermodynamics of the hydrogen-oxygen fuel-cell reaction.

Appreciation is also extended to Mrs. Barbara Adams for her help in the preparation and typing of this manuscript.

TABLE OF CONTENTS

LIST OF TABLES

LIST OF ILLUSTRATIONS

CHAPTER I

THE PROBLEM

1.1 Introduction. The bulk of the energy used to power the industries of the world is derived from hydrocarbon fuels such as coal, oil, and natural gas. The transformation of the energy which is stored in an orderly manner within the chemical bonds of such fuels into useful power is generally accomplished by a process of combustion, in which the highly orderly chemical energy becomes highly disorderly thermal energy. The inexorable second law of thermodynamics dictates that such an energy transformation will be inefficient. The search for a means of transforming chemical energy into electrical energy which does not suffer from the Carnot Cycle efficiency limitations implied by the second law of thermodynamics has reawakened interest in a relatively old engineering device, the hydrogen-oxygen fuel cell. This thesis consists of an analysis of the most promising such device, the hydrogen-oxygen high-pressure, high-temperature fuel cell, and its counterpart, the high-pressure, high-temperature hydrogen-oxygen electrolysis cell.

1.2 History of Fuel Cells. In 1801, Humphrey Davy, one of the pioneers in electrochemical research, built a fuel cell that used carbon and nitric acid. However, another English investigator, William R. Grove, is generally acknowledged as the originator of the

fuel cell. Paradoxically, the work of Grove was initially devoted to a study of electrolysis cells; and his interest in fuel cells was motivated primarily by an interest in the back electromotive force characteristics of electrolysis cells. In 1839 he reported that two strips of platinum immersed in sulfuric acid, one in contact with hydrogen and the other with oxygen, caused the steady deflection of a galvanometer connected to them (1). Further experiments resulted in the construction of a battery of such hydrogen-oxygen cells having sufficient electromotive force to electrolyze water (2). The application of the output electrical energy of a battery of fuel cells to electrolyze water constituted the primary interest of Grove, who presented papers on this subject in 1842, 1843, and 1845 (3, 4).

In 1889, Ludwig Mond and Carl Langer developed a more elaborate hydrogen-oxygen cell which employed platinum foil electrodes which were perforated and platinized. These electrodes were pressed against layers of absorbent asbestos which were saturated with sulfuric acid (5). The successful development of the dynamo at the time of Mond's and Langer's research overshadowed their work; and fuel cells dropped into relative obscurity until the early 1940's, in spite of an impassioned plea by Ostwald (6) at the first meeting of the Bunsen Society in 1894, where he called for the replacement of heat engines by fuel cells as the most practical way of increasing the conversion efficiency of fuels.

From 1910 until World War II, Emil Baur (7) was the foremost contributor to the advancement of fuel-cell technology. The work of Baur and his associates covered nearly all types of fuel cells. However, their work was given little credence, primarily due to the

extremely short operating life of their cells.

In the years following World War II, many prominent researchers made significant contributions to fuel-cell technology. Edward Justi of Germany (8) developed a unique double skeleton electrode structure which utilized Raney nickel to establish an extremely active hydrogen electrode. W. T. Grubb (9) and L. W. Niedrach (10) of General Electric developed a fuel cell which utilized an ion-exchange membrane to replace the conventional liquid electrolyte. A team of researchers at Allis Chalmers (11) developed a fuel cell which was distinguished primarily by an asbestos membrane which used capillary pressure to maintain a reasonably constant level of electrolyte concentration. A cell developed by K. Kordesch and his associates at Union Carbide (12) which made use of electrodes fabricated from carbon was shown to have good lifetime characteristics. Finally, and perhaps most significantly, Francis T. Bacon (13) and a research group at Cambridge University announced the development of a high-pressure fuel cell which had energy density and efficiency characteristics which were superior to the characteristics of the fuel cells discussed above.

The preceding summary of the history of hydrogen-oxygen fuel cells clearly demonstrates the current world-wide interest in fuel-cell technology. Several excellent summaries of modern work in this field may be found in the literature (14, 15, 16, 17).

1.3 History of the Electrolysis of Water. Shortly after the development of the voltaic pile in 1796, Nicholson and Carlisle demonstrated in 1800 the electrolytic decomposition of water (18). These investigators found that hydrogen and oxygen were evolved at

the surface of gold and platinum wires if they were connected to the terminals of a voltaic pile and dipped in water. W. R. Grove, however, from 1835 to 1850 was the first quantitative researcher in the field of water electrolysis (1, 2, 3). In the interval between the time of Grove and the development of the first electromechanical generators of electricity, electrolysis cells were relegated to the position of a scientific curiosity; and little work of significance was attempted in this area.

The development of the dynamo in the last decade of the past century gave impetus to the field of water electrolysis. The production of electrolytic hydrogen for use in fertilizers, dirigibles, and chemical manufacture became a profitable sideline for electrical power companies from 1895 to 1925 (19). Many different types of electrolysis cells, all of which were of essentially the same construction, were developed during this period. Among these were the Electrolabs Cell, the Knowles Cell, the Shriver Filter Press Electrolyzer, the Penchkranz Electrolyzer, the Stuart Cell, and the Noeggerath Cell (20). Of all of these cells, the Noeggerath Cell was the most efficient. Further, it was a pressure electrolysis cell, so gas compressors were not needed in such a facility (21).

From 1930 to 1943, improved modifications of the Noeggerath Cell were made by D. M. Newitt and H. K. Sen of India (22) and by A. E. Zedansky of Germany (23). Commercial facilities utilizing these cells are still in use.

Work on water electrolysis was drastically curtailed during the 1930's when other techniques of producing hydrogen were perfected. Techniques such as reducing hydrogen-rich natural gas to obtain

hydrogen, liquefaction and fractional distillation of coke oven gas, special treatment of water gas, etc. (24), have largely replaced electrolysis for the commercial production of hydrogen.

1.4 Need for Research in Hydrogen-Oxygen Electrolysis Cells and Fuel Cells. The great current interest in hydrogen-oxygen fuel-cell technology has been motivated primarily by the space program. Artificial satellites and manned space probes which remain aloft for several days or longer require a compact, light-weight, and efficient source of electrical energy. It appears that such power requirements can best be filled by hydrogen-oxygen fuel cells (25).

Research at Oklahoma State University and elsewhere (26, 27, 28) in the field of energy storage has led to an increased interest in hydrogen-oxygen electrolysis-cell and fuel-cell technology. For some time, engineers have recognized that conventional electrical power stations could operate with greater economy if an energy storage facility could be made a part of their power system. Such a storage facility could store energy when electrical power demands are below an average value, then insert the stored energy back into the power system when the electrical load demand increases. A corresponding decrease in the initial capital investment for the facility could result (29).

An energy storage system consisting of a bank of electrolysis cells to dissociate water, pressure tanks to collect and store the evolved gases, a fuel-cell system to recombine the hydrogen and oxygen into water and electrical power, and inverters to convert the d-c electrical output of the fuel cells into a-c power could, theoretically,

comprise an ideal energy storage facility for use in conjunction with conventional power stations. A further advantage of a power system which utilizes a storage facility is that it could draw power from such energy sources as the sun, the wind, and the tides and still supply relatively constant amounts of power to a consumer (30). The fuel-cell and the electrolysis-cell configurations discussed in this thesis were designed specifically for ultimate use in an energy storage facility of the type described above. Such a system is shown schematically in Figure 1.4.1.

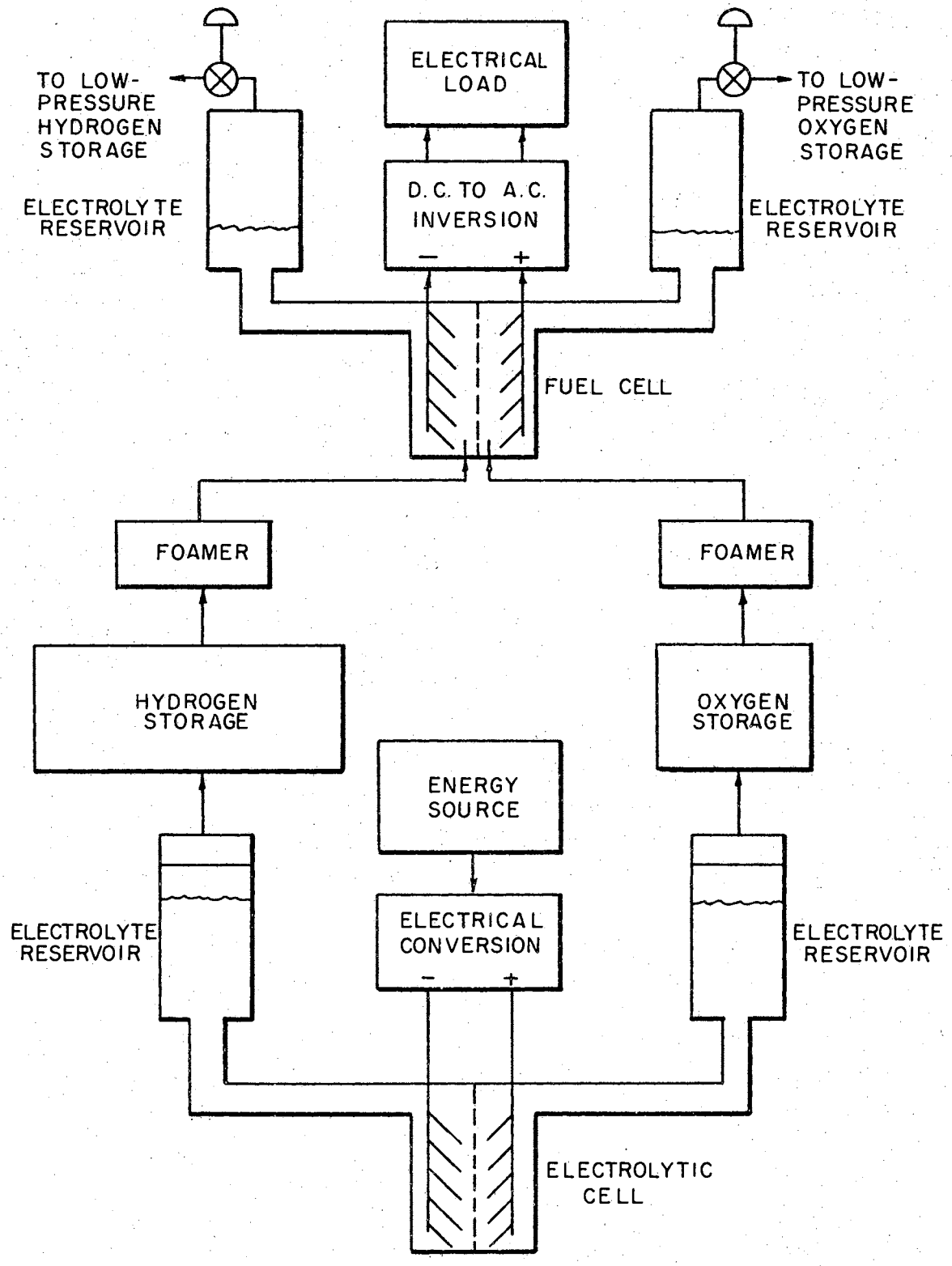

Figure 1.4.1. A System for Energy Conversion and Storage Relying on High-Pressure, High-Temperature Operation to Enhance Performance of the Cells

CHAPTER II

BASIC ELECTROCHEMICAL AND THERMODYNAMIC RELATIONSHIPS ASSOCIATED WITH HYDROGEN-OXYGEN FUEL CELLS AND ELECTROLYSIS CELLS

2.1 Introduction. This chapter consists of a summary of some of the more important and fundamental electrochemical relationships associated with hydrogen-oxygen fuel cells and electrolysis cells. The analysis will consider the efficiency, polarization, voltage versus current, pressure, and temperature characteristics of fuel cells and electrolysis cells. Hydrogen-oxygen fuel-cell technology will be emphasized, but the similarity between fuel-cell action and electrolysis action will make it possible to draw conclusions concerning the characteristics of both fuel cells and electrolysis cells.

2.2 Physical Characteristics of Hydrogen-Oxygen Fuel Cells and Electrolysis Cells. A schematic of a conventional hydrogen-oxygen fuel cell is shown in Figure 2.2.1. The cell consists of two parallel, porous electrodes which are separated by an electrolyte (usually concentrated potassium hydroxide). Hydrogen is injected into the electrode on the left where it combines with hydroxyl ions and forms water and electrons. These electrons travel through the external circuit to the oxygen electrode where they combine with oxygen and water to form hydroxyl ions. The hydroxyl ions migrate through the

electrolyte to the hydrogen electrode, thus completing the reaction. The cell will continue to supply electrical energy to a load as long as hydrogen and oxygen continue to be supplied to the cell and the resulting water by-product is periodically removed (31).

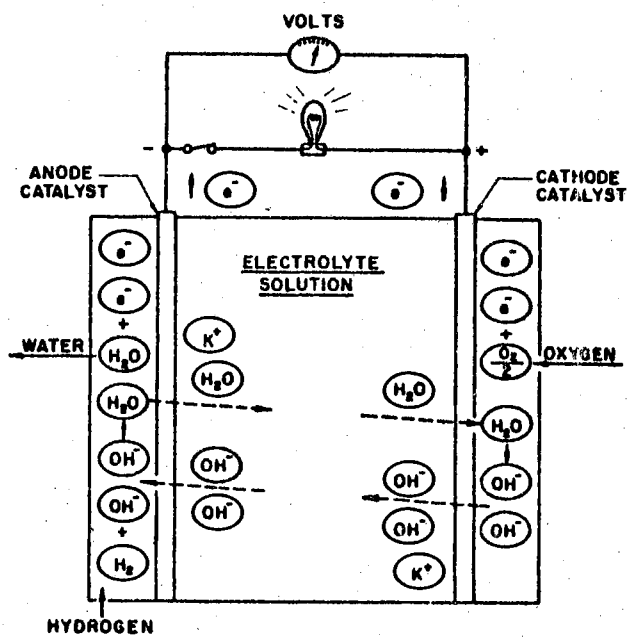

Figure 2.2.1. Basic Schematic of the Hydrogen-Oxygen Fuel Cell

Note that the cell described above requires porous electrodes so the necessary solid-liquid-gas interface can be maintained. If excessive pressure is applied to the electrolyte, however, the electrolyte will flood the electrode and halt the action of the cell. If excess gas pressure is present, the gases will pass through the porous electrodes. The possibility of an explosion caused by the mixing of hydrogen and oxygen gases then occurs. An alternate approach to the establishment of this interface will be considered in Chapter III.

A typical pressure electrolysis cell is shown in Figure 2.2.2.

The cell shown is similar to the type developed by Newitt and Sen (22). The cell electrodes are concentric steel cylinders. The application of d-c voltage of the polarity indicated will cause oxygen to be formed inside the inner cylinder and hydrogen to be formed at the surface of the outside cylinder. The electrolysis action depends on the migration of hydroxyl ions from the hydrogen electrode to the oxygen electrode--a fairly considerable distance. Further, the cell is unsuitable for reversible action as a fuel cell, since hydrogen and oxygen cannot be applied to the active sites of the electrodes. A different type of electrolysis-cell system, devised at Oklahoma State University, will be discussed in Chapter III.

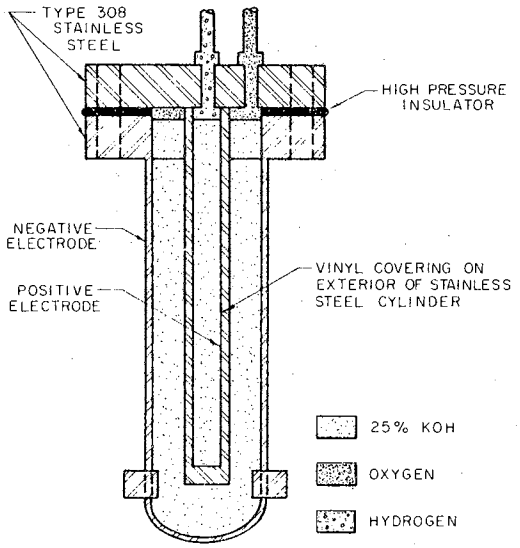

Figure 2.2.2. Conventional Electrolysis Cell

2.3 The Electromotive Force of a Hydrogen-Oxygen Fuel Cell. The theoretical value of the output voltage of a hydrogen-oxygen fuel cell is determined by the thermodynamics of the overall reaction

$$H_2 + 1/2\ O_2 \rightarrow H_2O \quad ,$$

under no-load conditions. According to the second law of thermodynamics, the e.m.f. of a reversible chemical reaction which operates at constant temperature is a measure of the driving force behind the reaction (32). The product of this thermodynamically calculated potential (E_{th}) and the quantity of electricity supplied gives the maximum amount of reversible work, W_e, of the reaction. Applying this principle to 1 mole of monovalent ions, the amount of electricity converted, according to Faraday's law, is 96,497 coulombs or 1 Faraday (33). In the more general case of a reaction with z charge equivalents, the maximum reversible work of the reaction is given by (34)

$$W_e = - z \mathcal{F} E_{th} \qquad \text{(Watt-seconds/mole)} \ . \qquad (2.3.1)$$

The negative value of work indicates that work is given up by the chemical conversion.

Appendix A consists of a conventional summary of the concept of Gibbs Free Energy as it applies to the hydrogen-oxygen fuel-cell reaction. The Gibbs Free Energy, G, of the reaction relates the energy associated with the reaction to the electrical energy which can be derived from the reaction (35).

For the reaction

$$H_{2(gas)} + 1/2\ O_{2(gas)} \rightarrow H_2O_{(liquid)} \ ,$$

by addition of the enthalpies of the components, one may obtain the change in enthalpy of the reaction as follows:

$$\Delta H = \sum \nu_i H_i = - H_{(H_2)} - 1/2\ H_{(O_2)} + H_{(H_2O)} \qquad (2.3.2)$$

A similar expression for the change in entropy is

$$\Delta S = \sum \nu_i S_i = - S_{(H_2)} - 1/2\ S_{(O_2)} + S_{(H_2O)} \qquad (2.3.3)$$

In the above equations, H_i and S_i correspond to the total molar enthalpies and entropies, respectively, of the material i with the stoichiometric factor ν in the reaction equation. The latter is negative for reactants (hydrogen and oxygen) and positive for products (water or water vapor) (35).

Table 2.3.1 lists the molar values of enthalpy and entropy at 300°K and one atmosphere of pressure for the reactants associated with the hydrogen-oxygen fuel cell (36). From Table 2.3.1 the following data can be obtained: ΔH = -68,350 cal/mole or -2.86 watt-sec./mole; ΔS = -38.99 cal/mole or -163.37 watt-sec./mole °K, from which ΔG = -56,653 cal/mole or -2.378×10^5 watt-sec./mole °K. Substituting this value in Equation A.9 in Appendix A with z = 2, the basic e.m.f. (E_{th}) is determined to have a value of 1.23 volts at standard temperature and pressure.

TABLE 2.3.1

MOLAR VALUES OF ENTHALPY AND ENTROPY AT 300°K AND ONE ATMOSPHERE

	Enthalpy		Entropy	
Substance	cal/mole	Ws/mole	cal/mole	Ws/mole
H_2	0	0	31.23	130.85
O_2	0	0	49.03	205.43
H_2O (gaseous)	-57,840	-2.42×10^5	45.14	189.14
H_2O (liquid)	-68,350	-2.86×10^5	16.75	70.18

2.4 The Effect of Temperature on the Output Voltage of a Hydrogen-Oxygen Fuel Cell. The preceding discussion has shown that the theoretical open-circuit voltage of a hydrogen-oxygen fuel cell is 1.23 volts. This figure, however, is based on pressure and temperature conditions of one atmosphere and 300°K, respectively. To continue the analysis still further, it is necessary to know something about the effect on the basic e.m.f. of changes in the environmental temperature (37).

For a reversible electrochemical process, Equation A.9 in Appendix A may be written as

$$- z \mathcal{F} E_{th} = \sum_i z_i (U_i + p V_i - TS_i) \qquad (2.4.1)$$

Differentiating Equation 2.4.1 with respect to temperature while holding pressure constant gives

$$- z \mathcal{F} (\partial E_{th}/\partial T) = \sum_i z_i (\partial G_i/\partial T) = - \sum_i z_i S_i \qquad (2.4.2)$$

Multiplying Equation 2.4.2 by T and substituting $H_i - G_i$ for TS_i leads to

$$- z \mathcal{F} T (\partial E_{th}/\partial T) = \sum_i z_i G_i - \sum_i z_i H_i = z \mathcal{F} E_{th} - \sum_i z_i H_i$$

The preceding equation can be written as

$$E_{th} - T (\partial E_{th}/\partial T) = - (1/z \mathcal{F}) \sum_i z_i H_i \qquad (2.4.3)$$

Equation 2.4.3 shows that the temperature coefficient of the e.m.f. is negative in a reversible process of the type under discussion.

It would appear that a fuel cell which is to obtain as much as

possible of the free energy of the hydrogen-oxygen reaction should be operated at as low a temperature as possible, in order to obtain a high open-circuit voltage. However, the preceding analysis fails to consider certain other design parameters for a fuel cell. For example, if the reaction is to take place at all, the cell electrodes must contain a catalyst which is sufficiently active to allow it to proceed. Most of the conventional catalysts have catalytic parameters which are enhanced with temperature, and they will fail to perform their function if the environmental temperature drops below a given value. Further, if the cell is operated at a sufficiently high temperature, inexpensive materials can be used as a catalyst (38). Finally, the potassium hydroxide electrolyte which is generally used in such cells has a resistance which decreases with increasing temperature, thus allowing the cell to operate at higher current densities as temperature is increased (39).

2.5 The Effect of Pressure on the Output Voltage of a Fuel Cell.

The effect of pressure on the output voltage of a fuel cell may be predicted by differentiating Equation 2.4.1 with respect to pressure. Thus (40)

$$- z \mathcal{F} E_{th} = \sum_i z_i (U_i + p V_i - TS_i) \qquad (2.4.1)$$

becomes

$$- z \mathcal{F} (\partial E_{th}/\partial p) = \sum_i z_i (\partial G_i/\partial p) . \qquad (2.5.1)$$

Multiplying both sides of Equation 2.5.1 by $-(1/z \mathcal{F})$

$$\partial E_{th}/\partial p = - (1/z \mathcal{F}) \sum_i z_i V_i \qquad (2.5.2)$$

Assuming that the ideal gas law, $pV = nRT$, is valid, the above equation becomes

$$\partial E_{th}/\partial p = - (1/z \mathcal{F}) \sum_i z_i (nRT/p) \qquad (2.5.3)$$

It is apparent that the hydrogen-oxygen fuel-cell reaction has a positive pressure coefficient for the cell open-circuit voltage. This indicates that pressure can improve the characteristics of a fuel cell by increasing the output voltage of the cell (41).

2.6 Voltage Versus Current Curve for the Hydrogen-Oxygen Fuel Cell. A typical V-I curve for the hydrogen-oxygen fuel cell is shown in Figure 2.6.1. From no load to point A, the cell is said to operate in an activation polarization region in which the cell voltage drops rapidly with increasing current, due primarily to catalytic inadequacies at the electrode surfaces. From point A to point B, the cell operates in an ohmic polarization region where the very gradual drop in cell voltage with increasing load current is attributed primarily to an IR drop in the electrolyte. From point B, a concentration polarization region is encountered in which the rate of ion migration through the electrolyte is inadequate to support the operation of the cell at a reasonable value of voltage. The operating point of hydrogen-oxygen fuel cells is generally chosen to be within the ohmic polarization region of the cell characteristics as a concession between current density, voltage stability, and efficiency.

Precise knowledge of the various polarization effects associated with hydrogen-oxygen fuel cells is indispensable to the designer of such cells. An excellent discussion of polarization effects is

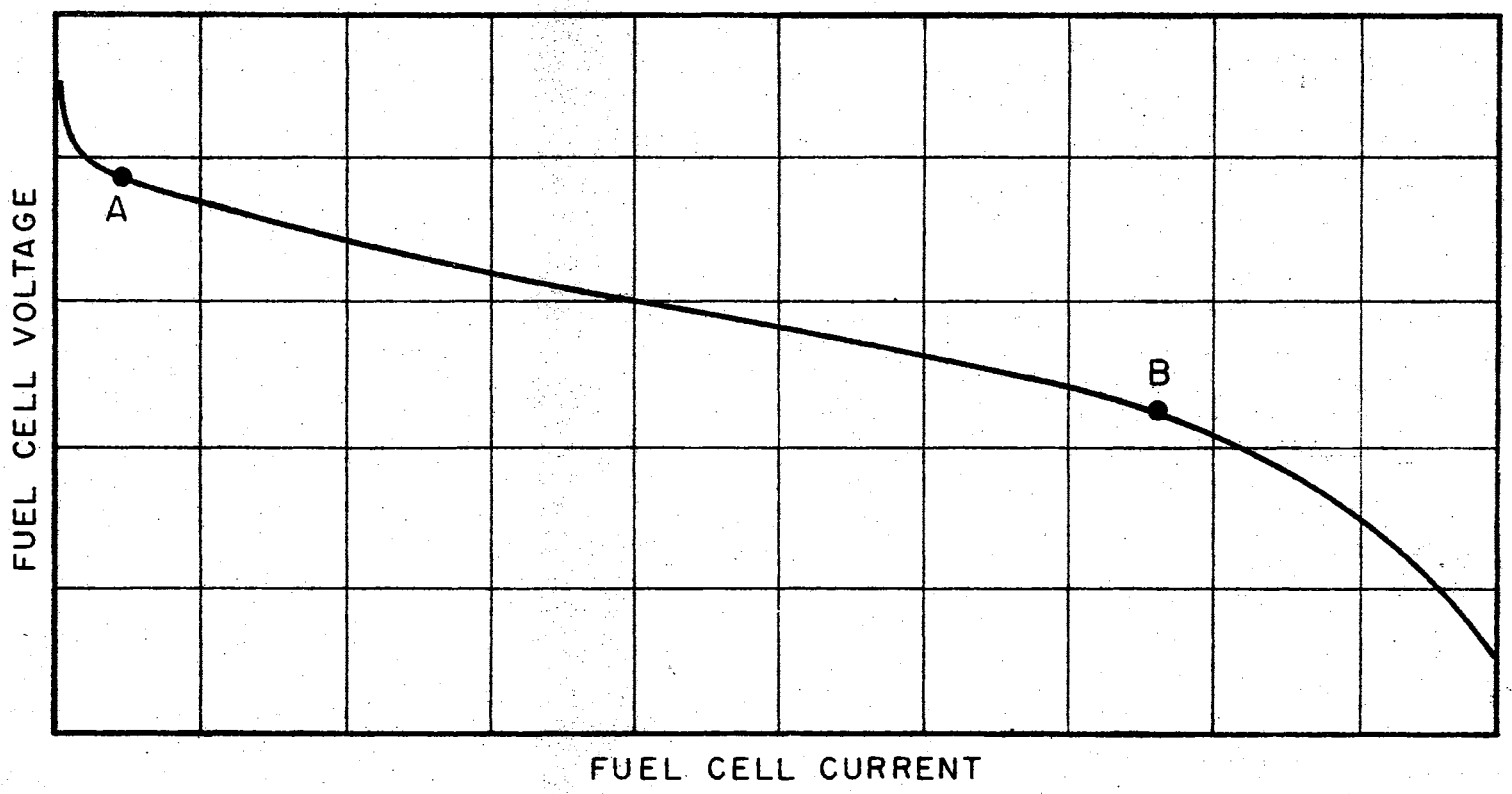

Figure 2.6.1. Typical Voltage Versus Current Curve for a Hydrogen-Oxygen Fuel Cell

contained in reference 42.

If polarization is defined as any characteristic of an electrochemical reaction which causes a decrease in output voltage, it can be caused by the following: inadequate rate of hydrogen and oxygen flow into the cell, dissolution of hydrogen and oxygen in the electrolyte, inadequate rate of transport of reactants through the electrolyte to the active sites of the electrode surfaces, electrical resistance effects in the electrode and electrolyte, slow reaction rate of the overall fuel-cell process, undesirable side reactions which contaminate the electrolyte or electrode, environmental pressure, and system temperature.

2.7 Efficiency of the Hydrogen-Oxygen Fuel Cell. The ideal efficiency of the hydrogen-oxygen fuel cell is defined to be the change in free energy, which is the maximum useful work obtainable from any system, divided by the heat of reaction. That is,

$$\eta_i = \frac{\Delta G}{\Delta H} = 1 - \frac{T\ \Delta S}{\Delta H} . \qquad (2.7.1)$$

This value is always less than unity, even in a cell operating reversibly, so long as heat (T ΔS) is being rejected (43). The heat of reaction is used in the above equation in order to compare the efficiency of a fuel cell with that of a conventional power plant. The efficiency defined by Equation 2.7.1 represents in one sense the thermal efficiency of the fuel cell alone and does not include losses that would be associated with the attendant accessories required in any real installation (43). In terms of the reversible electromotive force of the cell as given in Equation 2.3.1, the efficiency can be written as

$$\eta_i = - z \mathcal{F} E_{th}/\Delta H = - It\ E_{th}/\Delta H \ , \qquad (2.7.2)$$

where I is the current and t the time for which the current flows.

Equation 2.7.2 is actually an unfair estimate of the efficiency of a fuel cell in that it assumes that the output voltage of the cell does not change with variations in current. As discussed in the preceding section of this thesis, the output voltage of a fuel cell decreases with increasing load current due to the various polarizing agents associated with the reaction. An equation for the actual efficiency of the cell, obtained by substituting the actual cell voltage for E_{th} in Equation 2.7.2, is

$$\eta_i = - It\ E_{ac}/\Delta H \qquad (2.7.3)$$

A simpler and more widely used estimate of fuel-cell efficiency is obtained by dividing E_{ac} by E_{th}. This figure is convenient for its simplicity and for the fact that it is a convenient indication of the irreversibilities, or polarization characteristics, of the cell.

2.8 Theoretical Characteristics of Hydrogen-Oxygen Electrolysis Cells. In Section 2.3 of this thesis, a value of 1.23 volts was derived as the open-circuit voltage of a hydrogen-oxygen fuel cell operating at 300°K and one atmosphere of pressure. This value is also a valid statement of the minimum open-circuit voltage that an electrolysis cell can have under the same environmental pressure and temperature conditions. The over-voltage of an electrolysis cell is measured by the difference between the working voltage of the cell and that required for the decomposition of water, due allowance being made for the voltage required to overcome the resistance of the electrolyte and

the other polarization effects associated with the cell. In general, most cells cannot operate below 1.43 volts due to electrode polarization effects.

A typical voltage versus current curve for a hydrogen-oxygen electrolysis cell is shown in Figure 2.8.1. Points A and B of the curve shown in Figure 2.8.1 have the same significance as the corresponding points in Figure 2.6.1, which represented the output characteristics of a fuel cell. The polarization effects documented in Section 2.6 of this thesis are, with minor differences, identical to the effects which shape the character of the V-I curve for electrolysis cells.

Since electrolysis-cell action is essentially the reverse of fuel-cell action, it is reasonable to state that the efficiency considerations discussed in Section 2.7 apply to electrolysis cells as well as fuel cells. Since the output-input characteristics of an electrolysis cell are the reverse of the output-input parameters of a fuel cell, it follows that the equations for electrolysis-cell efficiency will be the inverse of the equations derived in Section 2.7 for fuel-cell action. As a consequence of the above, the generally utilized equation for electrolysis-cell efficiency is

$$\eta_i = E_{th}/E_{ac} \qquad (2.8.1)$$

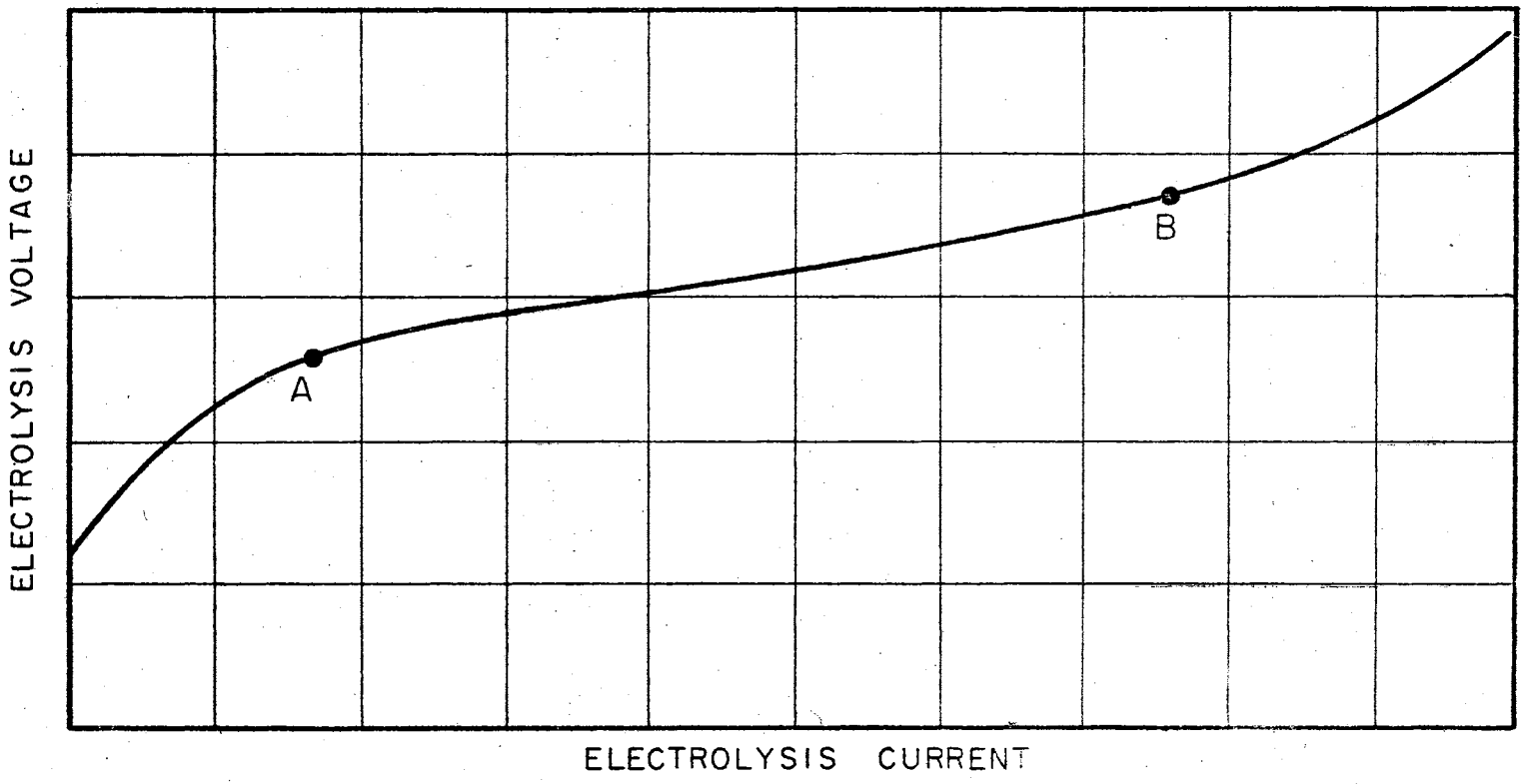

Figure 2.8.1. Typical Voltage Versus Current Curve for a Hydrogen-Oxygen Electrolysis Cell

CHAPTER III

A NEW APPROACH TO HIGH-PRESSURE, HIGH-TEMPERATURE FUEL-CELL AND ELECTROLYSIS-CELL DESIGN

3.1 Introduction. The preceding chapters of this thesis have demonstrated that a fuel cell or electrolysis cell which is operated at high temperature and high pressure can have characteristics which are superior to cells which are operated at low pressures and temperatures. This chapter will analyze some of the problems associated with such cells, and a new type of electrode structure which might help to minimize such problems will be discussed.

3.2 High-Pressure, High-Temperature Electrolysis Cells. Conventional high-pressure, high-temperature hydrogen-oxygen electrolysis cells consist essentially of parallel-plane electrodes separated by a 25 to 50 percent solution of potassium hydroxide. As shown in Figure 2.6.1, the application of a d-c voltage of 1.5 to 2.5 volts causes hydrogen and oxygen gases to be evolved. The applied voltage for 100 percent conversion efficiency is theoretically 1.23 volts. As discussed in Chapter II, however, polarization characteristics of such cells prevent operation at 1.23 volts. A practical operating voltage for such cells is 1.7 volts, and the performance characteristics of electrolysis cells are usually listed in amperes per square foot of electrode surface for this applied voltage.

Various problems are associated with the conventional parallel-plate electrolysis cell. For example, as the gases evolve from the electrode surfaces, there is considerable danger of their mixing and creating an explosion hazard. To avoid this problem, heavy asbestos membranes are used between the electrodes--thus increasing the internal resistance of the cell and decreasing its efficiency. Further, as the evolved gases flow upward through the electrolyte, they create turbulence which decreases the mean free path of the hydroxyl ions which must migrate from the hydrogen electrode to the oxygen electrode so the cell reaction may be completed. Again, the cell resistance rises--in a manner which increases with increasing quantities of gas evolved by the reaction.

Some cell manufacturers have attempted to solve the above problems by utilizing porous electrodes and an asbestos membrane which is partially saturated with a potassium hydroxide solution. The membrane acts both as a gas separator and as a container for the electrolyte. The cell electrodes are pressed tightly against the membrane. The evolved gases are prevented from passing through the membrane by the capillary characteristics of the asbestos; and they, therefore, move away from the membrane, through the electrodes, and into separate pressure vessels. The gas turbulence and the gas mixing problems associated with the "wet" type of electrolysis cells are thus solved. Unfortunately, such cells are not without shortcomings. Hot spots can develop in the cells which can dry the membrane and create an explosive hazard. Pressure gradient problems are fairly severe in such cells, and a special technique must be utilized to maintain the concentration of the electrolyte confined in the asbestos membrane. Nevertheless, a

research group working on such cells has quoted an energy density in excess of 250 amperes per square foot for an applied voltage of 1.7 volts for their cells in private communications.

The various problems associated with conventional parallel-plate electrolysis-cell systems suggest that some alternative to the parallel-plate electrodes might have some merit. In Figure 3.2.1 a conformal transformation has been used to convert the conventional parallel-plane electrode configuration into a set of electrodes which lie in the same plane. Since conformal transformations meet the requirements of Laplace's equation, the transformed set of electrodes have electrical characteristics mathematically relatable to the conventional parallel-plane electrodes. It is obvious that a set of electrodes such as those on the left of Figure 3.2.1 are not necessarily as effective as those on the right, but the mathematical relationship which can be established between them is of interest. Appendix B consists of a detailed comparison of the electrostatic potential distribution of a finned electrode with a set of parallel-plane electrodes of the conventional type.

To pursue the matter further, examine Figure 3.2.2. At the top of the figure is a set of electrodes for which the field plot is almost as good as a field plot for two parallel plates. So far, nothing of value has been gained. Another transformation, however, results in the electrode configuration shown at the bottom of Figure 3.2.2. Notice the advantages which this electrode design would have in an electrolysis system. The effective surface area of an electrode is increased over that of conventional parallel-plate electrodes. The effective surface area of an electrode is here defined to be the area of the

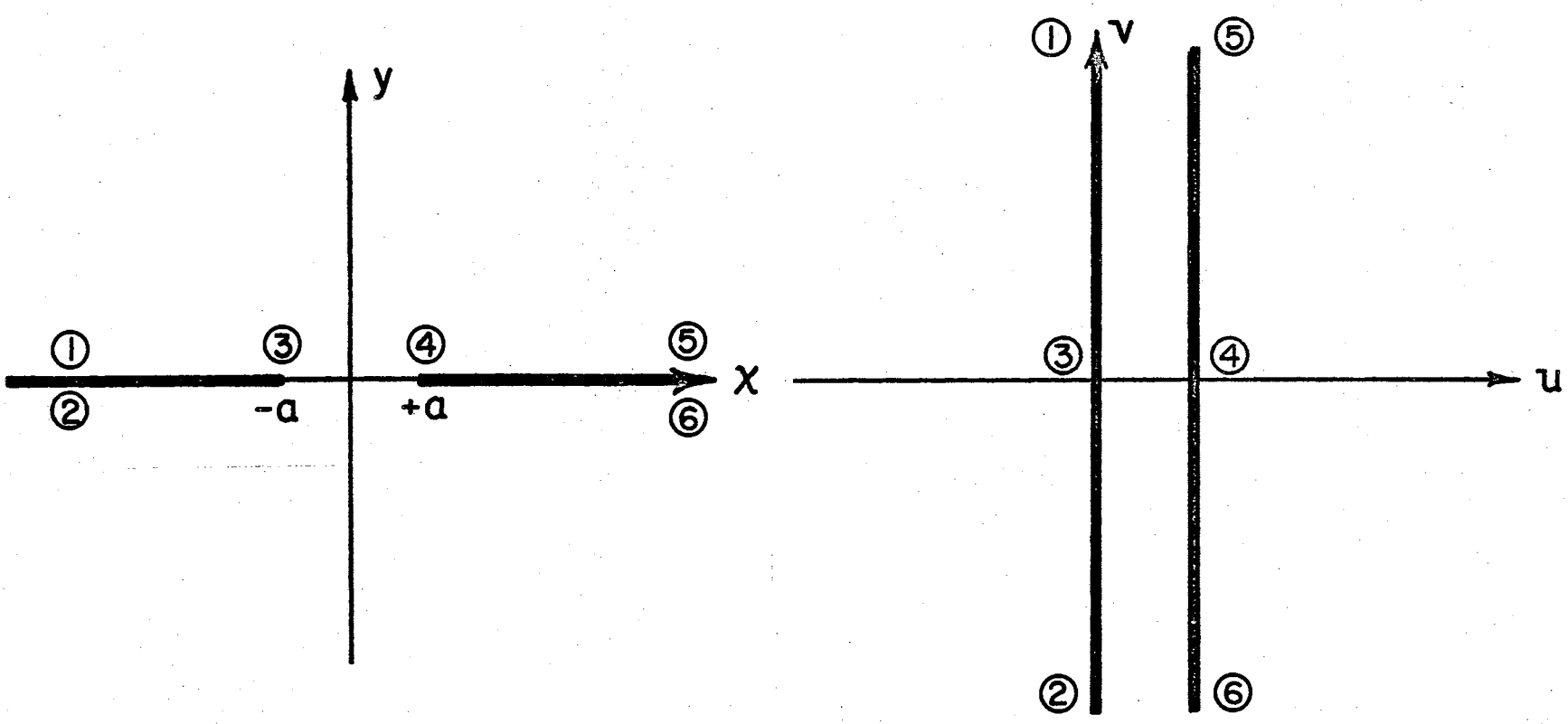

$$\omega = C_1 \cos^{-1} k Z + C_2$$

Figure 3.2.1. Conformal Transformation Converts Parallel-Plane Electrodes into Electrodes Which Lie in the Same Plane

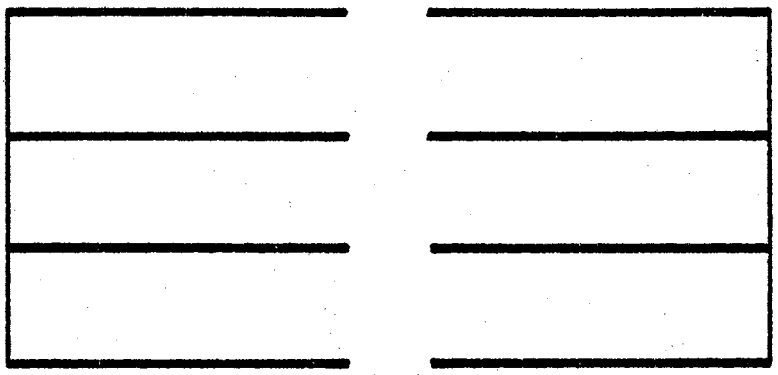

IDEALIZED "EQUIVALENT"
OF
FLAT PARALLEL PLATES

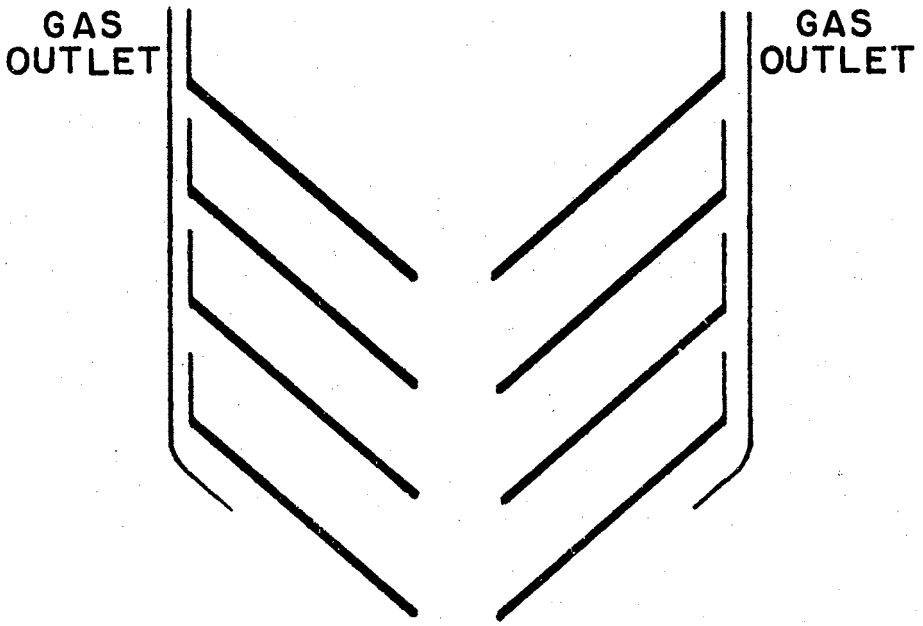

RESULTING ELECTROLYSIS CONFIGURATION
WITH SLANT TO ACCOMMODATE GAS REMOVAL

Figure 3.2.2. Transformation of Flat Parallel Plates to Slanted Plates to Enhance Gas Flow From Electrolysis-Cell Reaction Zone

reaction zone of the electrodes. The evolved gases flow by gravity through the holes at the upper edge of the plates, reducing the turbulence in the electrolyte solution that lies between the electrodes and enhancing the chances for optimum ion migration.

An experimental set of electrodes of this type is shown in Figure 3.2.3. The electrodes are separated by a thin membrane made of asbestos when the cell is in operation to prevent the mixing of gases. Extensive experiments were run on the set of electrodes shown in Figure 3.2.3 and on other electrodes based on a similar design. The most significant results of these experiments are tabulated in Chapter IV of this thesis.

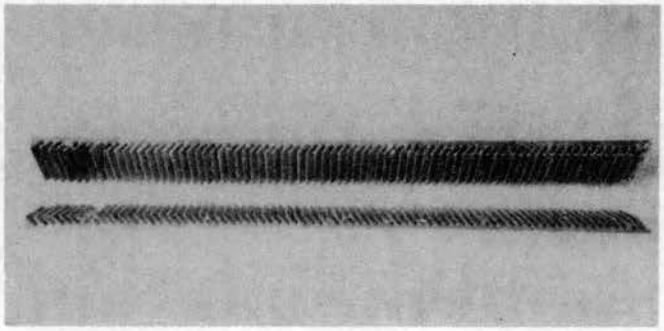

Figure 3.2.3. Photograph of the Milled-Fin Electrodes Used to Obtain Electrolysis-Cell Characteristics

3.3 High-Pressure, High-Temperature Fuel Cells. At the present state of the art of hydrogen-oxygen fuel-cell development, it is apparent that high-pressure, high-temperature hydrogen-oxygen fuel cells are capable of higher energy densities than other types of cells. The theoretical advantages of pressure on fuel-cell action are well

documented in the literature (13). Operating the cells at high temperature offers the additional advantage that nonnoble metal catalysts may be used as electrode materials, greatly decreasing their cost. Various difficulties are associated with high-pressure, high-temperature cells, however, which limit their present usefulness in an engineering application.

In general, high-pressure fuel cells consist essentially of two porous electrodes which are separated by an electrolyte. The solid-liquid-gas interface necessary to cell operation is maintained within the electrodes. Complicated control apparatus is required for the maintenance of the interface, however. A pressure of two to five pounds per square inch imposed on the fuel gases is generally sufficient to sustain the interface. Controlling this pressure in an environmental pressure which is 500 psi minimum implies that the gas regulating apparatus must be capable of a regulation corresponding to approximately one percent of the environmental pressure. This regulating ability is accomplished in the Bacon cell by holding the oxygen pressure and the environmental pressure constant, then adjusting the pressure of the hydrogen gas to sustain the interface conditions so necessary for proper cell performance (44). A precise differential pressure gauge and associated solenoid valve is required in this application.

The function of the electrodes in a fuel-cell system is threefold. First, since the reactant is a gas and the electrolyte is a liquid, the electrode must provide an interface between the liquid and gaseous phases. Second, the electrode must provide a low resistance path for the transfer of electrons to and from the site of the reactions. Third, the electrode must provide reactive sites for the electrode reactions

to occur. The standard approach to provide these functions is to utilize a porous electrode fabricated from a low resistance material which is also a good catalyst, insert the gas into one side of the electrode, and insert electrolyte into the other side of the electrode (45). The junction of the electrolyte and the fuel gas with the surface of the electrode comprises the active site of the reaction. The active site depends on the wetting characteristics of the electrolyte on the metal surface, the surface tension of the electrolyte-gas interface, the environmental pressure and temperature, the over-pressure of gas on the porous metal, and the capillary pressure of the electrolyte in the finely divided pores of the electrode.

The above discussion has implied that there are problems associated with maintaining a proper interface condition in the conventional high-pressure fuel cell. Observe, however, that the formation of the active site is not sufficient of itself to guarantee the successful completion of the reaction (46). In order for the reaction to be completed in an alkaline electrolyte, for example, it is necessary that a hydroxyl ion move from the oxygen electrode to the hydrogen electrode of the cell. One problem associated with this requirement is shown in Figure 3.3.1.

Note that the solid-liquid-gas interface, or active site, occupies only a small part of the electrode. The relative "sharpness" of the angle, θ, of intersection of the surface of the liquid electrolyte with the electrode walls becomes critical when the thickness of the meniscus layer is insufficient to allow the free passage of the hydroxyl ions necessary for the completed reaction. This restriction sets a lower limit on the size of the pores in the electrode and an upper limit on the over-pressure of the fuel gas.

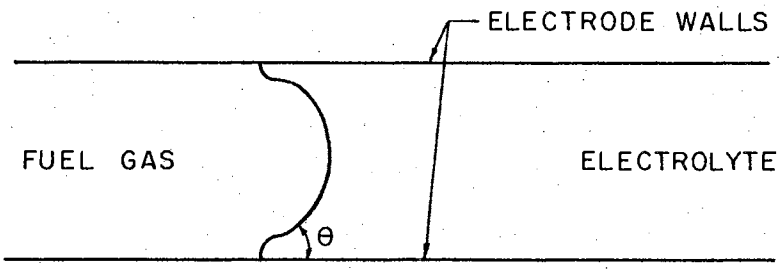

Figure 3.3.1. Elementary Diagram of the Three-Phase Interface Required for Reaction to Occur in a Fuel Cell

It should also be observed that the active site shown in Figure 3.3.1 represents an idealized case. In actual fact, the construction of a porous electrode from sintered powder results in an extremely irregular interface. It is possible, therefore, that hydroxyl ions on their way through the electrodes toward the site of the reaction may be surrounded by an equipotential surface--the electrode--and thus exhibit no tendency to move on to the active site and complete the reaction. The work required to form such ions is, therefore, lost to the reaction. These factors limit the size of the metal particles used in porous electrodes to a low of five to ten microns, and they also set the upper limit of thickness of the electrodes to approximately one-eighth inch. Further, they place rather severe restrictions on the regularity of the geometry of the individual particles which comprise the electrodes.

A fuel-cell electrode configuration which will eliminate or minimize the above problems which occur in conventional parallel-plate

porous electrodes can be devised, based on the conformal transformation technique discussed in Appendix B of this thesis. Figure 3.3.2 indicates how a fuel cell would work using such a set of electrodes. The electrodes can be either nickel screens or sintered-nickel powder, and they are electrically tied together through the load. A thin asbestos membrane is required to keep the gases from mixing. Notice that this electrode configuration has no pressure differential problem of the type existing in conventional fuel cells. The solid-liquid-gas interface problem in conventional cells is greatly improved with the electrodes shown in Figure 3.3.2 due to the nature of the gravitational force on the gas bubbles released at the bottom of the cell. Hydroxyl ions can reach the active sites of the hydrogen electrode either by diffusing directly into the fins or by drifting into the space between the electrodes and being moved to the bottom surface of the fins by the upward motion of the gas bubbles. Further, the total surface area of the electrodes can easily exceed the area of conventional parallel-plane electrodes of the same width and height. Finally, the only pressure limitation on a cell using the above electrodes would lie in the structural capability of the vessel which confines the system.

One of the problems associated with a fuel cell which utilizes finned electrodes is the fact that it is difficult to supply gases uniformly to each fin. Various modifications of the finned electrode concept were examined experimentally in an effort to subvert this difficulty. A photograph of one modification is shown in Figure 3.3.3. Gases were inserted into the bottom of the electrodes. Gas bubbles came into contact with the diamond-shaped fins of the electrodes, forming the necessary solid-liquid-gas interface necessary for fuel-cell

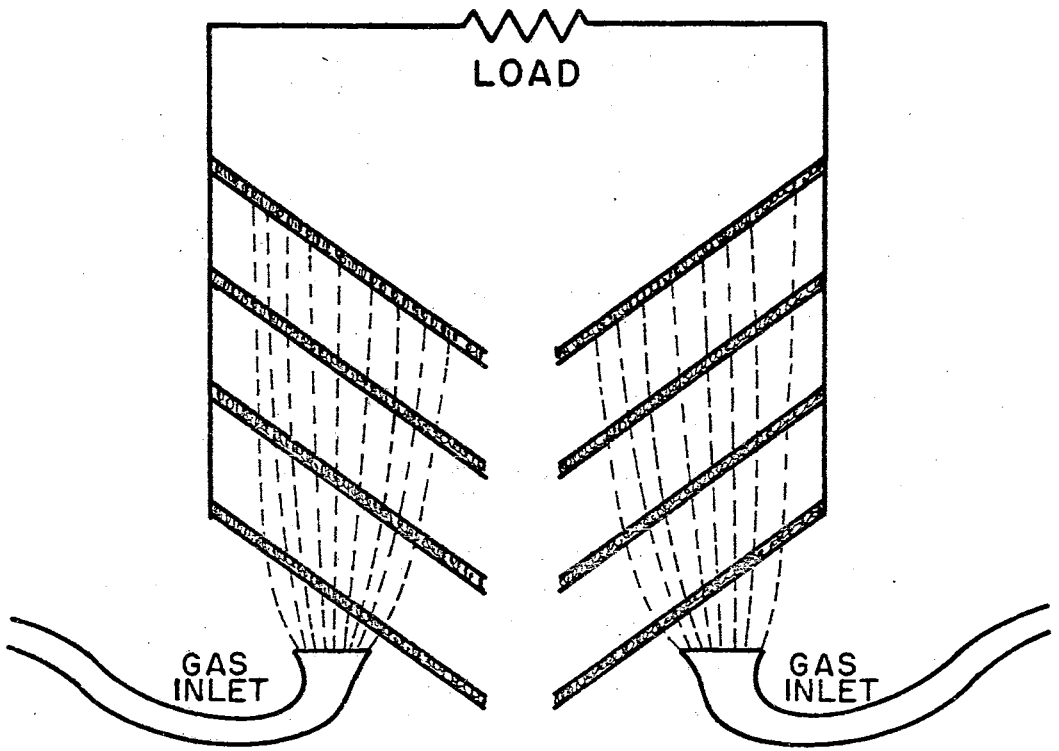

Figure 3.3.2. Diagram Showing a Method of Providing Gas to the Reaction Surfaces of a Porous-Finned Electrode System

operation. Other bubbles moved through the diamond lattice until the bottom part of each fin was covered with gas. Thus, the entire electrode was in the path of gas flow. Notice that the interface formed in these electrodes might be considered to be dynamic as compared to the conventional static interface established in porous electrode fuel cells. The diamond-lattice fuel cell will operate at any environmental pressure which can be sustained by the vessel which confines the electrodes.

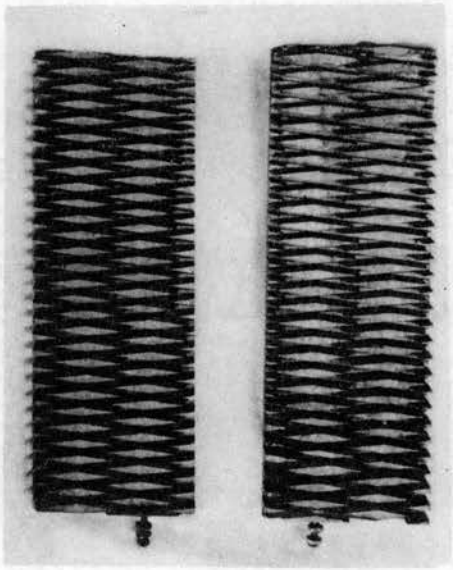

Figure 3.3.3. Photograph of Diamond-Lattice Shaped Fuel-Cell Electrodes Designed to Facilitate Gas Flow

In the solid electrode approach to fuel-cell electrode design, the fuel gases and the oxidizing gases are injected into the electrolyte at the bottom of the cell; then they move upward by gravitational force to their respective electrodes. The electrode geometry must be such that the gas bubbles impinge on the electrode surfaces and remain at the active sites of the electrodes for a period of time sufficient to allow the cell reaction to be completed. In the diamond-lattice

configuration shown in Figure 3.3.3, the active sites available for the hydrogen-oxygen reaction to occur are at the bottom of each of the diamond-shaped segments of the electrodes. Such an arrangement does not provide the maximum number of active sites possible in a solid electrode structure. Further, the manifolding characteristics of the diamond-lattice structure allows an excessive quantity of gas to pass through the cell without entering into the fuel-cell reaction.

A modification of the diamond-lattice electrode configuration which might improve the manifold system and increase the number of active sites available for the cell reaction is the spiral electrode structure shown in Figure 3.3.4. The cell consists of two pure nickel cylinders, each of which has a spiral manifold cut into its surface. A gas bubble injected at the bottom of one of the spirals would move along the bottom surface of the spiral until it entered into the fuel-cell reaction. It is apparent that the probability of hydrogen and oxygen bubbles getting through such a manifold without entering into the fuel-cell reaction is much less in this type of structure than it is in the diamond-lattice approach to fuel-cell electrode design.

Data concerning the characteristics of the fuel-cell types discussed in this section are tabulated in Chapter IV of this thesis.

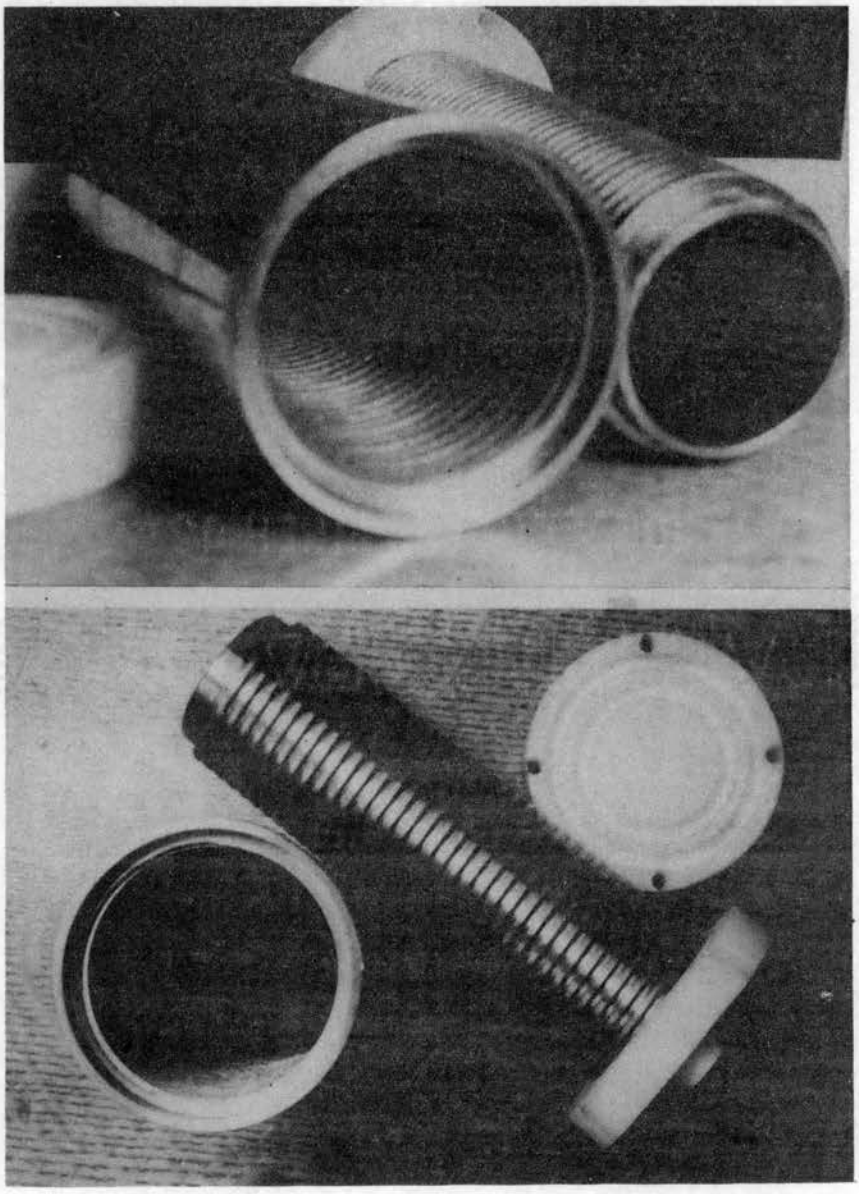

Figure 3.3.4. Photograph of the Spiral, Cylindrical Electrode Fuel-Cell Configuration

CHAPTER IV

EXPERIMENTAL RESULTS

4.1 Introduction. This chapter consists of a summary of the experimental results obtained on the high-pressure, high-temperature hydrogen-oxygen fuel cell and electrolysis-cell electrode structures discussed in Chapter III. The experimental work was devoted to a search for the optimum pressure and temperature environment for cell operation, electrode catalyst and material studies, the search for an optimum electrode configuration, and an attempt to justify the "finned" electrode approach to high-pressure, high-temperature fuel cell and electrolysis-cell electrode design.

4.2 Experimental Apparatus and Procedures. A fundamental problem which must be faced by any researcher in the area of high-pressure, high-temperature hydrogen-oxygen reactions is the potential explosion hazard which exists when experimental work becomes a part of the research effort. Experimental procedures and techniques must be carefully chosen to guard against an accidental mixing of hydrogen and oxygen gases which could cause an explosion. Further, safeguards must be built into the experimental system to protect the researcher and his experimental apparatus from the hazards associated with the reaction. The facility constructed as a part of this study is shown in Figure 4.2.1.

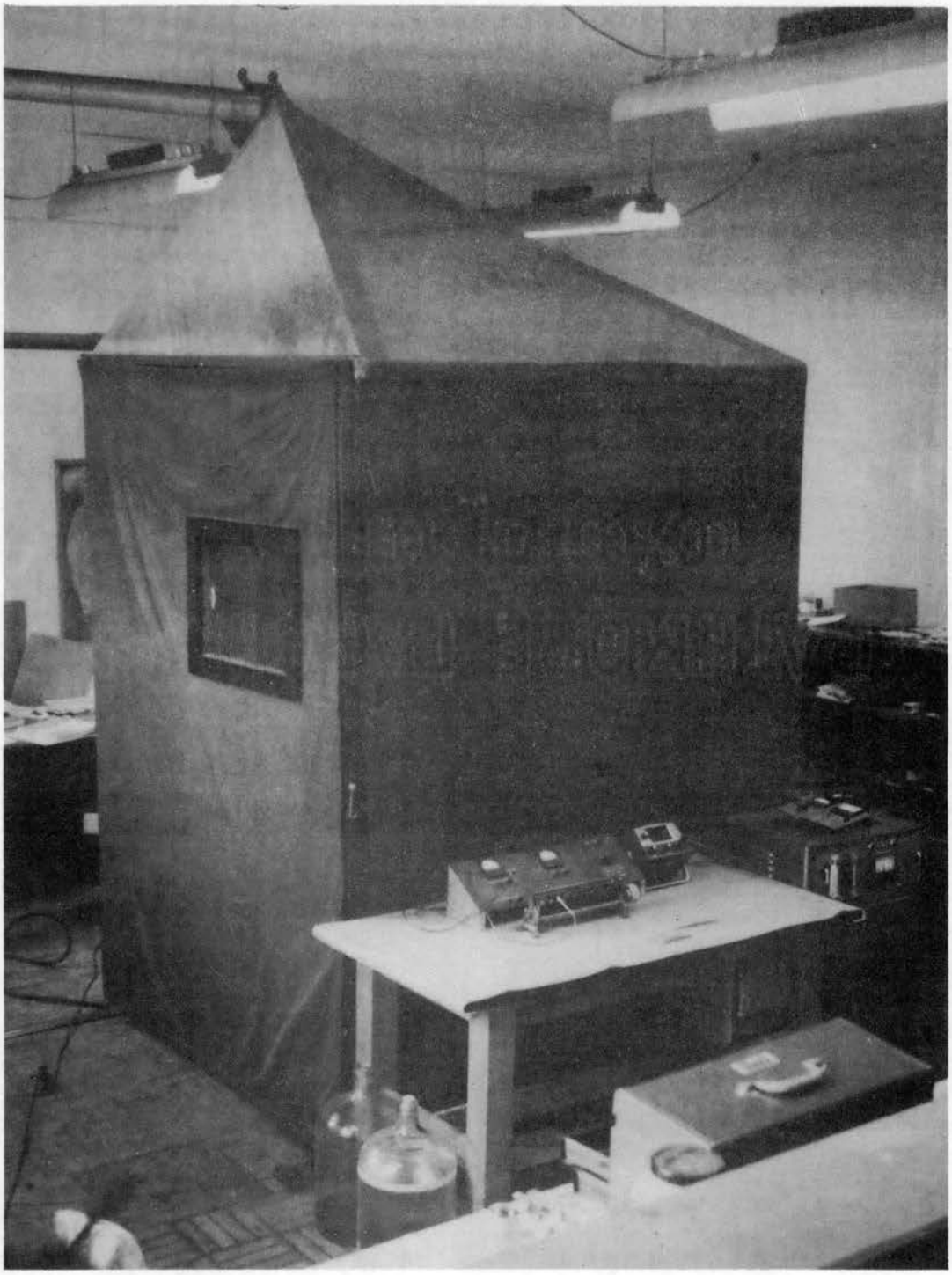

Figure 4.2.1. Photograph of Facility Used in High-Pressure, High-Temperature Experimental Work

The facility shown in Figure 4.2.1 is a rectangular cage constructed from heavy gauge steel screen covered with chemically-treated, fire-resistant canvas. The top of the reaction chamber consists of a sheet metal hood, whose seams were carefully welded to prevent gas leakage. An exhaust fan driven by a quarter-horsepower universal motor was installed at the apex of the hood to insure a rapid egress of any gases or fumes associated with the reactions which occurred inside the cage. The blower motor was a sealed, brushless type that could not produce any sparks which could trigger an explosion. All of the experiments whose results are presented in this chapter were performed within this facility. The exhaust fan ran continuously, and the door of the cage was kept closed during the course of each experiment. A heavy-duty safety glass window installed in the door of the cage permitted visual observation of the progress of the experiments.

An interior view of the facility shown in Figure 4.2.1 is shown in Figure 4.2.2. The heavy gauge wire superstructure of the cage is shown in the figure. Also shown in the figure is a typical high-pressure electrolysis-cell system consisting of an electrolysis cell, defoamers, desiccators, and storage tanks. The electrolysis cell design was patterned after the work of Sen (22), and the details of its construction were shown in Figure 2.2.2 of this thesis.

The system shown in Figure 4.2.2 was constructed so that an indication of the problems associated with high-pressure electrolysis and high-pressure gas storage could be obtained. Experimental work on this system soon demonstrated that the internal resistance of the Sen cell was 4.7 ohms at 800 psi and 80°F, the temperature and pressure capability of the cell. Such a figure is far too high to allow the cell to

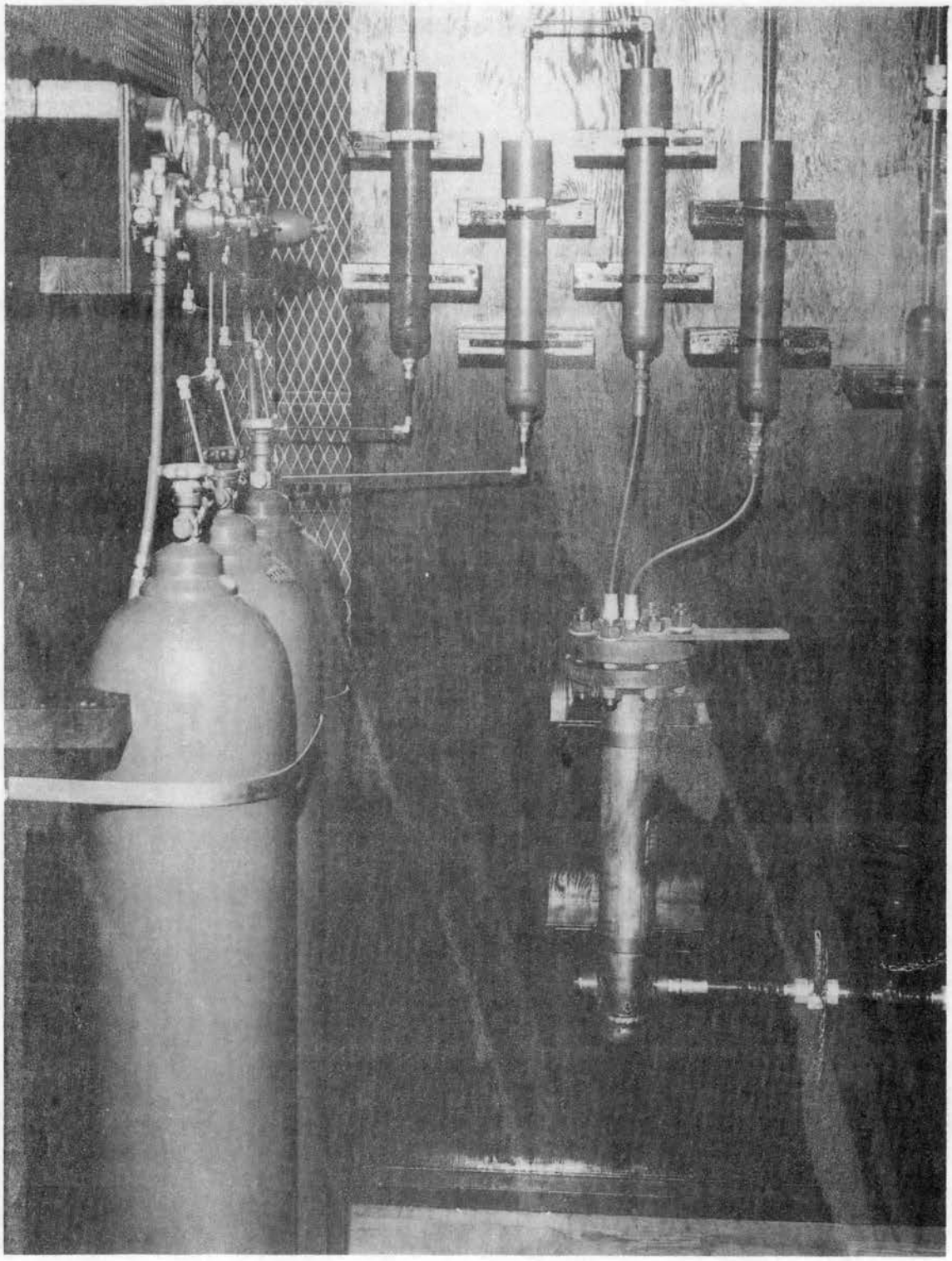

Figure 4.2.2. Photograph of High-Pressure Electrolysis-Cell System, Showing Experimental Facility Utilized to Dry Gases Prior to Storage

be used for the economic production of hydrogen and oxygen on a large scale, but it did provide impetus for the search for a better electrode configuration as discussed in Chapter III of this thesis.

Analysis of the system shown in Figure 4.2.2 also demonstrated that the gases which are evolved during the electrolytic process contained large quantities of water vapor and potassium hydroxide foam. Such contaminants had to be removed from the gases before the gases reached the storage tanks. Otherwise, the potassium hydroxide foam would corrode the pressure tanks; and the water vapor would condense inside the tanks, eventually filling them. The defoamer chambers shown immediately above the electrolysis cell in Figure 4.2.2 consist of stainless steel chambers which were loosely packed with shredded teflon to reduce the potassium hydroxide foam to a liquid which would drain back into the electrolysis tank. The pressure vessels which are shown in Figure 4.2.2 to be installed between the defoamers and the high-pressure storage tanks were packed with a commercial desiccant to collect the water vapor which was present in the gas stream and insure that the gases which reach the pressure tanks shown at the left of Figure 4.2.2 were sufficiently dry, to allow for convenient storage.

Another problem which is associated with high-pressure electrolysis cells is the fact that water must be periodically added to the electrolyte, replacing the water which is removed by the electrolytic process. Such action is necessary to the maintenance of an approximately constant value of electrolyte concentration. This problem could necessitate pumping water into the pressure chamber under pressure, which would introduce an appreciable loss to the system and thus decrease its efficiency. The water addition problem associated with such cells was

solved in the system shown in Figure 4.2.2 by the pressure tank and associated valves shown at the right of the figure. When it became necessary to add water to the system, the valve shown at the left of the pressure tank, or water reservoir, and the valve shown at the top of the pressure tank were closed, thus disconnecting the reservoir tank from the electrolysis-cell system. The pressure tank was then depressurized by an independent set of valves, and water was added to the reservoir tank. The independent set of valves was then closed; and the valves connecting the water reservoir to the electrolysis cell opened, thus allowing water to be added to the electrolysis cell without necessitating depressurization of the electrolysis cell proper or pumping water into the system at high pressures. The rather crude system of valves clearly demonstrated the workability of the process, and an automated control system based on the principle demonstrated could easily be installed in a commercial facility.

A set of electrolysis-cell electrodes, fabricated according to the finned electrode approach discussed in the preceding chapter, is shown in Figure 4.2.3. The electrodes were constructed from one-sixteenth-inch thick sheet nickel stock, and the one-inch long fins were spot welded to the electrode base plate. The holes drilled in the electrode base plate served as a convenient exit for the gases which were evolved during the electrolytic process. The relative merits of this electrode configuration were documented in the preceding chapter.

Before electrolysis-cell electrodes of the type shown in Figure 4.2.3 can be inserted into an environmental chamber, they must first be put into a container which will help to keep the evolved gases separated. Such a container is shown in Figure 4.2.4. The electrodes shown

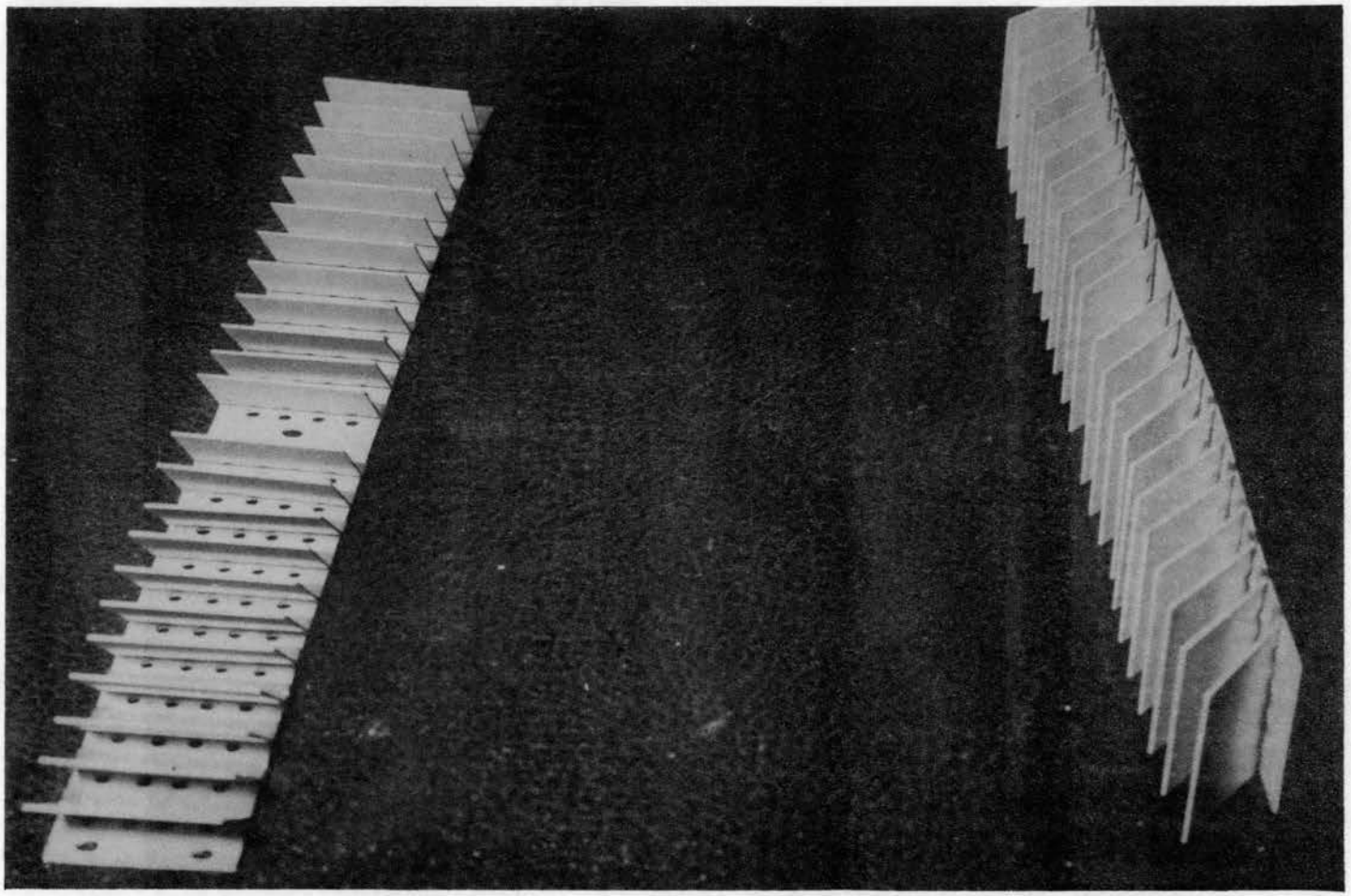

Figure 4.2.3. Photograph of a Test Set of Electrolysis-Cell Electrodes

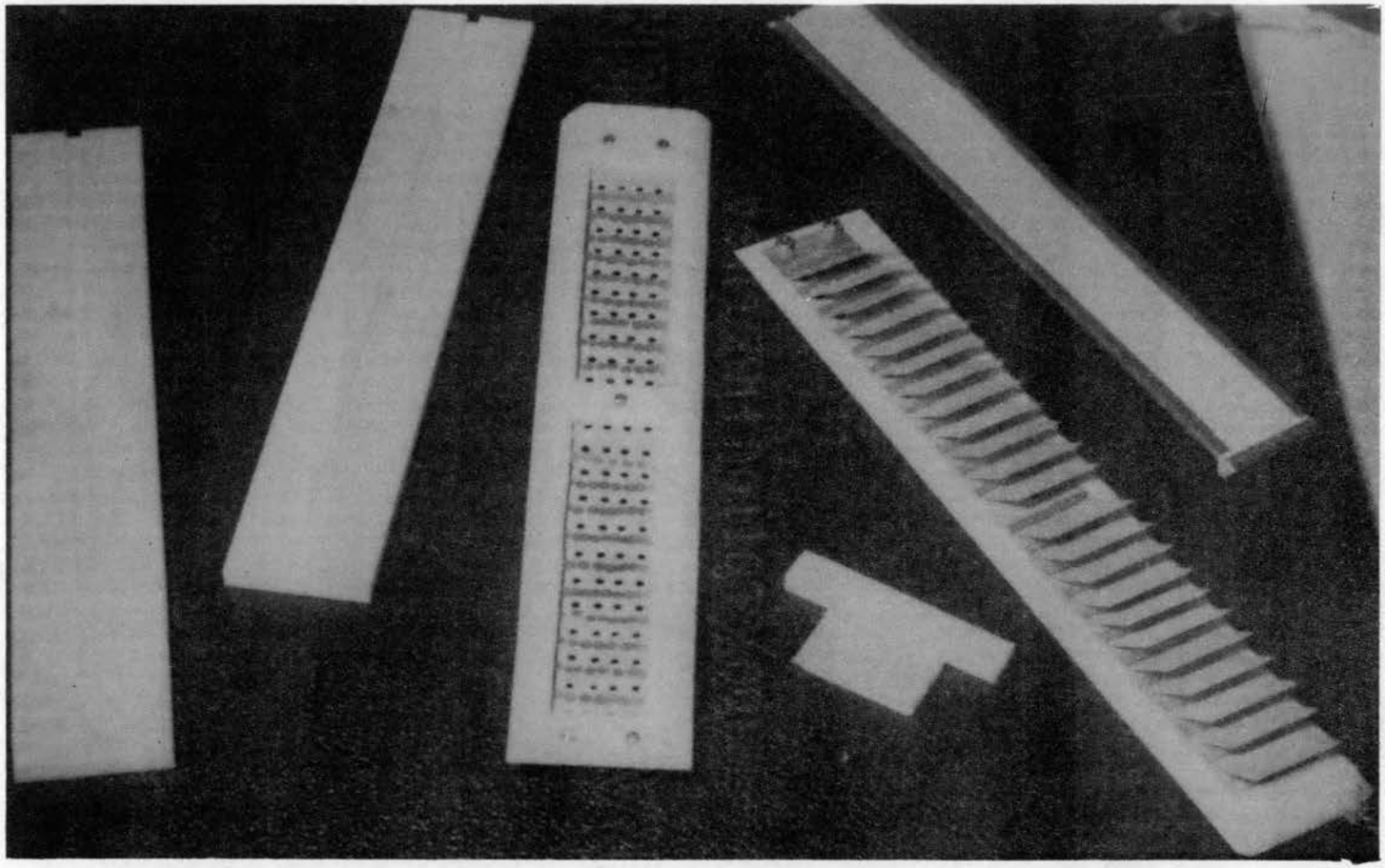

Figure 4.2.4. Photograph of a Disassembled Electrolysis-Cell Configuration, Showing Electrodes, Teflon Container, Asbestos Membrane, and Gas Separator

in Figure 4.2.3 are shown in Figure 4.2.4 to be attached to opposite walls of a teflon container, the other two walls of which are shown at the left of the figure. Teflon was used in the construction of all of the containers used in the experimental work which was conducted as a part of this study, due to the fact that this material proved to be impervious to the pressure, temperature, and corrosive aspects of the system environment. The asbestos membrane used in all of the experimental work on the electrodes shown in Figure 4.2.3 is displayed at the right of Figure 4.2.4. The membrane shown consists of two layers of woven asbestos cloth with a narrow border of sheet nickel to keep the membrane rigid. Since the earliest days of electrolysis-cell research, asbestos has been used as the membrane material, primarily due to its resistance to the potassium hydroxide environment associated with such a cell. Shown between the electrodes in Figure 4.2.4 is a teflon separator which is fitted on top of the cell membrane to help keep the evolved gases separate.

In Figure 4.2.5 the assembled cell is shown beside the high-pressure tank into which the cell assembly is inserted during environmental testing of the electrolysis-cell system. One side of the container was detached in the figure to show the orientation of the electrodes and membrane when the cell is assembled.

The system employed in all of the high-pressure, high-temperature fuel-cell and electrolysis-cell experiments conducted as a part of this research effort is shown in Figure 4.2.6. The system consists of three tanks, each of which is similar to the tank shown in Figure 4.2.5. The pressure and temperature limits imposed by the structural capability of the tanks were 3,000 psi and 400°F, respectively. The bottom tank

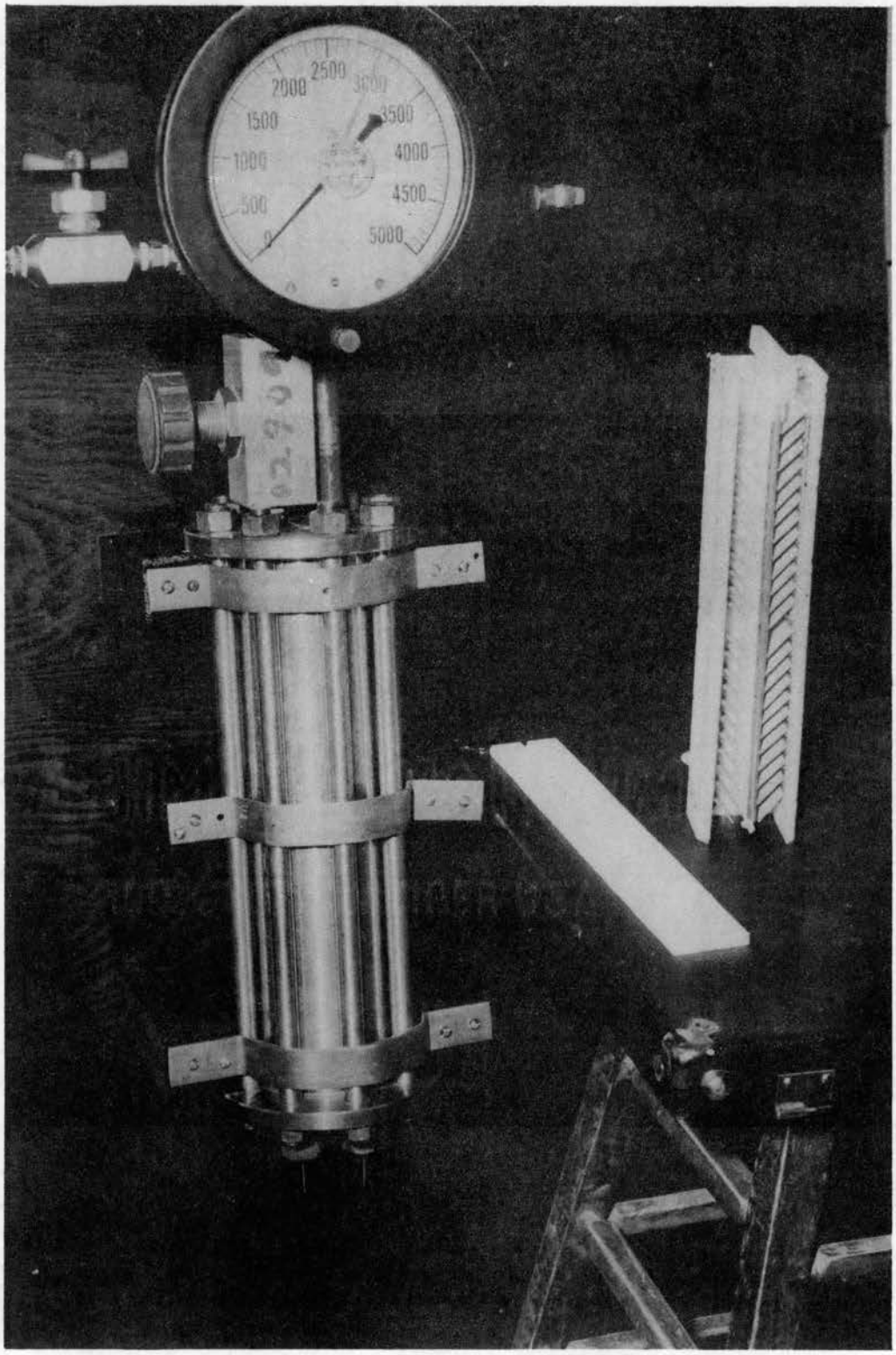

Figure 4.2.5. Photograph of High-Pressure Environmental Pressure Chamber in Which Fuel-Cell and Electrolysis-Cell Tests Were Run

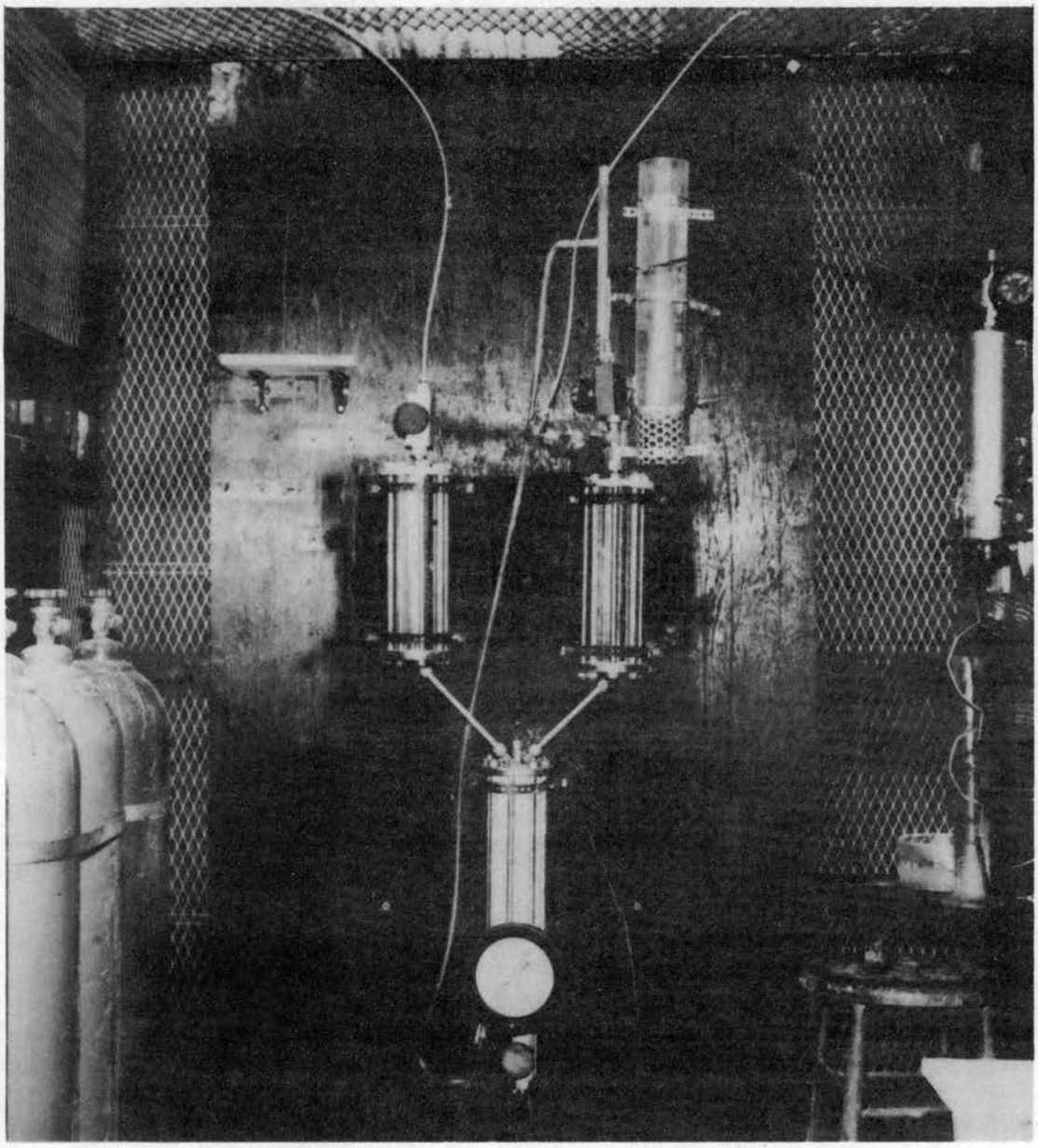

Figure 4.2.6. Photograph of Environmental Test Facility Installed in the Protective Facility

contained the electrolysis-cell or fuel-cell configurations required in a given experiment, and the pressure vessels above this tank served as a receptacle for the gases which were associated with the reactions in the bottom tank. By design, the volumes available for storage of the evolved gases were kept small in the environmental test facility shown in Figure 4.2.6. This was done to insure that the quantity of hydrogen gas available to an explosive reaction could be kept small, if such an explosion did occur.

Figure 4.2.7 is a photograph of the experimental apparatus used to instrument and control the fuel-cell and electrolysis-cell tests which were conducted as a part of this study. At the left of Figure 4.2.7 is an instrumentation panel which enables the researcher to monitor the temperature, voltage, and current parameters of the system under test. In addition, the instrumentation panel is connected through a switching circuit to the digital voltmeter shown in the center of the photograph in Figure 4.2.7. Such an arrangement greatly facilitates the data-taking process and enhances the reliability of the data by making it possible for one highly accurate meter to be used for all of the electrical measurements required in a given experiment. The voltmeter shown is a Digitex Model No. 201 digital voltmeter, which is capable of four-figure accuracy on its one-volt range.

The device below the digital voltmeter in Figure 4.2.7 is an Industrial Instruments Incorporated Therma Bridge Analyzer, Type No. TBA3-919. This instrument is an oxygen analyzer which provides a direct indication of the amount of hydrogen gas which is present in the oxygen side of the system. It allows the researcher to compare various membranes and gas separators in terms of their ability to keep separate

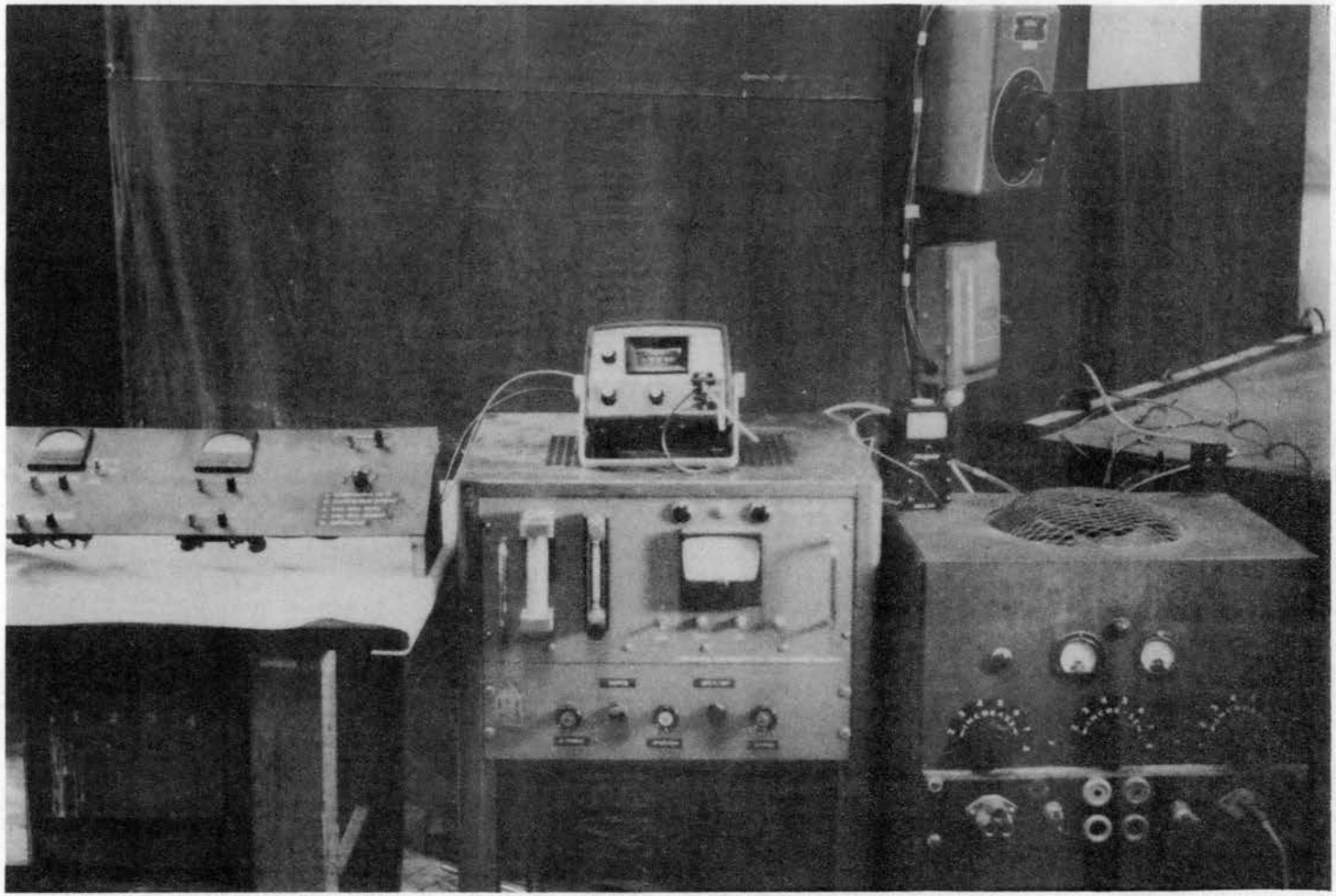

Figure 4.2.7. Photograph of Experimental Apparatus Used in Fuel-Cell and Electrolysis-Cell Tests

the gases which are evolved during the electrolytic process. Further, the device has a built-in alarm system which can give warning of an excessive quantity of hydrogen in the oxygen gas stream; and it thus provides insurance against the possibility of an explosion.

Shown at the right of the oxygen analyzer in Figure 4.2.7 is the power supply used to supply electrical energy to the electrolysis-cell systems examined by this researcher. Maximum voltage and current parameters of the power supply are 24 volts and 200 amperes, respectively. The power supply was driven by a three-phase power source, and it utilized ignitrons to provide a direct-current power which was relatively free from alternating-current ripple components. The apparatus shown above the power supply in Figure 4.2.7 is a twenty-ampere Variac which supplied power to the heating elements used to control the temperature of the system under test. The heating elements were attached directly to the pressure tank containing the cells being tested, and they were capable of increasing the cell temperature at a rate of 200°F per hour.

A schematic of the test facility used in all of the hydrogen-oxygen fuel-cell tests is shown in Figure 4.2.8. As shown in the figure, an electrolysis cell and a fuel cell were placed in the same environmental pressure chamber. When electrolysis action was initiated through the application of d-c electrical energy, the resulting hydrogen and oxygen gases rose from the surfaces of the electrolysis electrodes and moved, by gravitational force, to the fuel-cell electrodes. The necessary solid-liquid-gas interface for fuel-cell action was then established, and fuel-cell action was initiated. The physical distance between the electrolysis electrodes and the fuel-cell electrodes was made large with respect to the spacing between the electrode pairs so

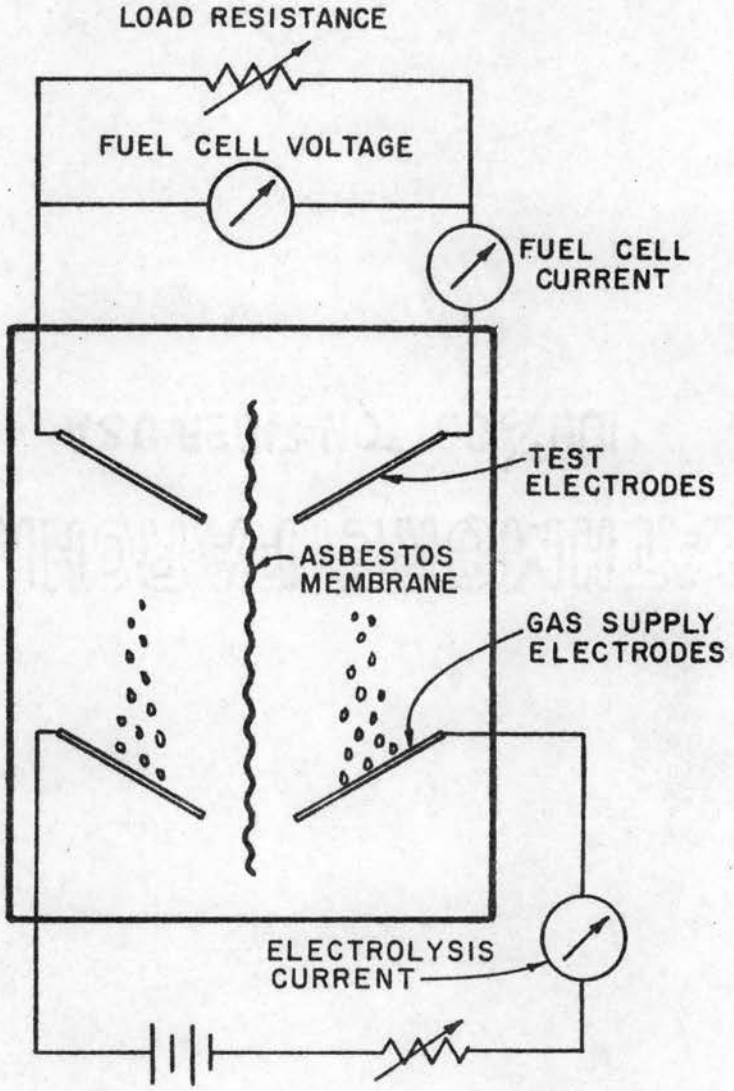

Figure 4.2.8. Schematic Diagram for Supplying Gas to and Testing for Fuel-Cell Action of Electrodes Based on the Finned-Electrode Approach to Cell Design

that ion fringing effects which would cause an undesirable interaction between the cells would be negligible. To further insure that fringing effects would not affect the fuel-cell data, the tests were run as shown in Figure 4.2.8 and then repeated with a Faraday screen surrounding the electrolysis electrodes. No change in fuel-cell performance was noted, so the effects of fringing were assumed to be negligible.

The process by which the required hydrogen and oxygen gases for fuel-cell action were supplied to the fuel cell by an electrolysis cell contained within the same pressure vessel made it unnecessary for the required gases to be pumped into the system under pressure. Such a procedure greatly simplified the experimental system and brought about a corresponding decrease in the cost of the system. It did, however, make it necessary for both fuel-cell and electrolysis-cell electrical data to be taken during the course of all fuel-cell experiments. The instrumentation panel and digital voltmeter discussed in conjunction with Figure 4.2.7 was designed to have this capability, as is shown in Figure 4.2.9, which consists of a close-up view of the instrumentation panel-digital voltmeter combination. The left side of the instrumentation contains a conventional d-c voltmeter with a 2.0 volt full-scale reading and a 25-ampere meter shunt which had a resistance of 0.001 ohm. The voltmeter was used to give a general indication of the electrolysis-cell voltage, and the voltage terminals of the meter shunt were tied through the switch shown at the right of the instrumentation panel to the digital voltmeter. In this way, the digital voltmeter could be used to measure the current associated with the electrolysis cell. The voltage associated with the electrolysis cell was also tied through the switch to the digital voltmeter to allow accurate

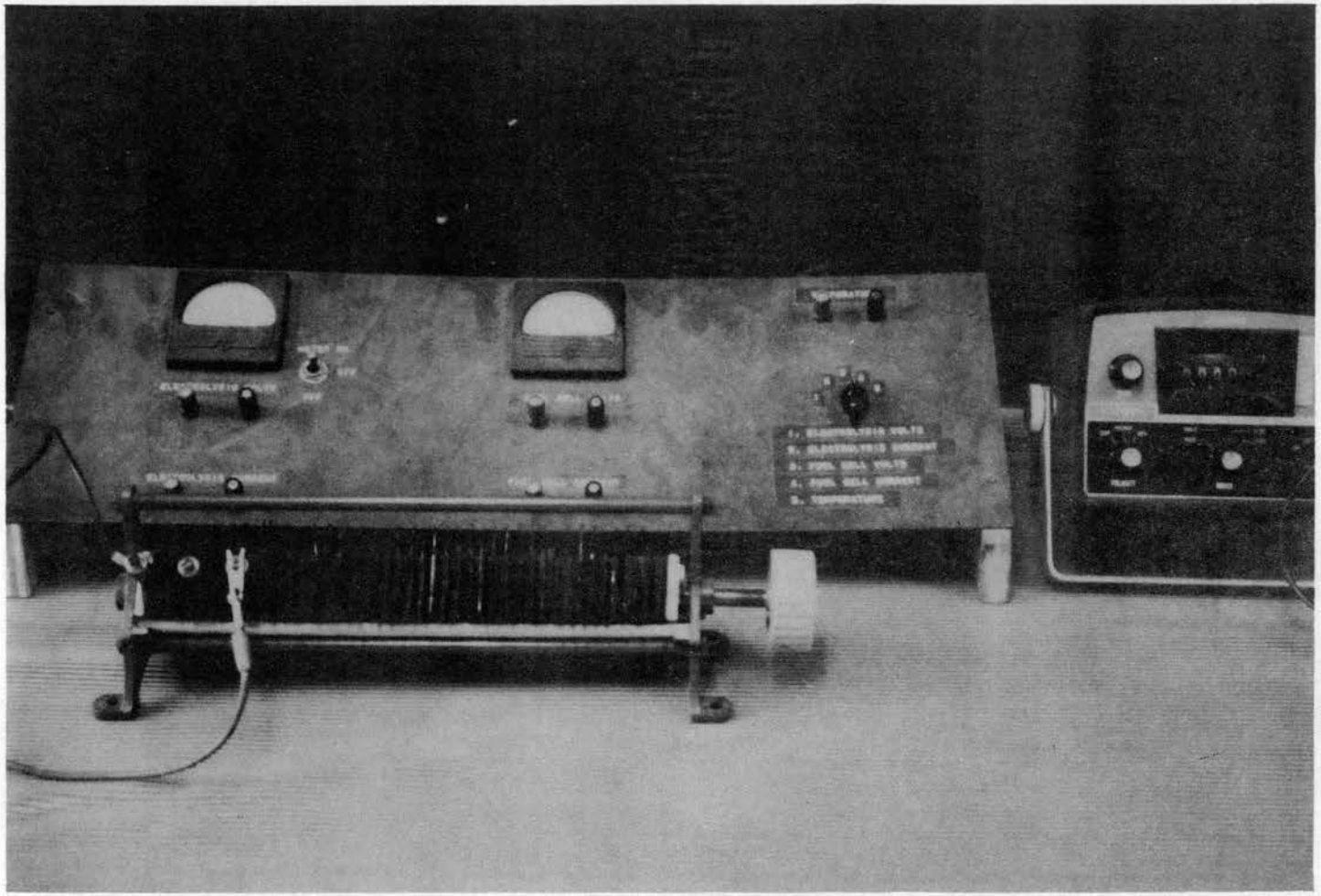

Figure 4.2.9. Photograph of Instrumentation Utilized to Obtain V-I Relationships Associated With Hydrogen-Oxygen Cells

tabulations of its value to be made. A similar voltmeter and meter shunt were installed in the center of the instrumentation panel to allow fuel-cell data to be tabulated. These instruments were connected through the switching circuit to the digital voltmeter in a manner identical to the techniques discussed above for the electrolysis cell.

The instrumentation panel and associated digital voltmeter provided a convenient and compact facility to measure the electrical characteristics of fuel cells and electrolysis cells. The only other electrical device required for the taking of such data was a variable resistor, one of which is shown in the foreground of the photograph in Figure 4.2.9. These variable resistors were inserted into the electrical circuit as is shown in Figure 4.2.8.

Various techniques were employed to fabricate the electrodes whose characteristics are tabulated in the following sections of this chapter. The electrodes with the most significant parameters are shown in Figures 4.2.10 and 4.2.11. They were fabricated from one-fourth-inch flat nickel stock, as shown in Figure 4.2.12. The milling machine shown in the figure was purchased for the specific function shown in Figure 4.2.12--to facilitate the fabrication of milled-fin electrodes. The complexity and expense of this process could easily be reduced if large quantities of such electrodes were required. Electrode casting or extrusion techniques which would eliminate the milling process are well within the range of present engineering technology.

4.3 Hydrogen-Oxygen Electrolysis-Cell Experimental Results. This section consists of a presentation and discussion of the data obtained during three years of experimental research on the finned-electrode

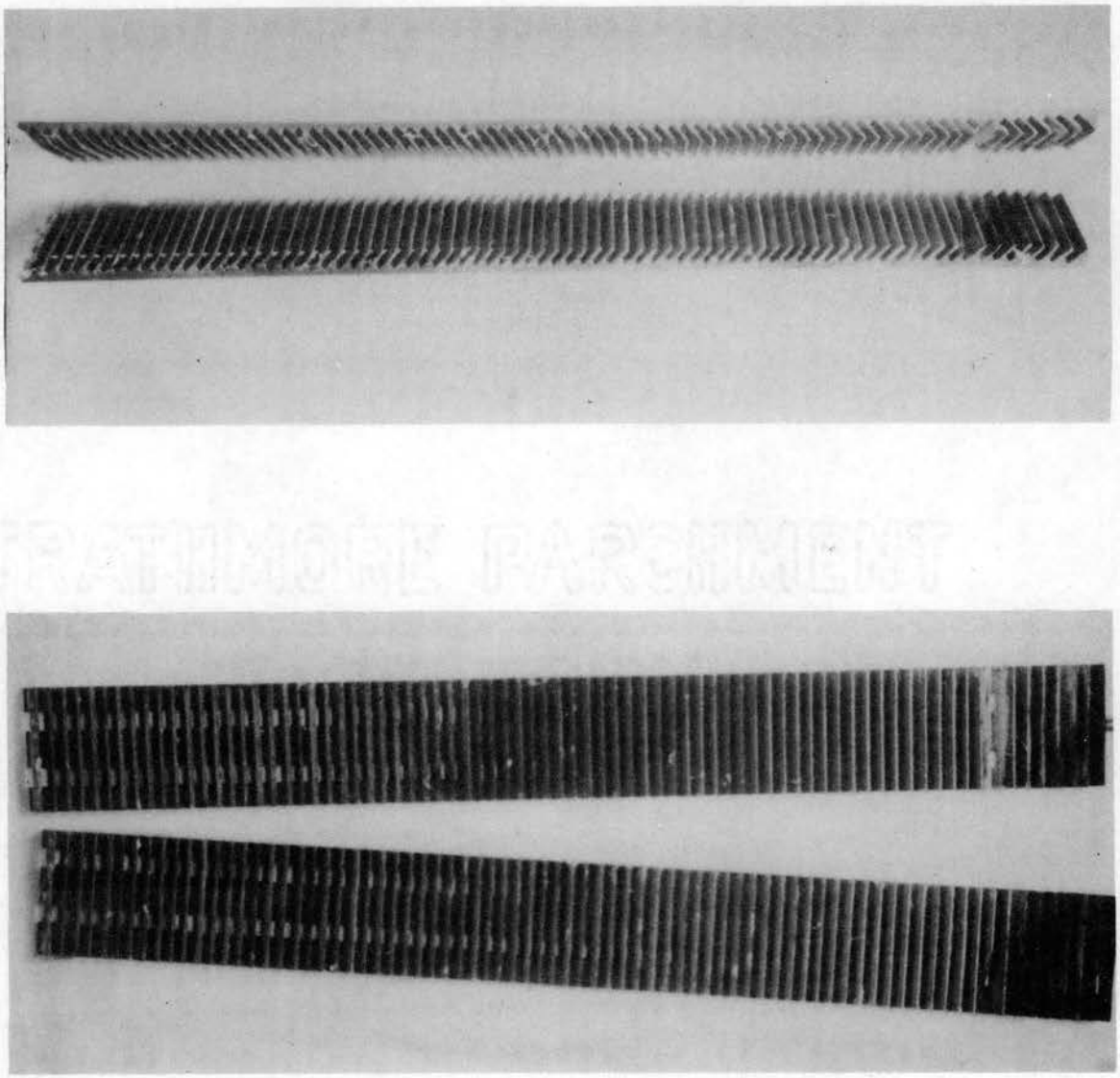

Figure 4.2.10. Photograph of Milled-Fin Electrodes Used to Obtain Electrolysis-Cell Characteristics

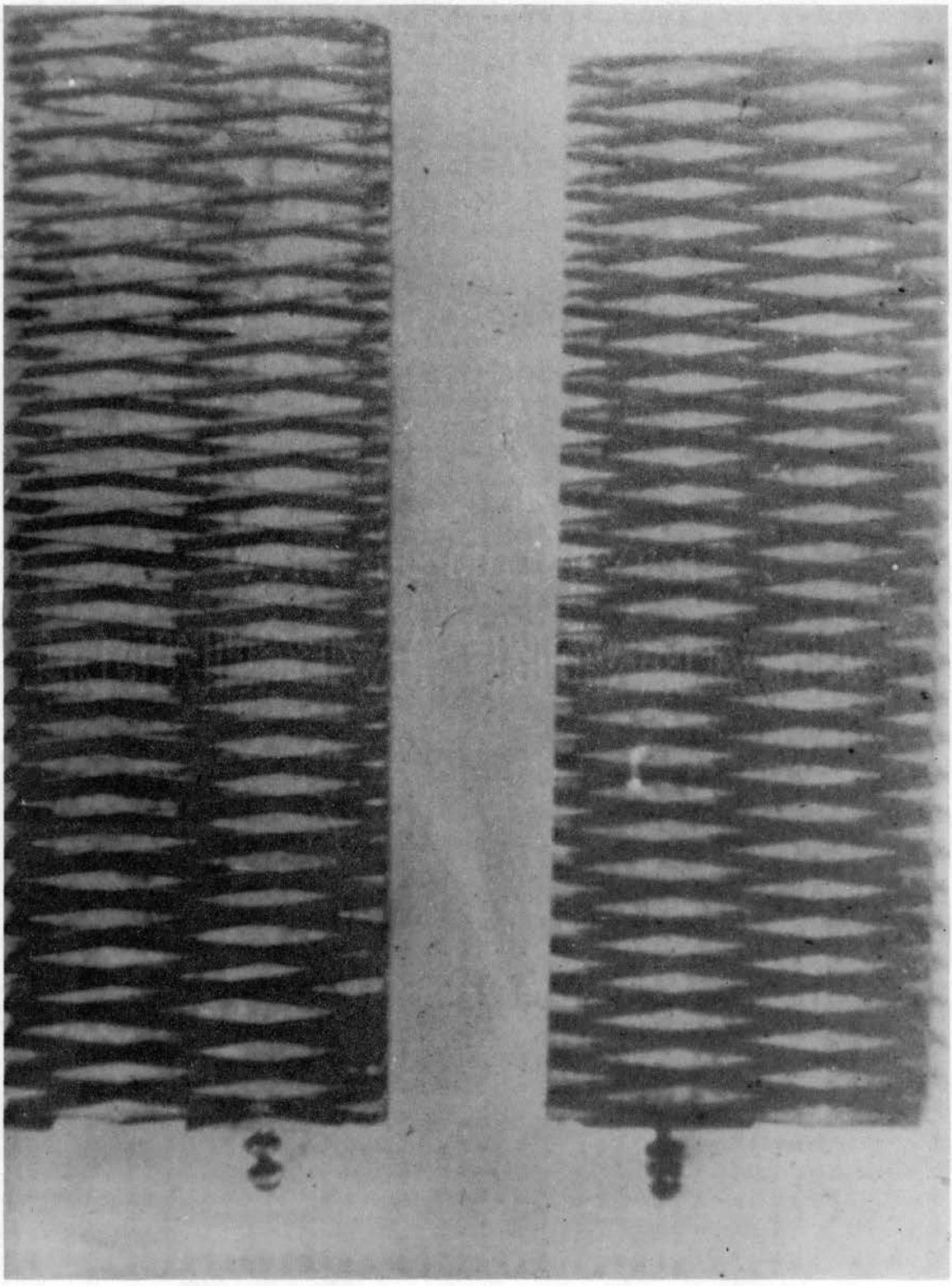

Figure 4.2.11. Photograph of Diamond-Lattice Electrode Approach to High-Pressure Fuel-Cell Design

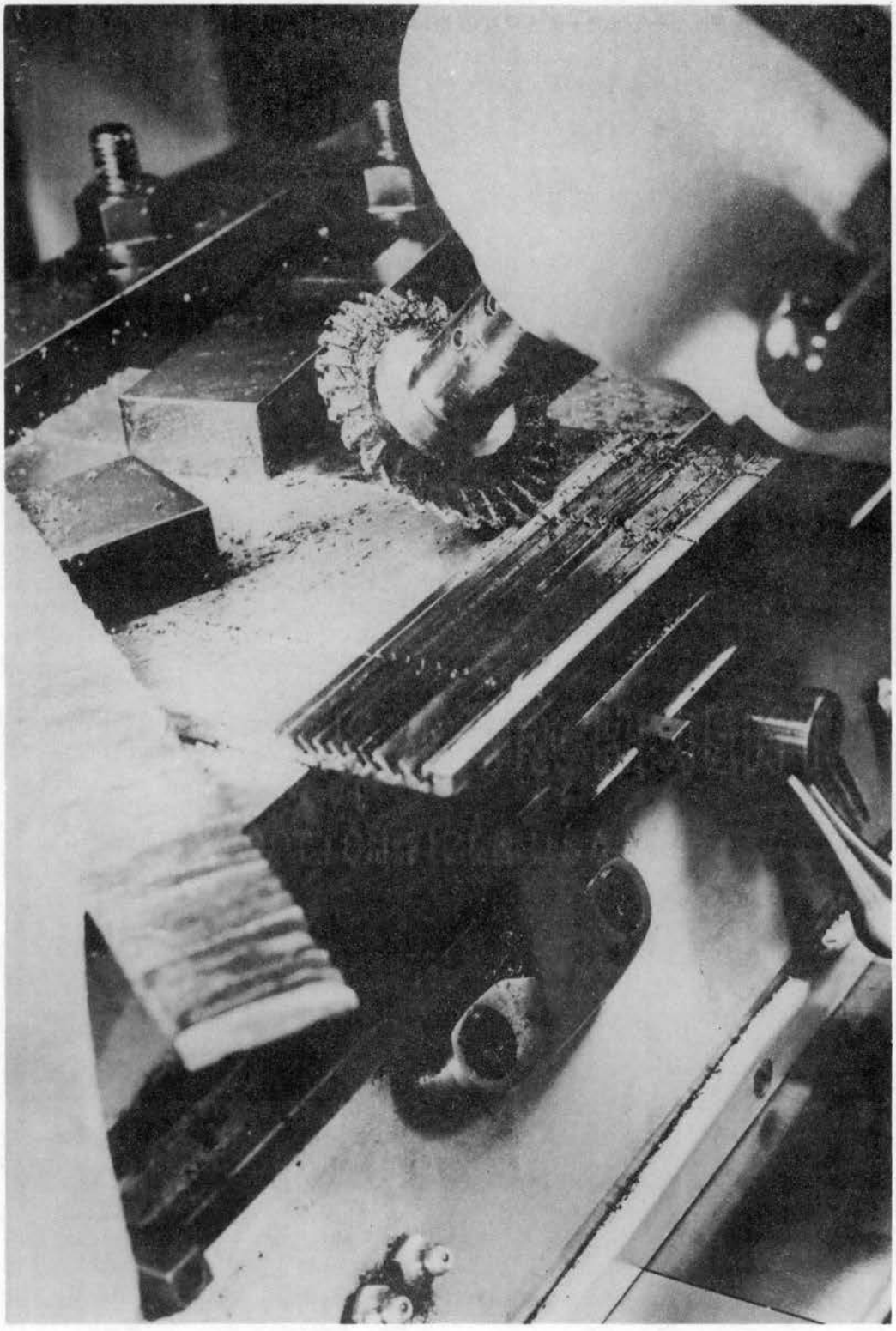

Figure 4.2.12. Photograph of Facility Utilized in Fabricating Milled-Fin Electrodes

approach to hydrogen electrolysis-cell design. Although research in this area is still being conducted, the results presented in this section will clearly show the usefulness of the technique.

The theoretical advantages of a finned-electrode approach to electrolysis-cell design were documented in the preceding chapter. Experiments were conducted to determine the optimum number, length, and angle of declination of various sets of fins in an effort to determine the optimum electrode configuration. Figure 4.3.1 shows that the effective resistance of the electrolysis cell decreases with an increasing number of fins, indicating that the fins are in parallel in the electrolyte. This implies that the number of fins per unit of vertical length should be as large as possible. The upper limit on the number of fins possible in a given cell is established by the vertical distance between the fins, which must not be so small as to constrict the flow of hydroxyl ions into the vicinity of the fins. Further, the distance between the fins must be large enough to provide for the free passage of the gases which result from electrolytic dissociation away from the active sites of the electrodes. However, neither of these limits can be approached in a real electrode due to difficulties associated with the fabrication process.

As discussed in Chapter III, the fins associated with this approach to electrode design are given a downward tilt so that gravitational force will cause the evolved bubbles to move rapidly away from the membrane used to keep the gases separate. Too steep a tilt in the electrodes, however, would increase the difficulty in fabricating the fins. These problems limited the fin tilt to 45°, and this angle was maintained in all of the electrodes constructed as a part of this study.

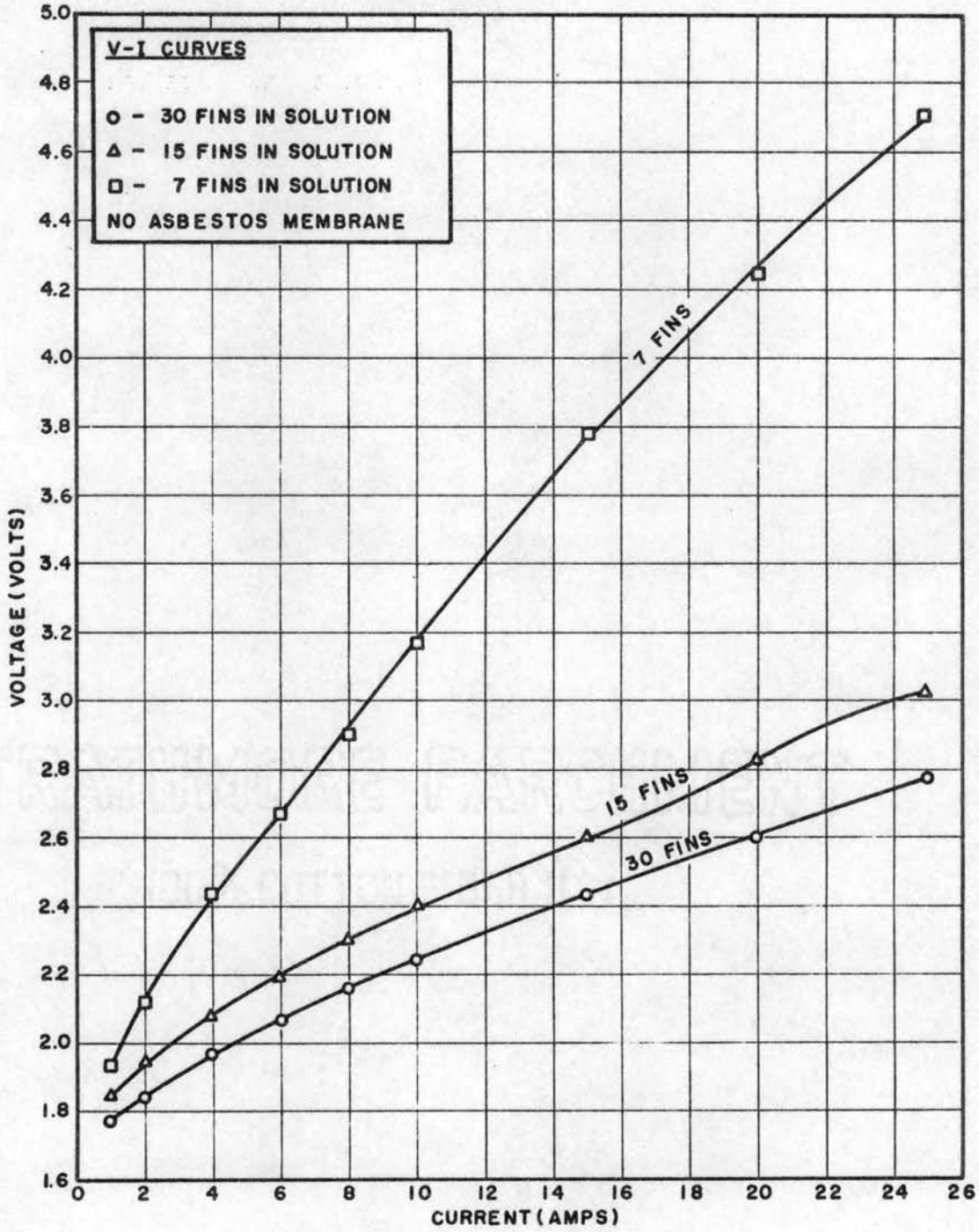

Figure 4.3.1. Effect of Number of Electrode Fins on the Voltage-Current Characteristics of Solid-Nickel, Milled-Fin Electrodes

The efficiency of the electrolytic process is known to be a function of the distance between the electrodes, due to the resistive character of the potassium hydroxide electrolyte. This implies that the effectiveness of the fin surfaces in a finned electrode decreases with distance away from the fin tips. This means that electrodes with extremely long fins would contain large areas of fin surface which would not contribute greatly to the electrolytic process. However, the fins should be long enough to allow for the safe separation of the evolved gases. A balance of these length-determining factors led to the establishment of a fin length of 1/8 inch for all of the milled-fin electrodes constructed as a part of this phase of the research effort.

The electrodes whose characteristics are discussed in this section were milled from solid nickel sheets. The data plotted in Figures 4.3.2 and 4.3.3 indicate that the characteristics of such electrodes are enhanced when the electrodes have been etched in a concentrated solution of nitric acid. It is anticipated that the electrolysis-cell characteristics can be improved still further by using porous electrodes, which would have an even greater effective surface area for a given mechanical configuration. Figures 4.3.2 and 4.3.3 also show that the addition of an asbestos membrane between the cell electrodes to keep the evolved gases separate does not affect the characteristics of the cell to any great extent. Figure 4.3.2 consists of a voltage versus current plot for a finned-electrode electrolysis cell which contained no protective membrane. In Figure 4.3.3, the same characteristics are plotted with the cell electrodes separated by three layers of asbestos membrane. Comparison of the two curves shows that only a slight voltage drop is associated with the membrane, proving that such membranes can

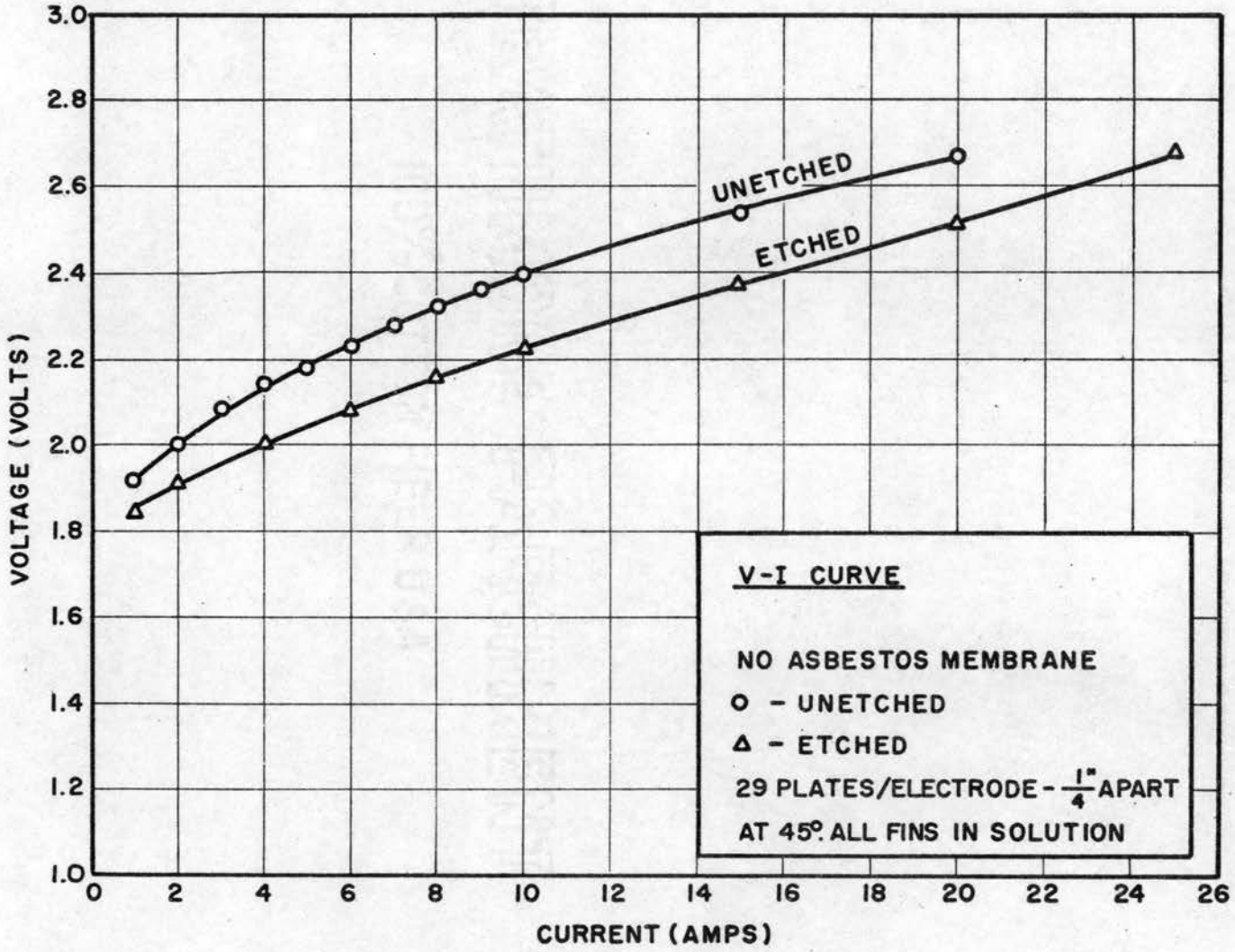

Figure 4.3.2. Effect of Etching Solid-Nickel Finned Electrodes on Electrolysis-Cell Performance

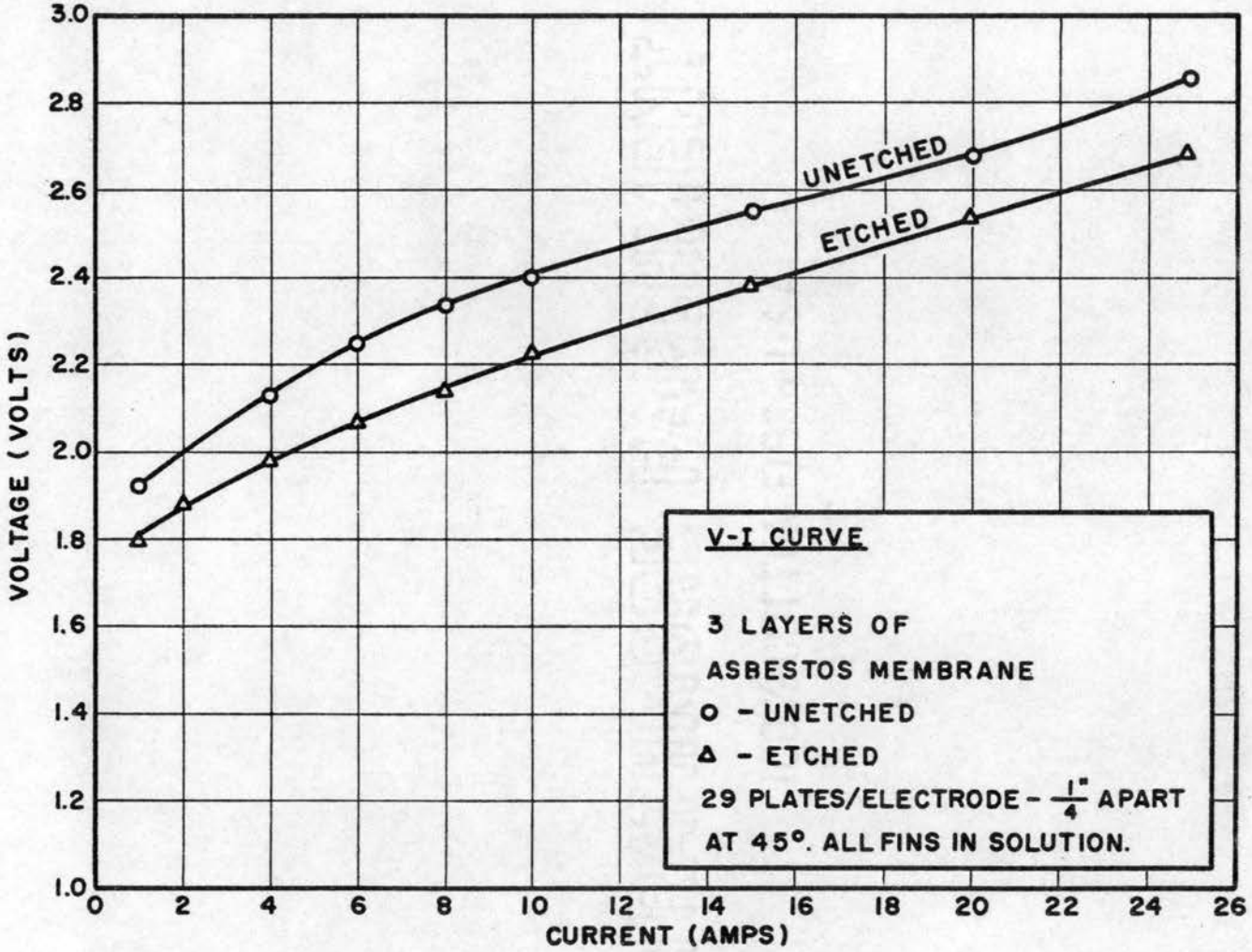

Figure 4.3.3. Effect of Asbestos Membrane on Cell Performance

be used in electrolysis cells without seriously affecting their performance characteristics or efficiency.

The effect of a catalyst on the performance of electrolysis cells was examined. A 25-percent solution of platinic chloride was applied to the etched electrodes, following procedures suggested by General Electric (47). As shown in Figures 4.3.4 through 4.3.7, the activated electrodes exhibited performance characteristics which were superior to those for the unactivated set over a pressure range of atmospheric to 3,000 psi, the upper pressure limit of the environmental pressure chamber used in the experiment. The electrodes used in this series of experiments were shown in Figure 4.2.3.

The curves shown in Figures 4.3.4 through 4.3.7 are also significant in that they demonstrate the effect of pressure on the voltage versus current curves for both activated and non-activated electrolysis cells. The curves show that a slight improvement in cell performance occurs as the environmental pressure of the system is increased. Although the improvement is slight, it is significant in that it shows that the gases which result from the electrolytic process can be evolved and stored under high-pressure conditions without increasing the input electrical power requirements of the cell. This indicates an advantage of a pressure electrolysis-cell system over a system which operates at atmospheric pressure and then utilizes a compressor to compress the gases to a pressure suitable for gas storage.

The improvement in cell performance which results when a catalyst is applied to the electrode surfaces becomes significant only if the effectiveness of the catalyst is not degraded by the environmental conditions of cell operation. Tests were run to determine the effect on

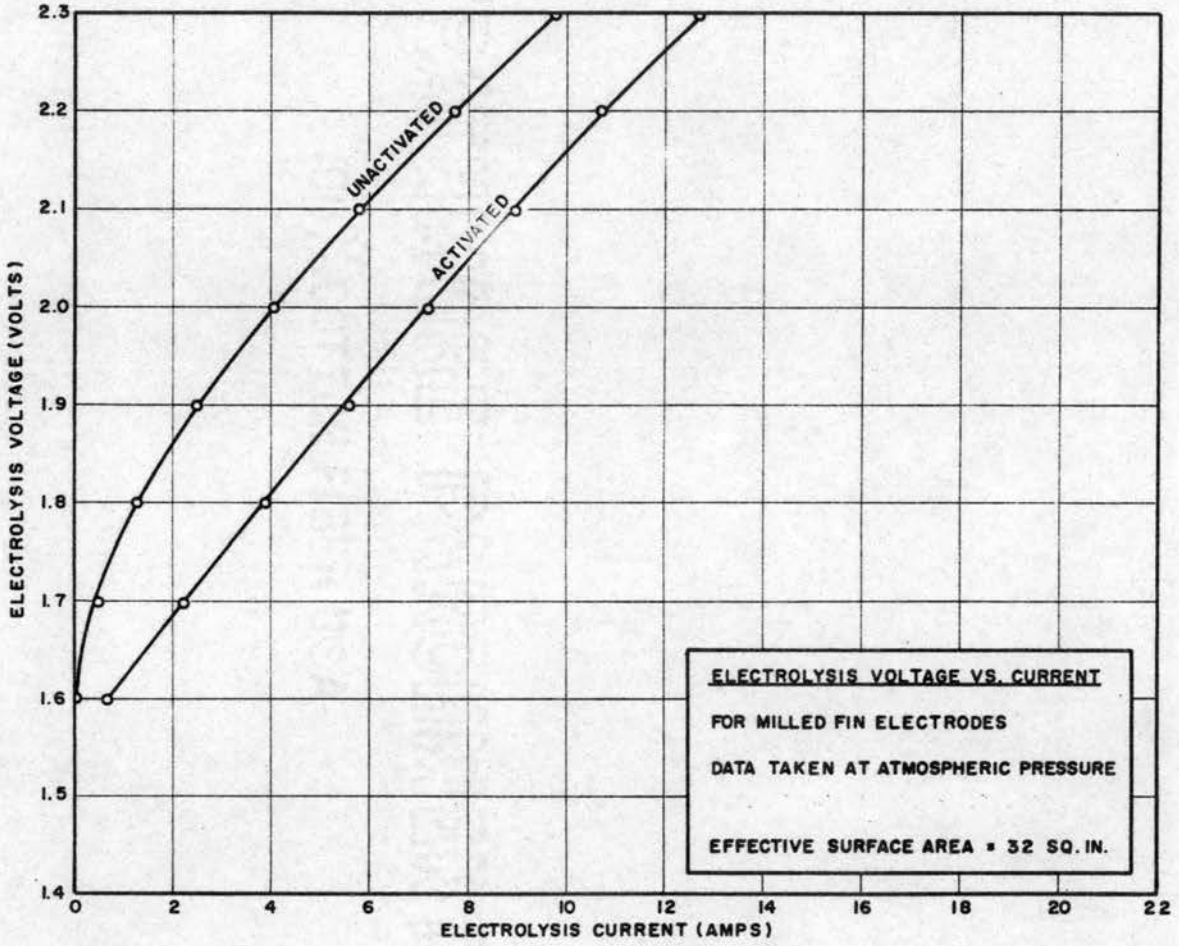

Figure 4.3.4. Curves Showing Effect of Activation With Platinic Chloride on Electrolysis-Cell Characteristics at Atmospheric Pressure

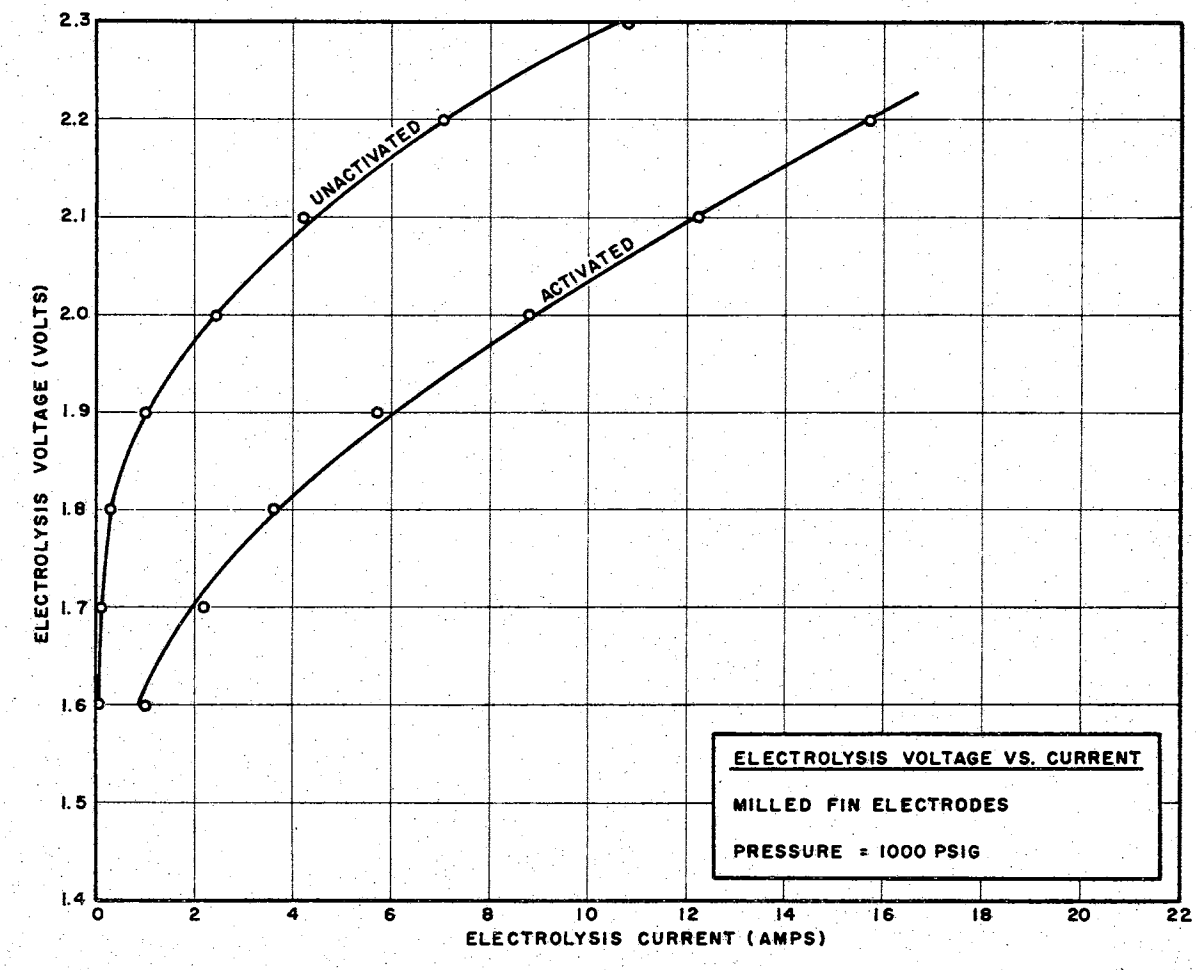

Figure 4.3.5. Curves Showing Effect of Activation With Platinic Chloride on Electrolysis-Cell Characteristics at 1,000 psig

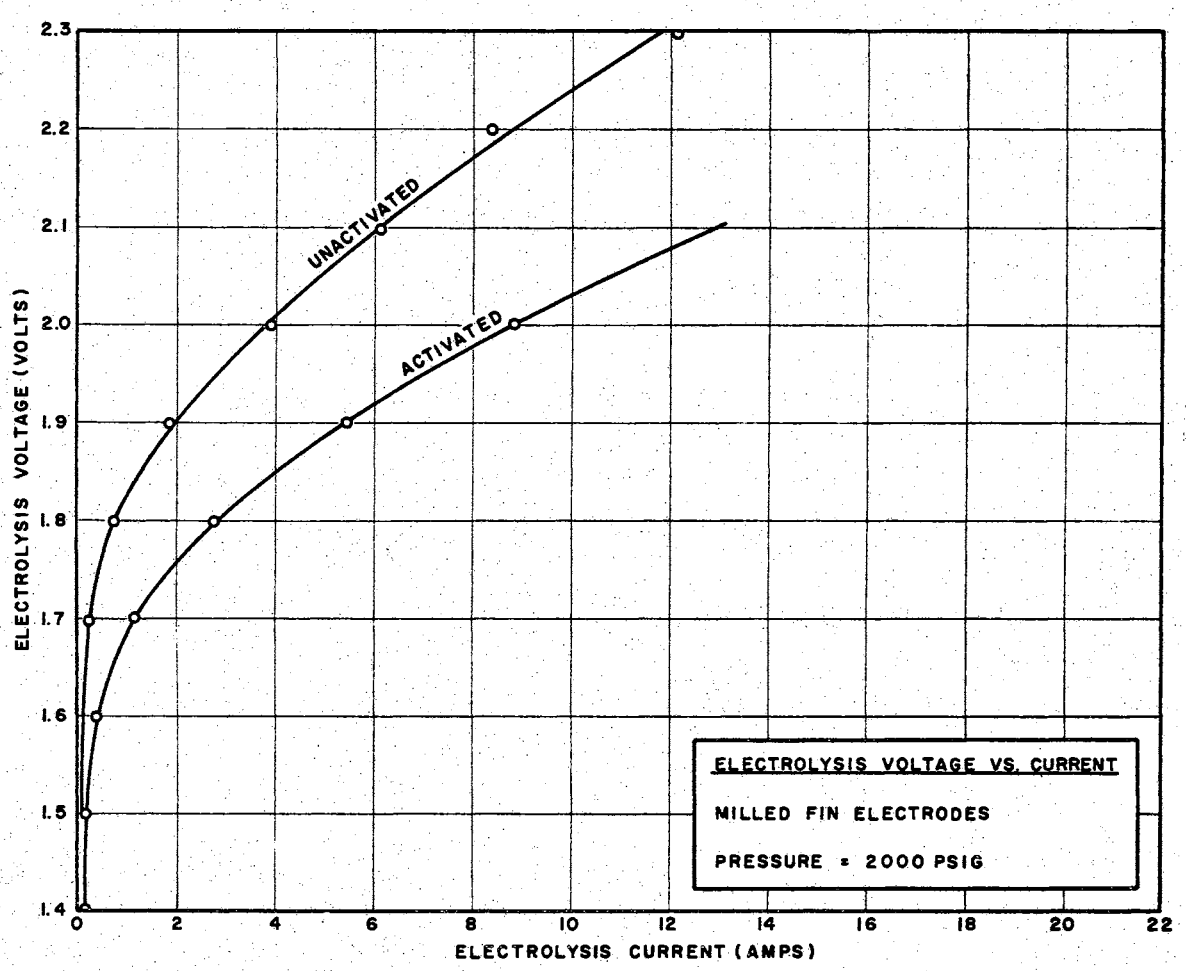

Figure 4.3.6. Curves Showing Effect of Activation With Platinic Chloride on Electrolysis-Cell Characteristics at 2,000 psig

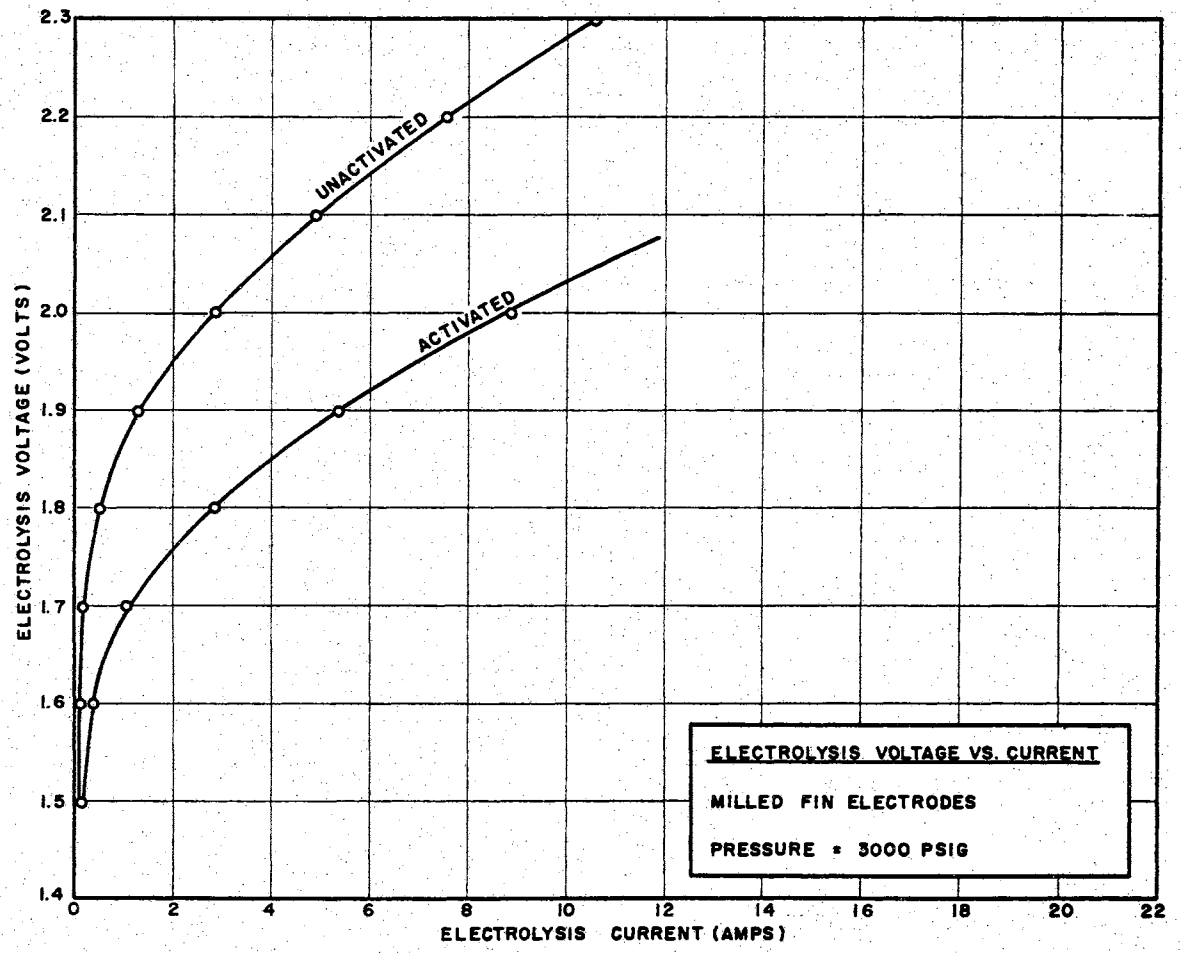

Figure 4.3.7. Curves Showing Effect of Activation With Platinic Chloride on Electrolysis-Cell Characteristics at 3,000 psig

the catalyst of environmental pressure ranges up to 3,000 psi and environmental temperatures up to 200°F. It soon became evident that the effectiveness of the catalytic deposition technique used was limited to temperatures lower than 150°F, due to the fact that the platinum coating on the electrodes went into solution with the electrolyte at temperatures above 150°F. The deterioration of the catalyst can be seen from a comparison of Figures 4.3.8 and 4.3.9. The experiment whose results were plotted in Figure 4.3.8 was the first effort to obtain a voltage versus current plot for various temperatures and a constant pressure of 3,000 psi for the catalyzed electrodes shown at the bottom of Figure 4.2.10. The curves shown in Figure 4.3.9 represent the second run of the same experiment. The curves in Figure 4.3.9 are clearly inferior to those shown in Figure 4.3.8 at each environmental temperature for which data was recorded. This indicates that the catalytic deterioration which occurred during the first run of the experiment caused the degradation in cell performance shown in Figure 4.3.9. Further evidence of the inadequacy of the catalytic deposition technique at high temperatures follows from the fact that the data plotted in Figure 4.3.8 was taken as the environmental temperature increased. The voltage versus current curve for 122°F is identical to the curve at 193°F, while the curve at 152°F is superior to both of these curves, thus proving that the cell characteristics deteriorated at temperatures in excess of 152°F.

Figure 4.3.10 indicates that electrolysis characteristics of the milled-fin electrodes are greatly enhanced by increasing environmental temperature. For a temperature of 400°F and a pressure of 2,000 psi, the current density for electrolytic action was 405 amperes per square

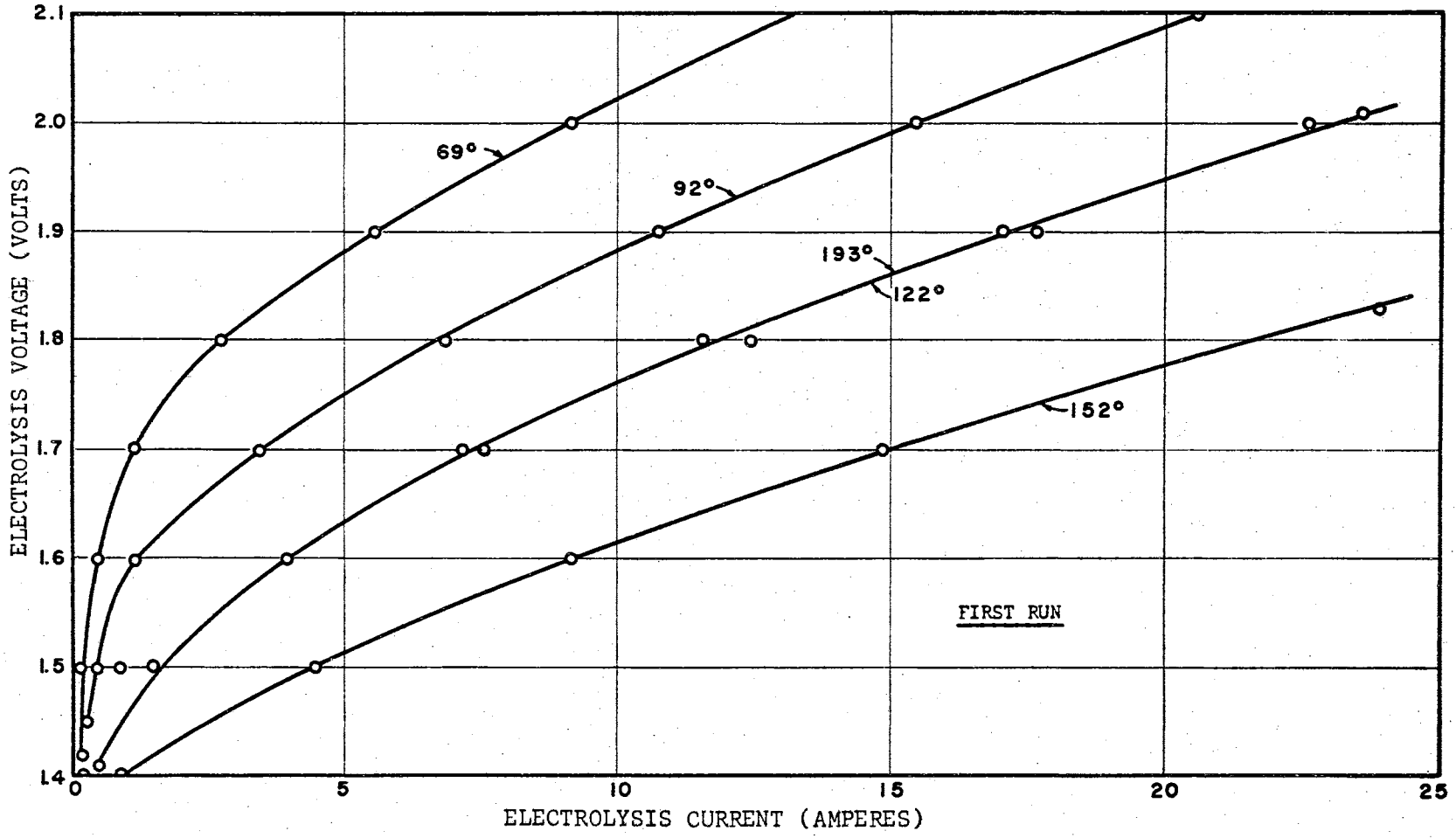

Figure 4.3.8. V-I Curves Resulting From First Experimental Run Using Activated Electrodes

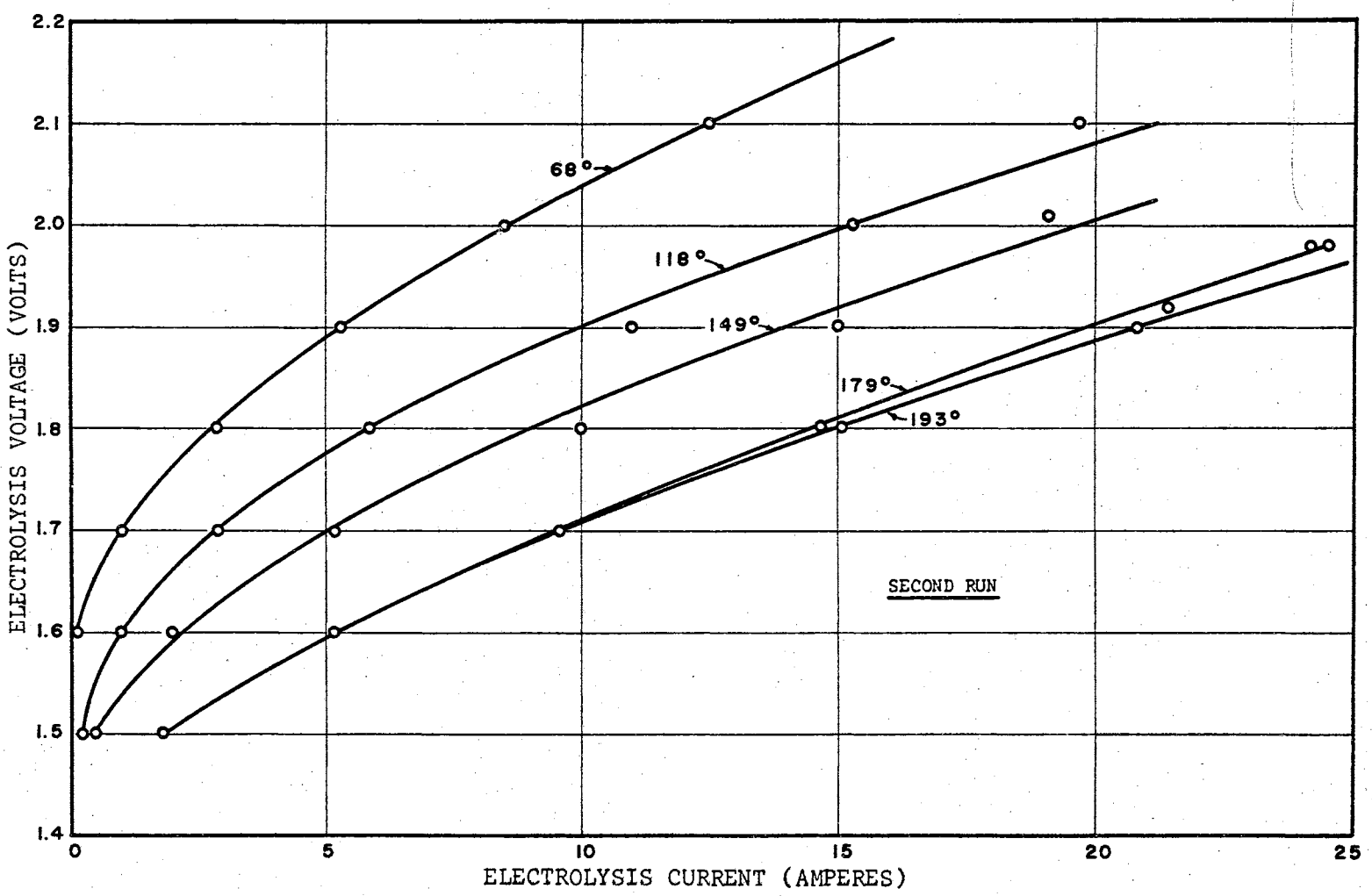

Figure 4.3.9. V-I Curves Resulting From Second Experimental Run Using Activated Electrodes

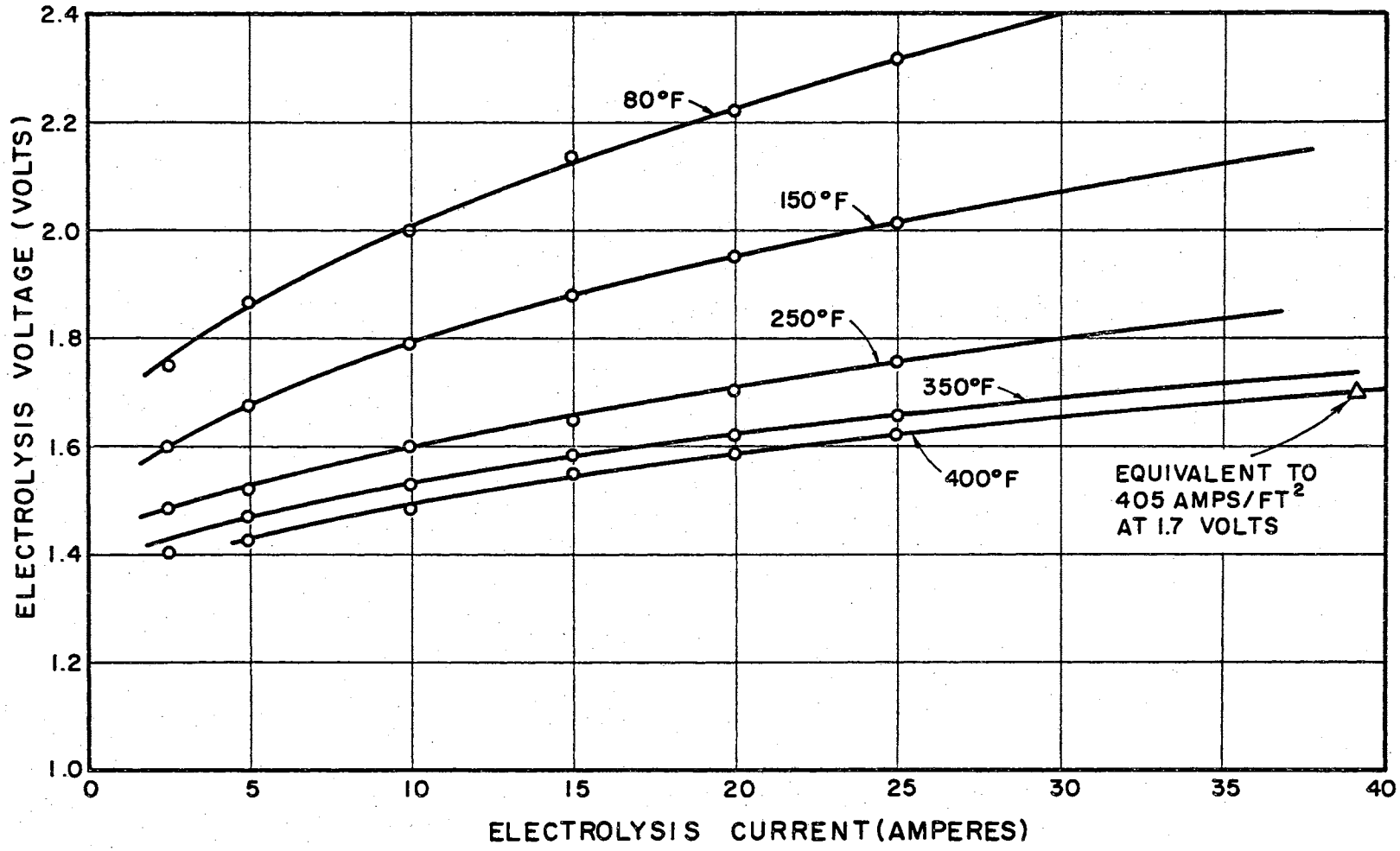

Figure 4.3.10. Effect of Temperature on Electrolysis-Cell Performance at 2,000 psi With Unactivated, Solid-Nickel, Milled-Fin Electrodes

foot for an applied voltage of 1.7 volts. This figure is significantly higher than any which this writer could find in the literature. This fact, coupled with the preceding discussion on the effect of pressure on the cell, demonstrates that the milled-fin, high-pressure, high-temperature electrolysis-cell configuration developed as a part of this study represents a noteworthy step toward the development of a superior electrolysis-cell system. The fact that temperature has a greater effect on the electrodes than pressure is seen from a comparison of Figure 4.3.10 with Figure 4.3.11, which shows the effect of pressure on the milled-fin electrolysis-cell electrodes.

Figures 4.3.12 through 4.3.16 are included in this thesis to show that the enhancing effect of temperature on activated milled-fin electrodes is independent of environmental pressure. These curves represent the completion of the experimental attempt to map the pressure and temperature effects on the voltage versus current curves for the new type of electrode structure developed at Oklahoma State University.

An experiment was devised to quantitatively measure the amount of gas evolved by the electrolytic process as a function of the applied voltage and current. In this way, a practical estimate of the actual conversion efficiency of the cell could be determined. The evolved gases were bled into an inverted, water-filled, calibrated glass cylinder which was attached to the top of the upper left-hand tank shown in Figure 4.2.6. Continuous observation of the electrical power required to produce the gases was made possible through the use of a recorder. Data taken as a part of this experiment is shown in Table 4.3.1. Also listed for comparison purposes is data concerning the characteristics of some of the more important commercially available

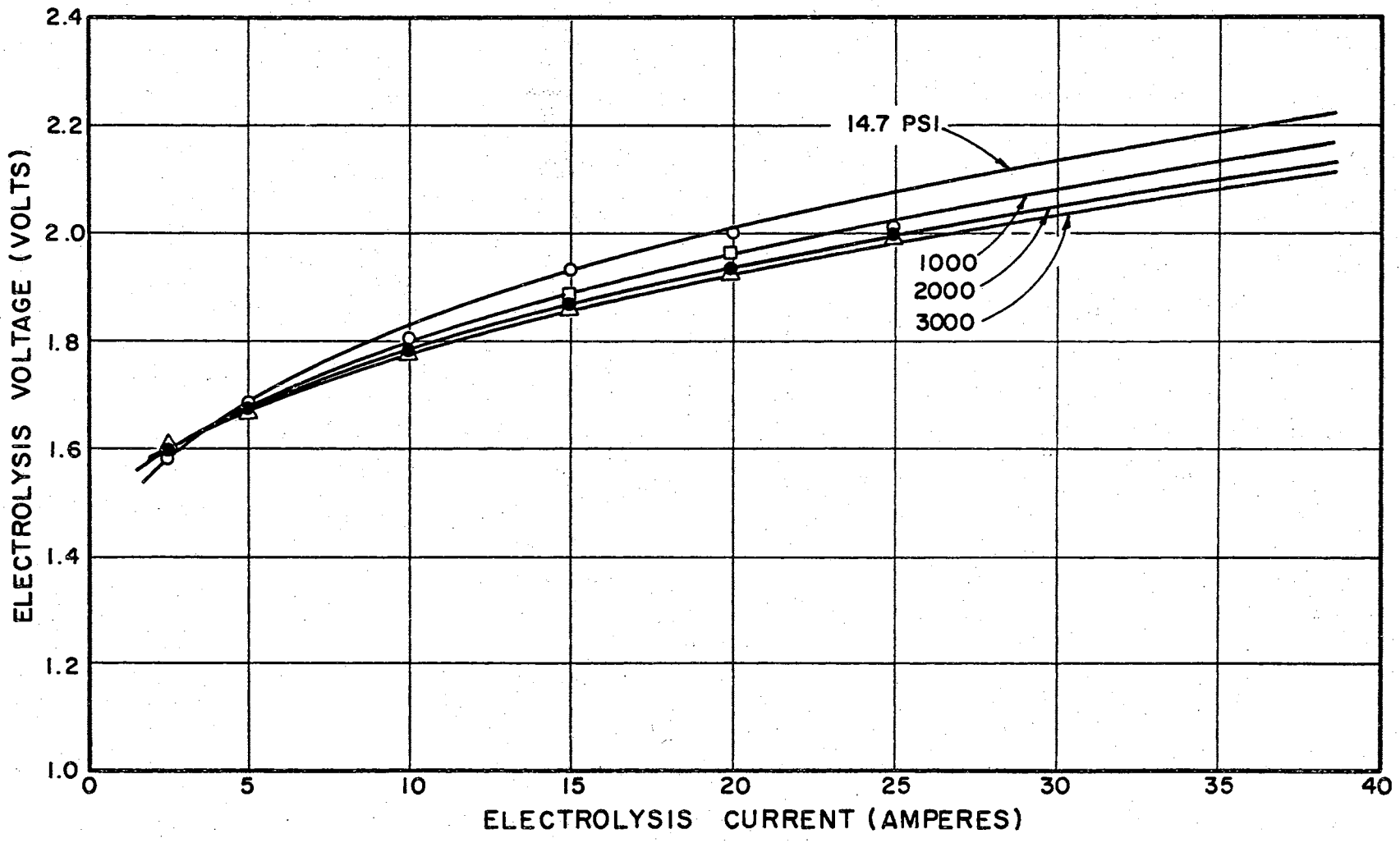

Figure 4.3.11. Effect of Pressure on Electrolysis-Cell Performance at 150°F With Unactivated, Solid-Nickel, Milled-Fin Electrodes

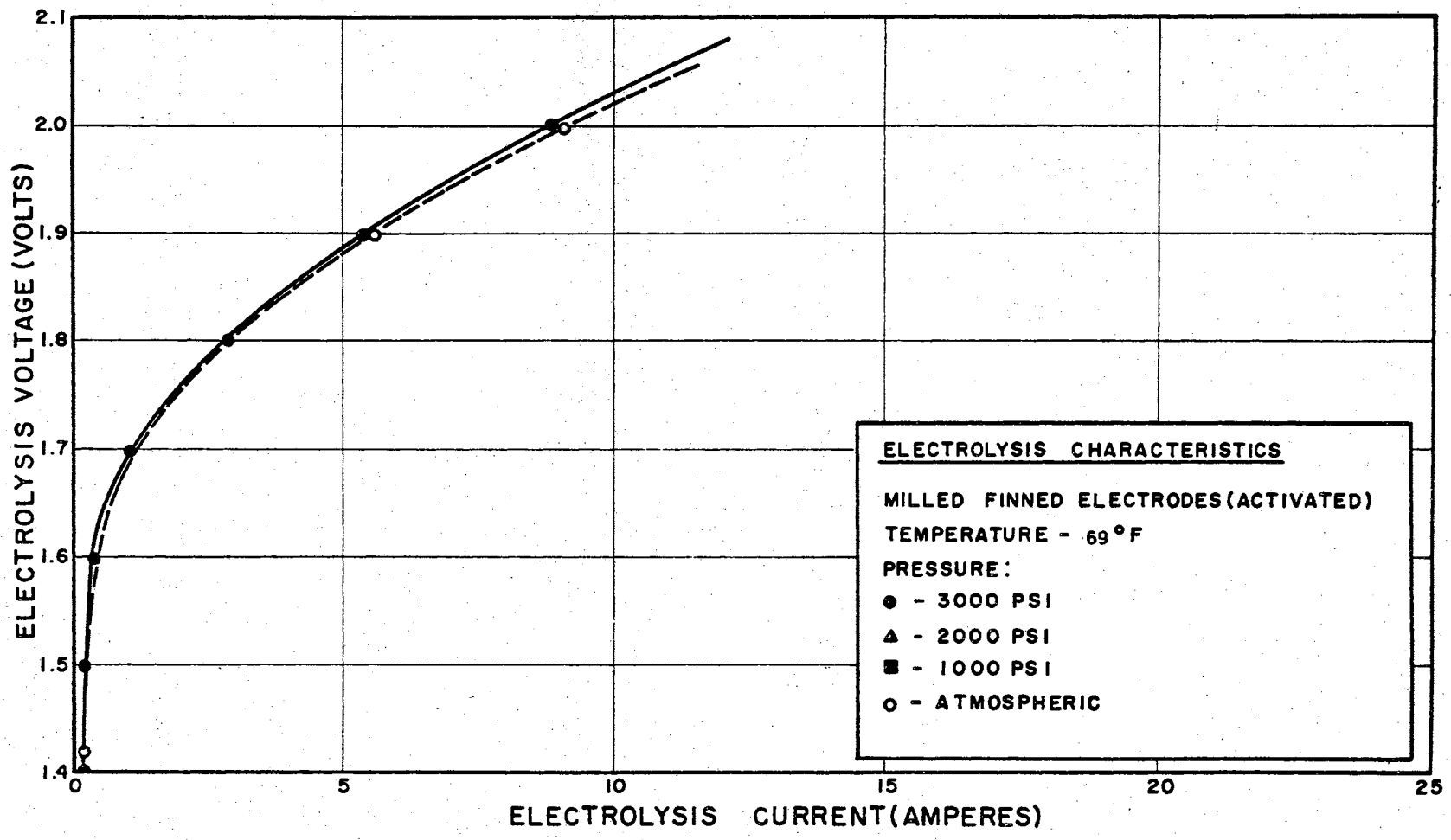

Figure 4.3.12. Curve Showing Effect of Pressure on Electrolysis-Cell Characteristics at 69°F

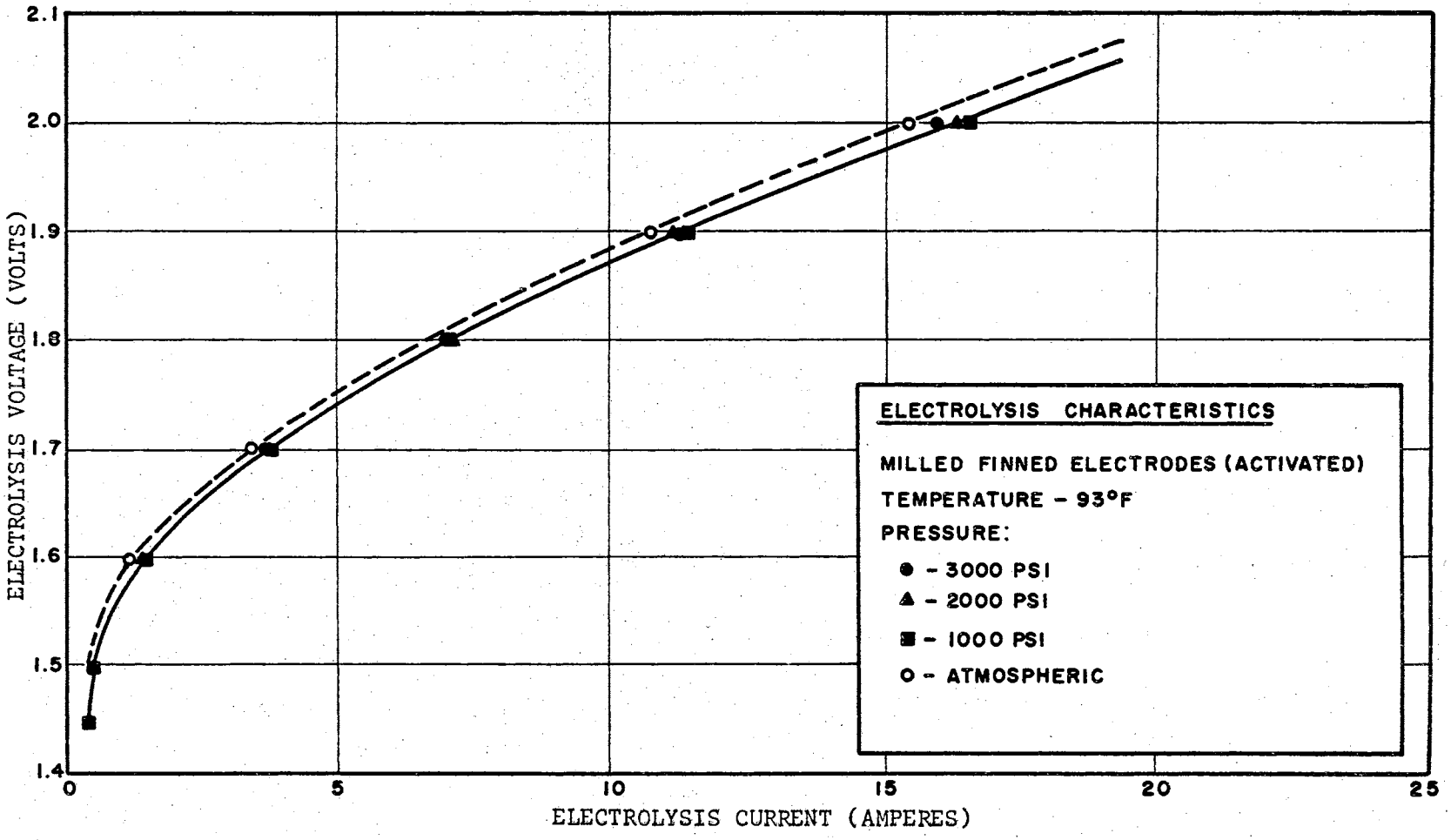

Figure 4.3.13. Curve Showing Effect of Pressure on Electrolysis-Cell Characteristics at 93°F

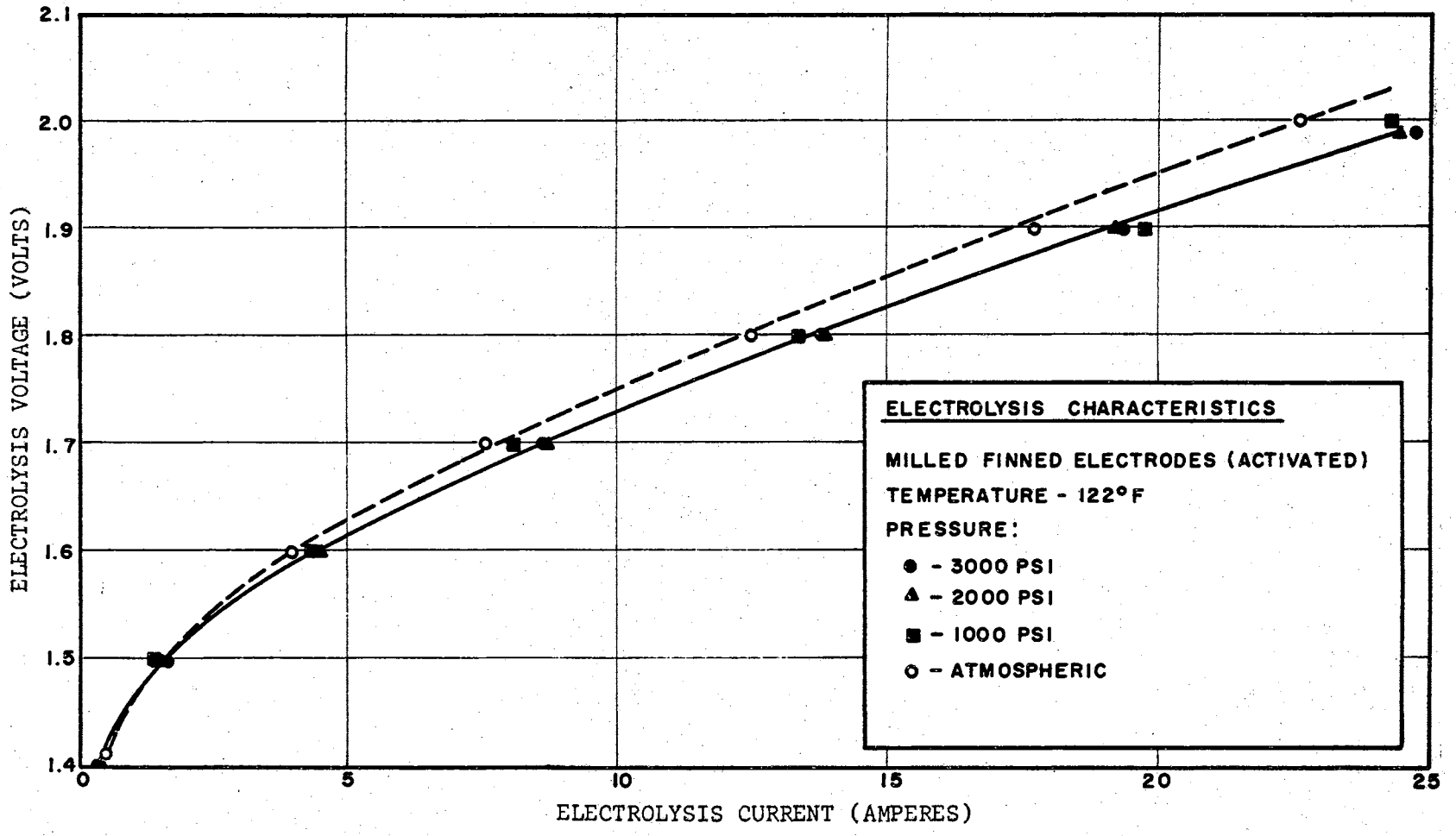

Figure 4.3.14. Curve Showing Effect of Pressure on Electrolysis-Cell Characteristics at 122°F

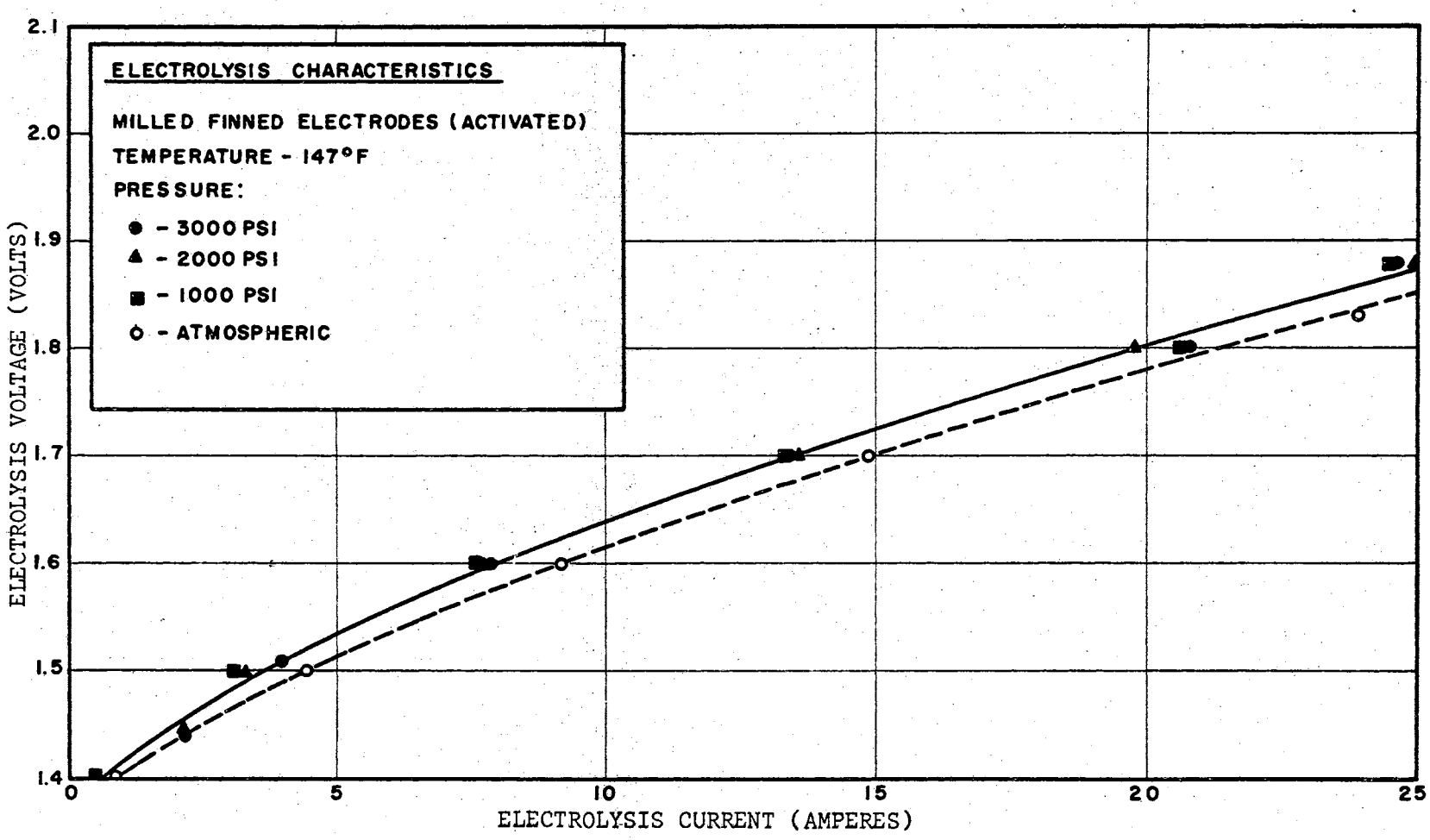

Figure 4.3.15. Curve Showing Effect of Pressure on Electrolysis-Cell Characteristics at 147°F

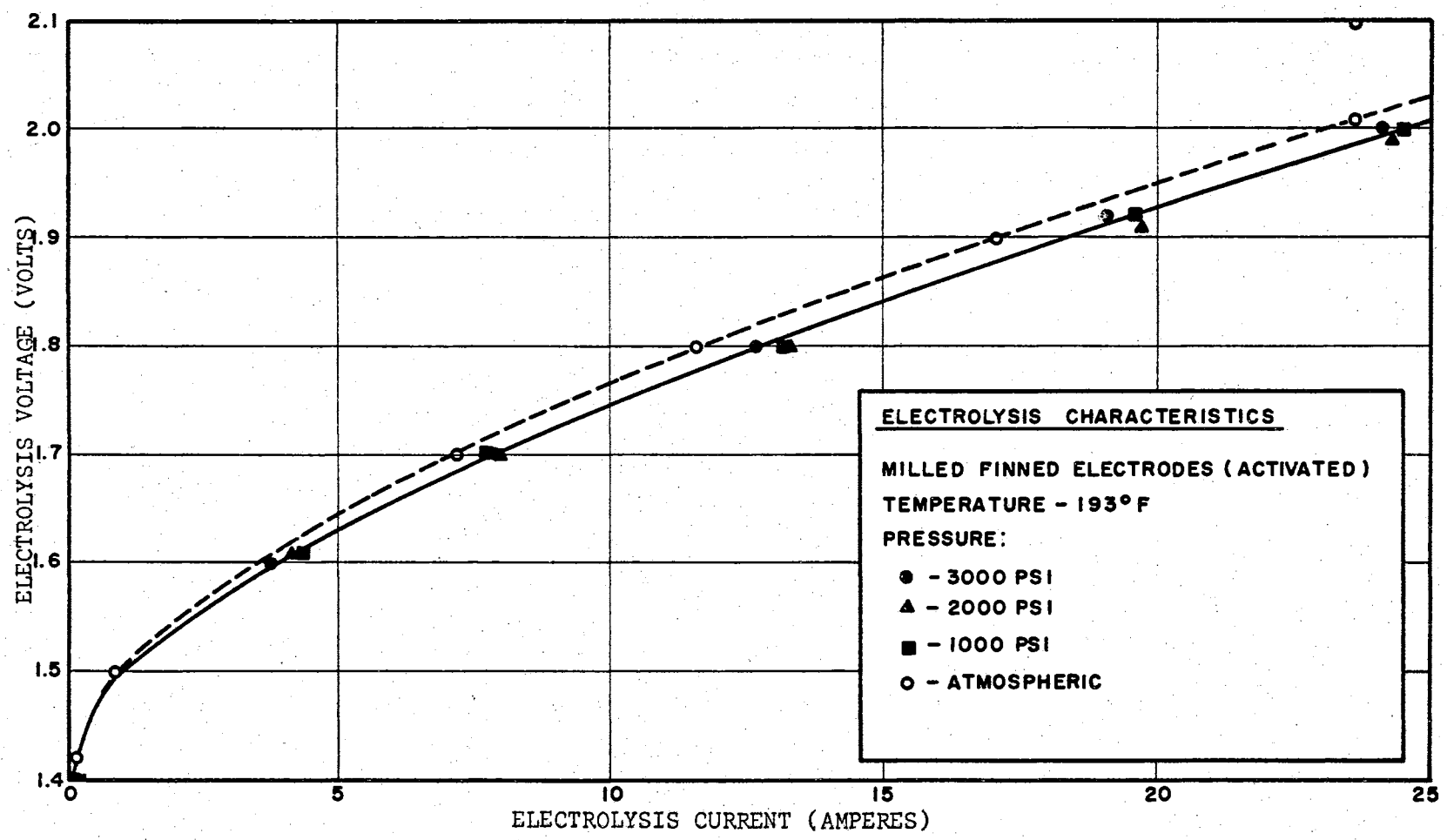

Figure 4.3.16. Curve Showing Effect of Pressure on Electrolysis-Cell Characteristics at 193°F

TABLE 4.3.1

A COMPARISON OF THE OKLAHOMA STATE UNIVERSITY MILLED-FIN CELL WITH CONVENTIONAL HYDROGEN-OXYGEN ELECTROLYZERS

Cell Type	Energy Density (Amps Per Sq. Ft.)	Kilowatt Hours Per Cubic Ft. H_2 Out	Efficiency %	Reference
OSU Milled-Fin Cell	710	.100	95.1	
Knowles Cell	300	.140	68.0	(20)
Shriver Filter Press	100	.139	68.5	(20)
H. K. Sen Cell	18	.112	85.0	(22)
Noeggerath	75	.100	95.1	(20)
Electrolabs Cell	86	.125	72.5	(20)

electrolyzers. It is apparent from the table that the Oklahoma State University cell has a significantly higher value of energy density than any of the other cell types. (The energy density figure is referenced to a cell voltage of two volts in each case listed.) The efficiency of the milled-fin approach to electrolysis-cell electrode design, as shown by columns three and four of Table 4.3.1, is extremely high; and it compares very favorably with the values listed for the other cells.

A significant difficulty associated with the construction of a large electrolysis system is the fact that the individual cells are characteristically high-current, low-voltage devices. It is desirable, therefore, that such cells be operated in a series connection, rather than in a parallel configuration, to reduce the current requirements for a large bank of the cells. Compounding the difficulty in connecting the cell electrode pairs in series is the fact that the electrolyte solution used in the system provides an extremely low-resistance path for the flow of ions and thus tends to connect the cell electrode pairs in parallel when the cells are operated in a common electrolyte.

In water electrolysis, it is necessary that hydroxyl ions pass through the electrolyte from the oxygen electrode to the hydrogen electrode if the reaction is to be completed. Therefore, those ions which are released from a given oxygen electrode must be available to its corresponding hydrogen electrode but not available to any other hydrogen electrode which might be in the same electrolyte. This is accomplished in the Oklahoma State University electrolysis cell as is shown in Figure 4.3.17. Between the finned electrode pairs is a nickel plate which serves both as a barrier to the free flow of hydroxyl ions and an extremely low-resistance contact which binds together the two electrodes

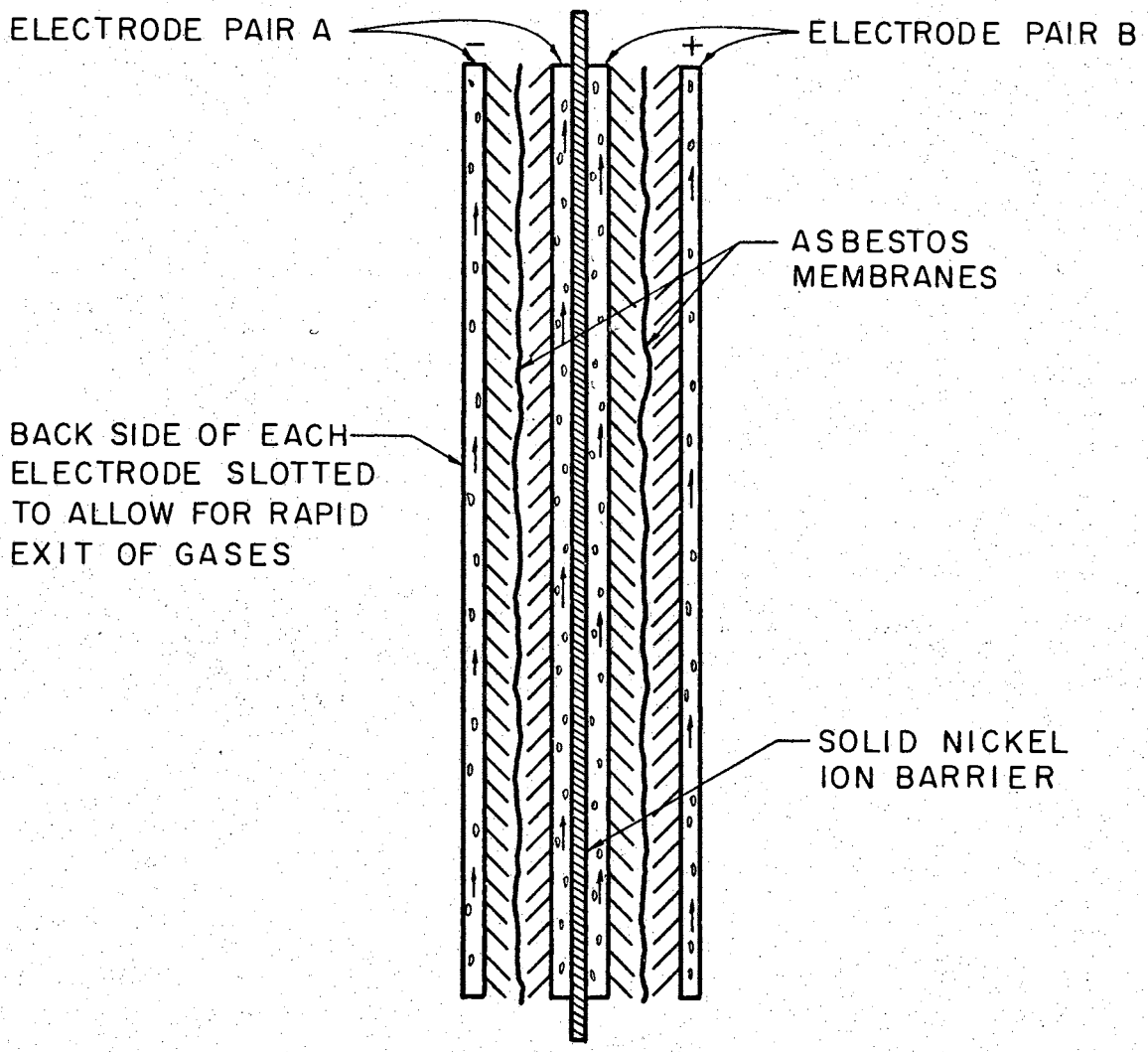

Figure 4.3.17. Schematic Diagram of Two Milled-Fin Electrolysis Cells Connected in Series Electrically

shown in the figure. It is interesting to note that the middle electrode will have oxygen gas evolved from the left-hand side and hydrogen gas from the right-hand side when the voltage of the polarity indicated is applied to the cell.

A series configuration of the type described above was constructed, and it is shown in Figure 4.3.18. Voltage versus current curves were plotted for the two electrodes shown in the figure, then a curve for the series arrangement was plotted from the results of the experiment. These results are shown in Figure 4.3.19. Also plotted in Figure 4.3.19 is the theoretical V-I curve which would result when the V-I curves for the individual electrode pairs were added arithmetically. Note that the curve obtained experimentally is superior to the curve obtained by simple arithmetic. This occurs because the current available to the center electrodes is injected uniformly into the electrode in the series configuration. When the curves were run for the individual cells, however, the current was injected into the bottom of the electrodes and was thus not distributed uniformly along the surface of the electrode. The nickel plate which served as a barrier to the passage of hydroxyl ions was seen to perform satisfactorily since gases evolved from only one side of the center electrode when the V-I curves for the individual cells were being obtained experimentally. Although this demonstrates the technical feasibility of this approach to placing the cells in series, more research is necessary to prove the practical value of the technique.

4.4 Hydrogen-Oxygen Fuel-Cell Experimental Results. Data for a single fin set of fuel-cell electrodes is presented as Figures 4.4.1

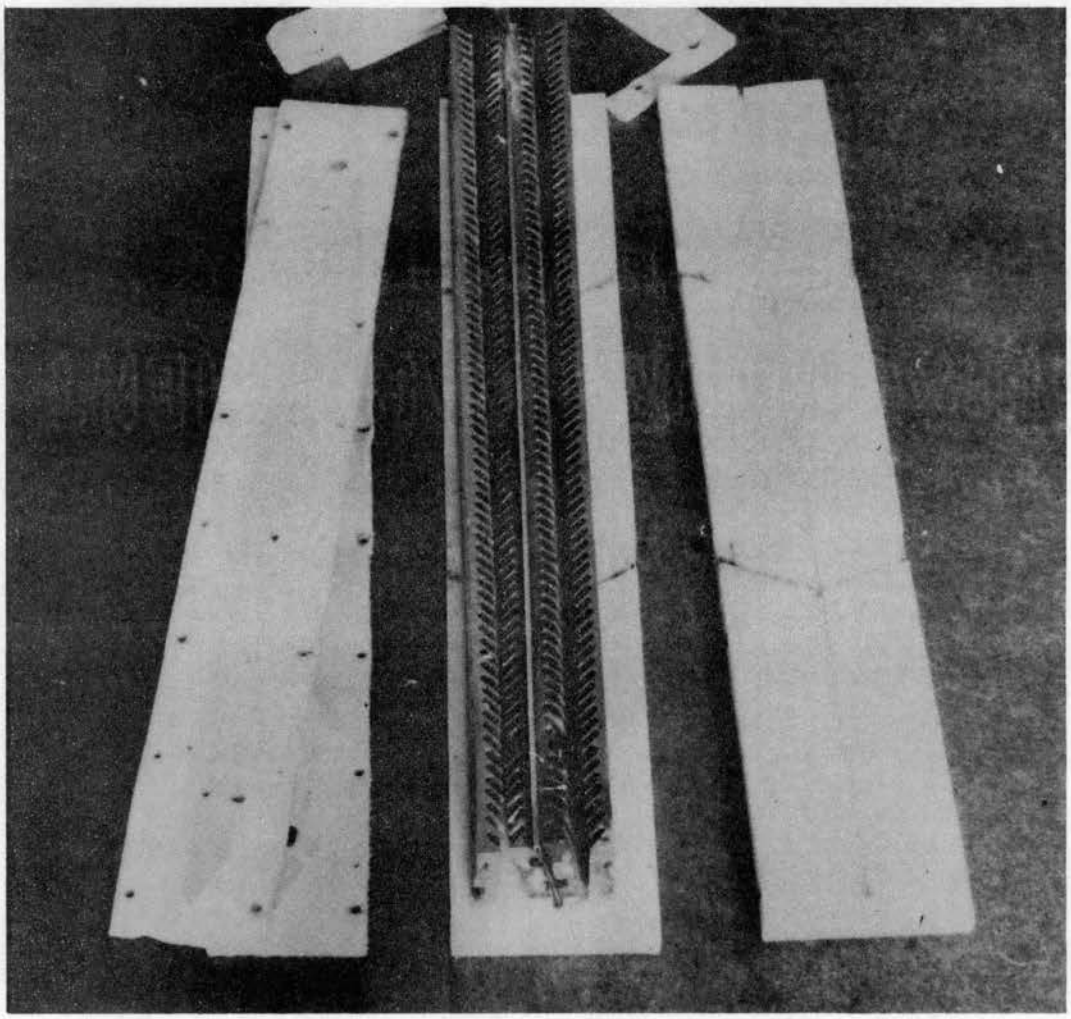

Figure 4.3.18. Photograph of Disassembled Unit of Two Milled-Fin Electrolysis Cells Tested in Series Electrically

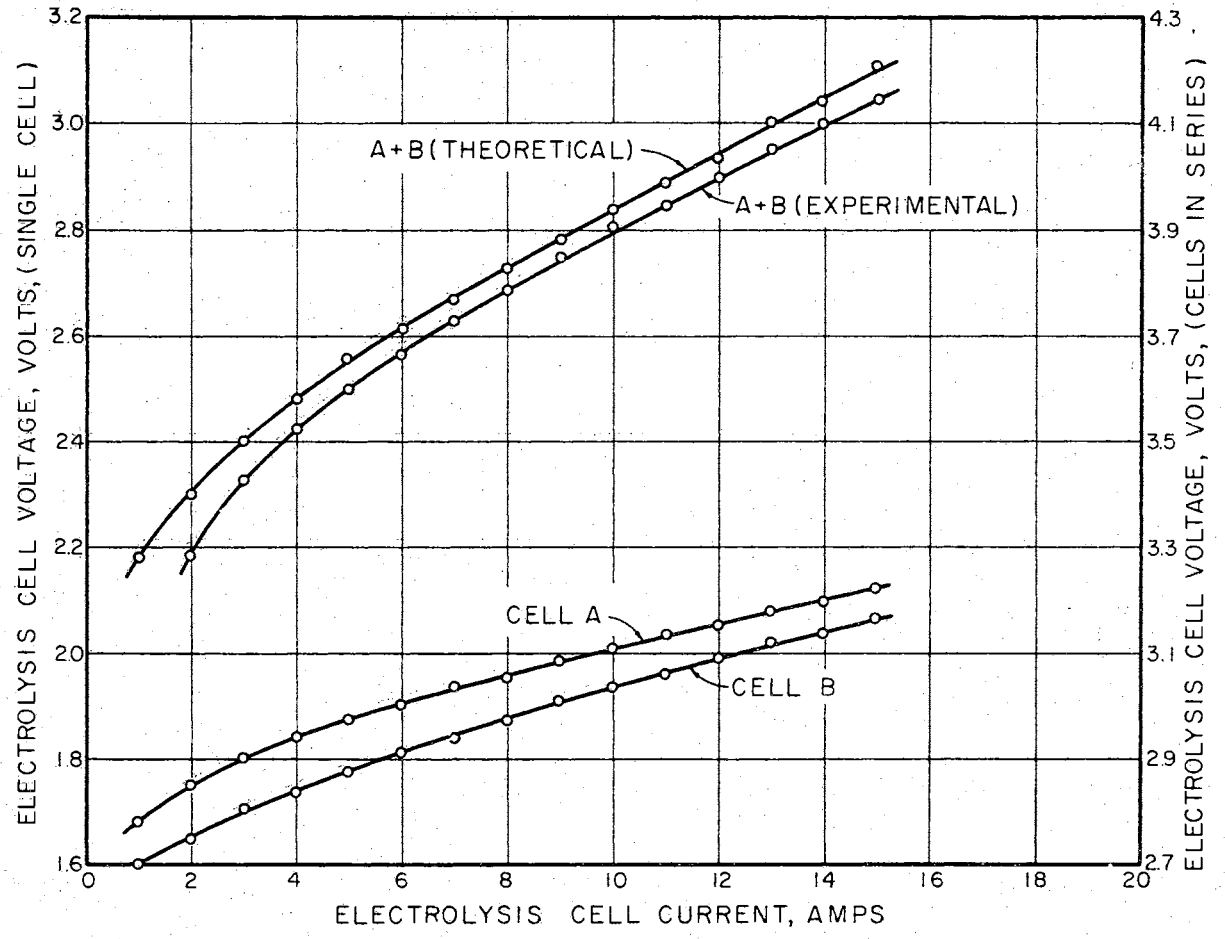

Figure 4.3.19. Comparison of Experimental and Theoretical V-I Curves for Individual Electrolytic Cells and Two Cells in Series

through 4.4.8 of this thesis. The curves indicate the effect of pressure and temperature on the set of nickel-fin fuel-cell electrodes which had been activated with a platinic chloride catalyst. A comparison of Figures 4.4.1 through 4.4.4 indicates the marked improvement in fuel-cell performance which results when the environmental pressure of the cell is increased. Not shown in the curves is the fact that the stability of the cell characteristics is also enhanced by increasing pressure. Stability in this case is an indication of the ability of the cell to maintain a given voltage and current without undesirable drift. The curves relating to fuel-cell performance were plotted as straight lines connecting the data points for the single-fin set of electrodes to indicate the stochastic nature of the data. Figures 4.4.5 through 4.4.8 demonstrate clearly that increasing temperature causes an improvement in fuel-cell performance.

An attempt was made to repeat the above experiments, using non-catalyzed nickel-fin electrodes. No fuel-cell operation of any consequence was noted for the unactivated electrodes within the environmental pressure and temperature limits of the cell. The results of the experiments run on the activated electrodes, however, clearly demonstrates the finned electrode approach to fuel-cell design can produce fuel-cell action.

Initial tests on the diamond-lattice electrode structure shown in Figure 4.2.11 were performed on solid electrodes which were fabricated from 3/8-inch nickel stock. Each electrode was ten square inches in area, and no catalyst was applied to the electrodes. No appreciable fuel-cell action was observed until the environmental temperature rose about 290°F, and a rather dramatic improvement in cell characteristics

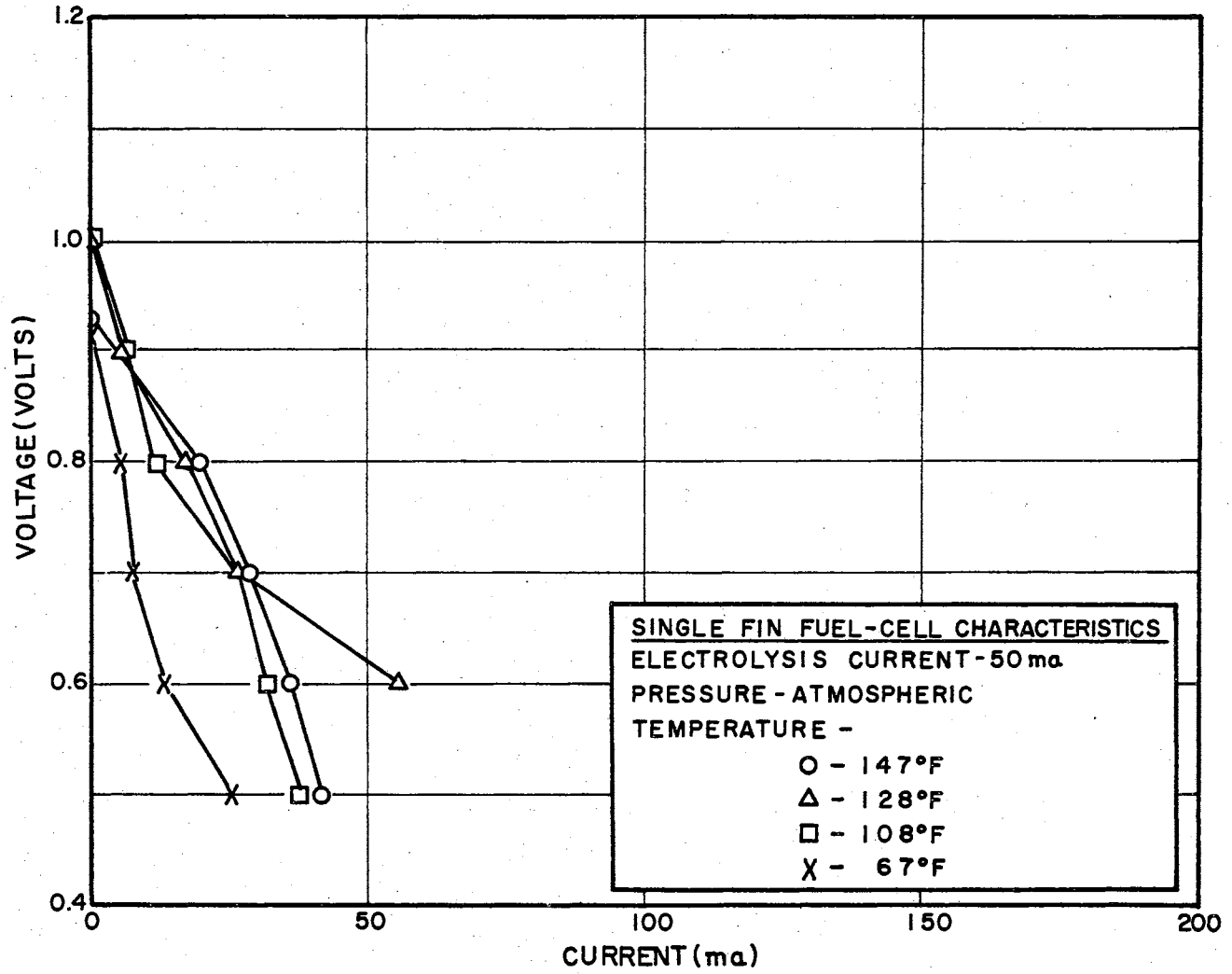

Figure 4.4.1. Effect of Temperature on the Fuel-Cell Characteristics of Activated-Nickel, Single-Fin Electrodes at Atmospheric Pressure

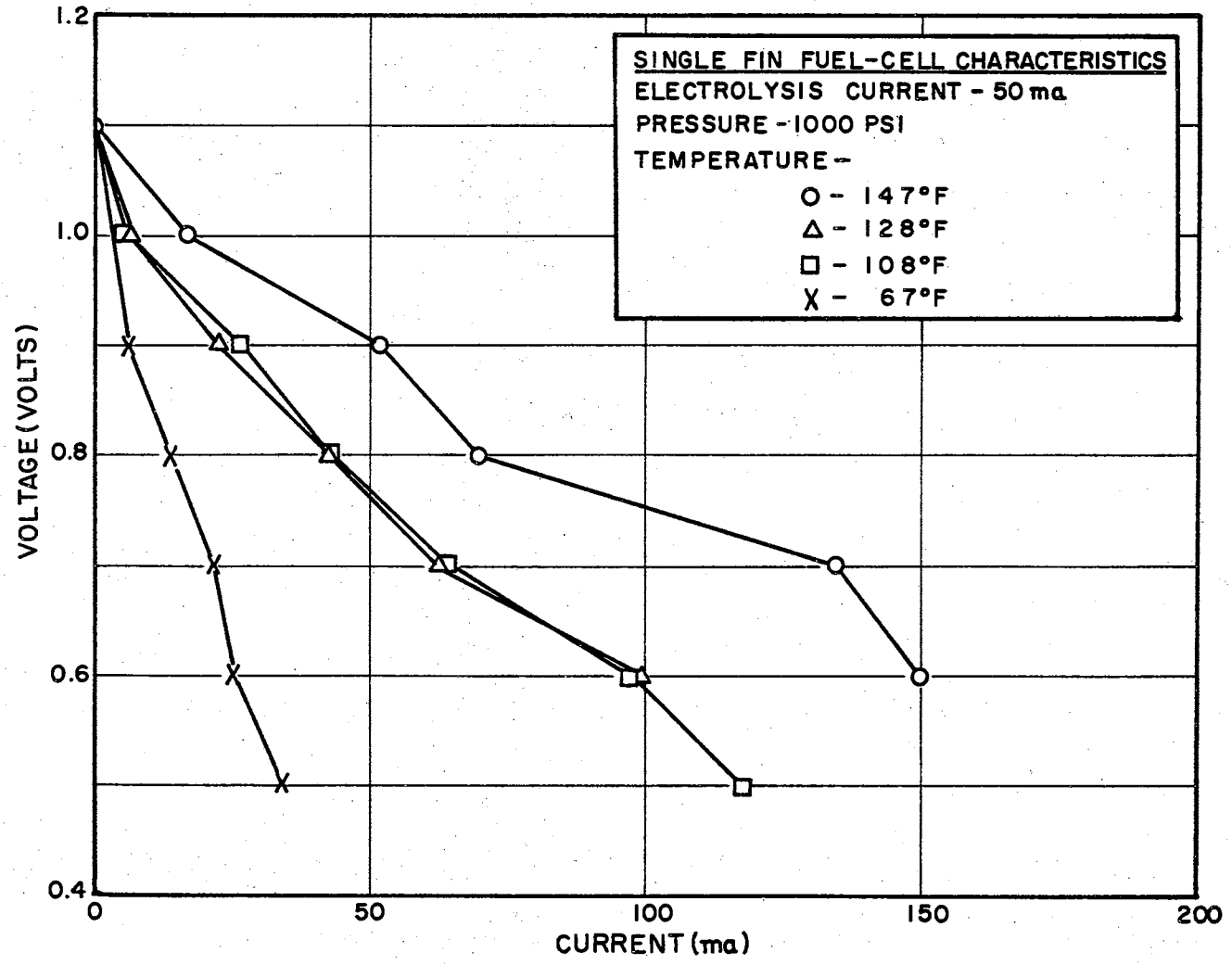

Figure 4.4.2. Effect of Temperature on the Fuel-Cell Characteristics of Activated-Nickel, Single-Fin Electrodes at 1,000 psi

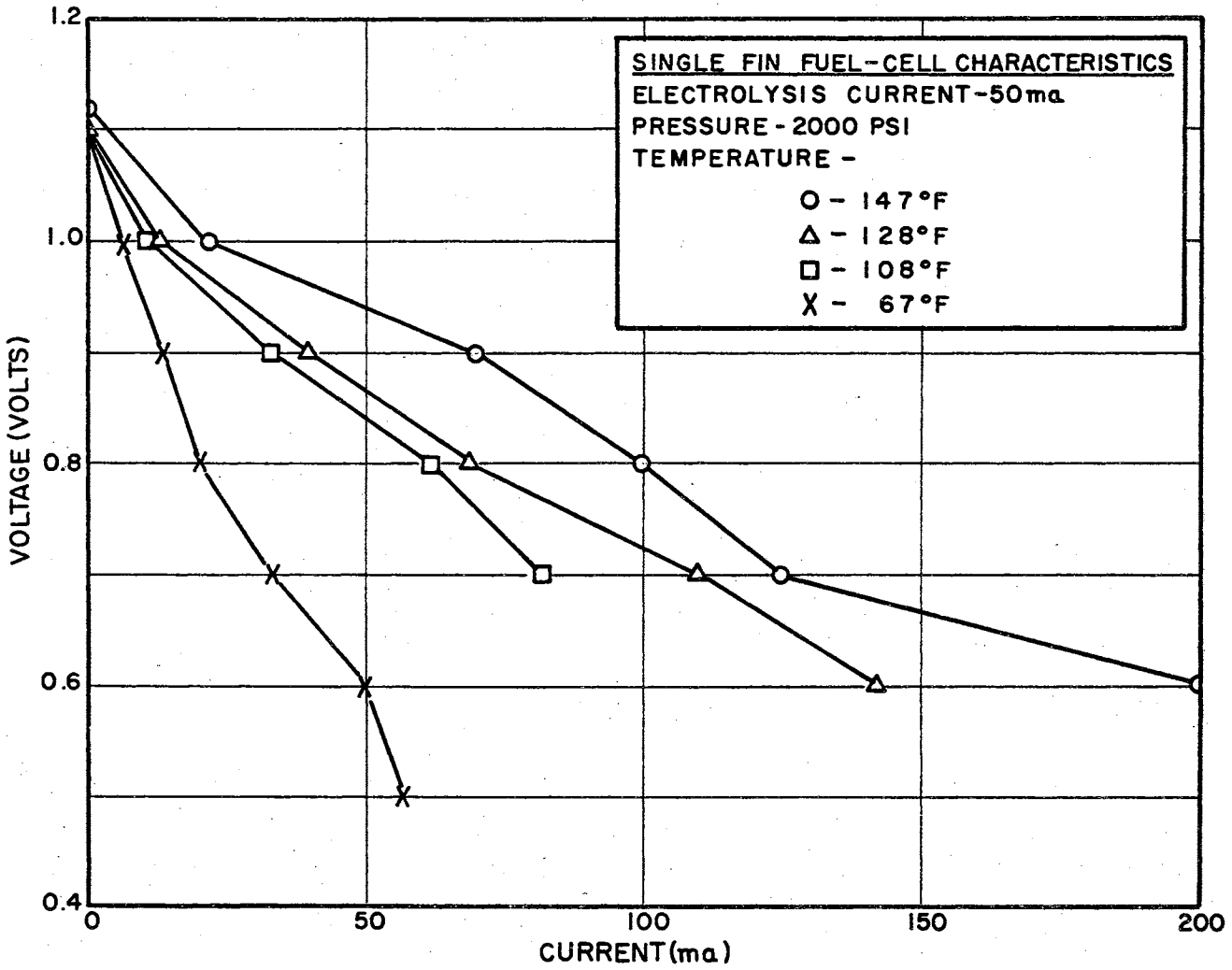

Figure 4.4.3. Effect of Temperature on the Fuel-Cell Characteristics of Activated-Nickel, Single-Fin Electrodes at 2,000 psi

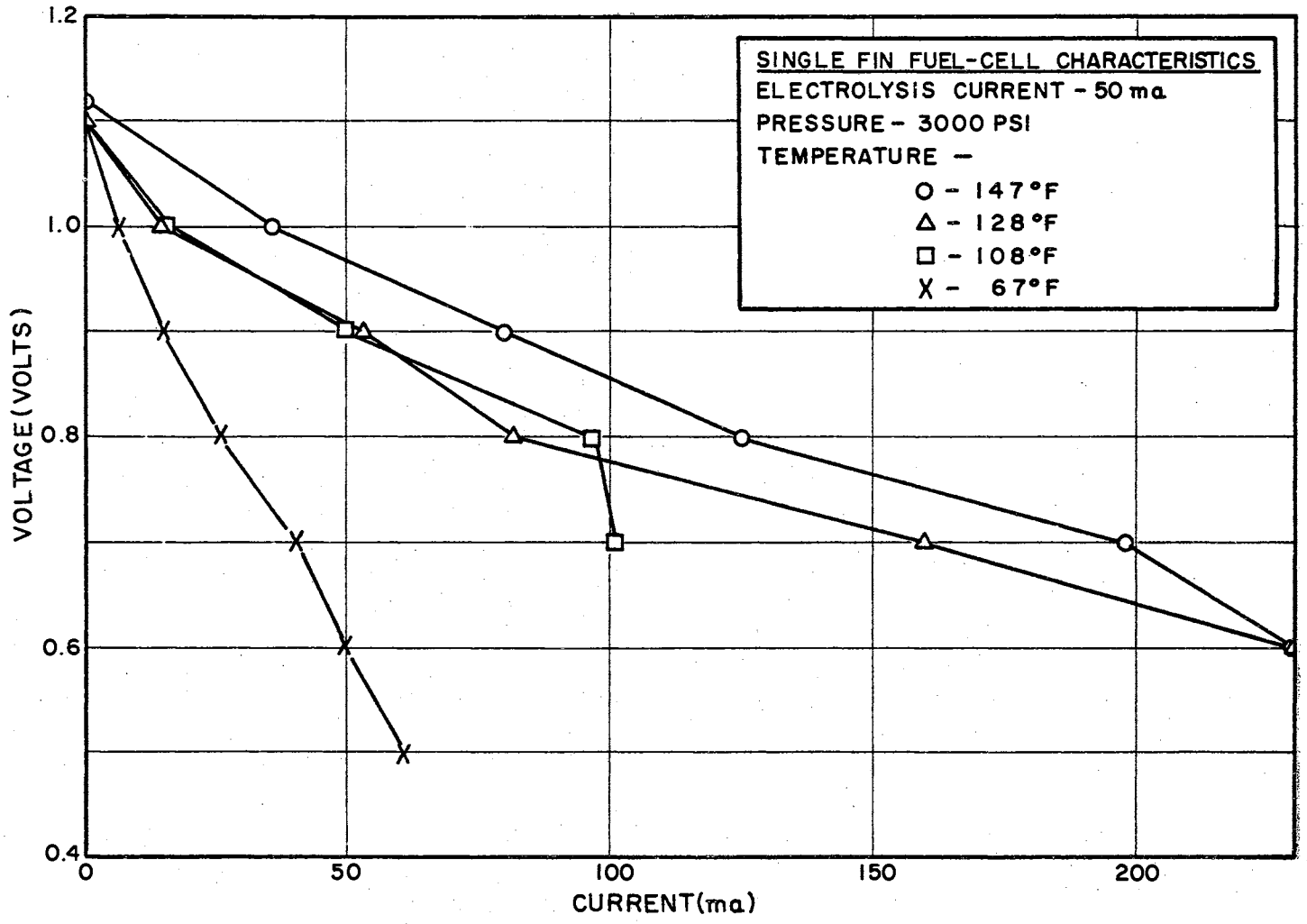

Figure 4.4.4. Effect of Temperature on the Fuel-Cell Characteristics of Activated-Nickel, Single-Fin Electrodes at 3,000 psi

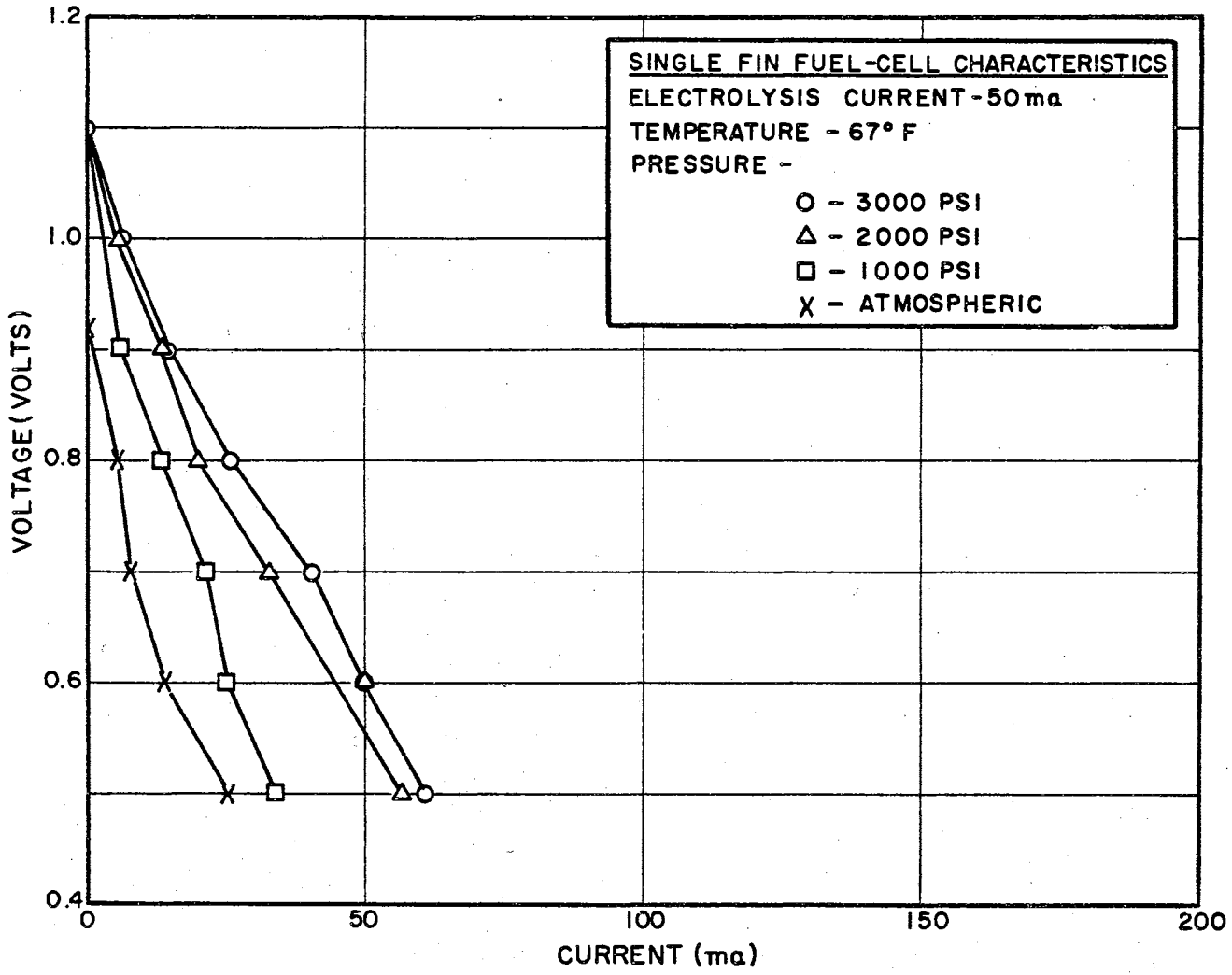

Figure 4.4.5. Effect of Pressure on the Fuel-Cell Characteristics of Activated-Nickel, Single-Fin Electrodes at 67°F

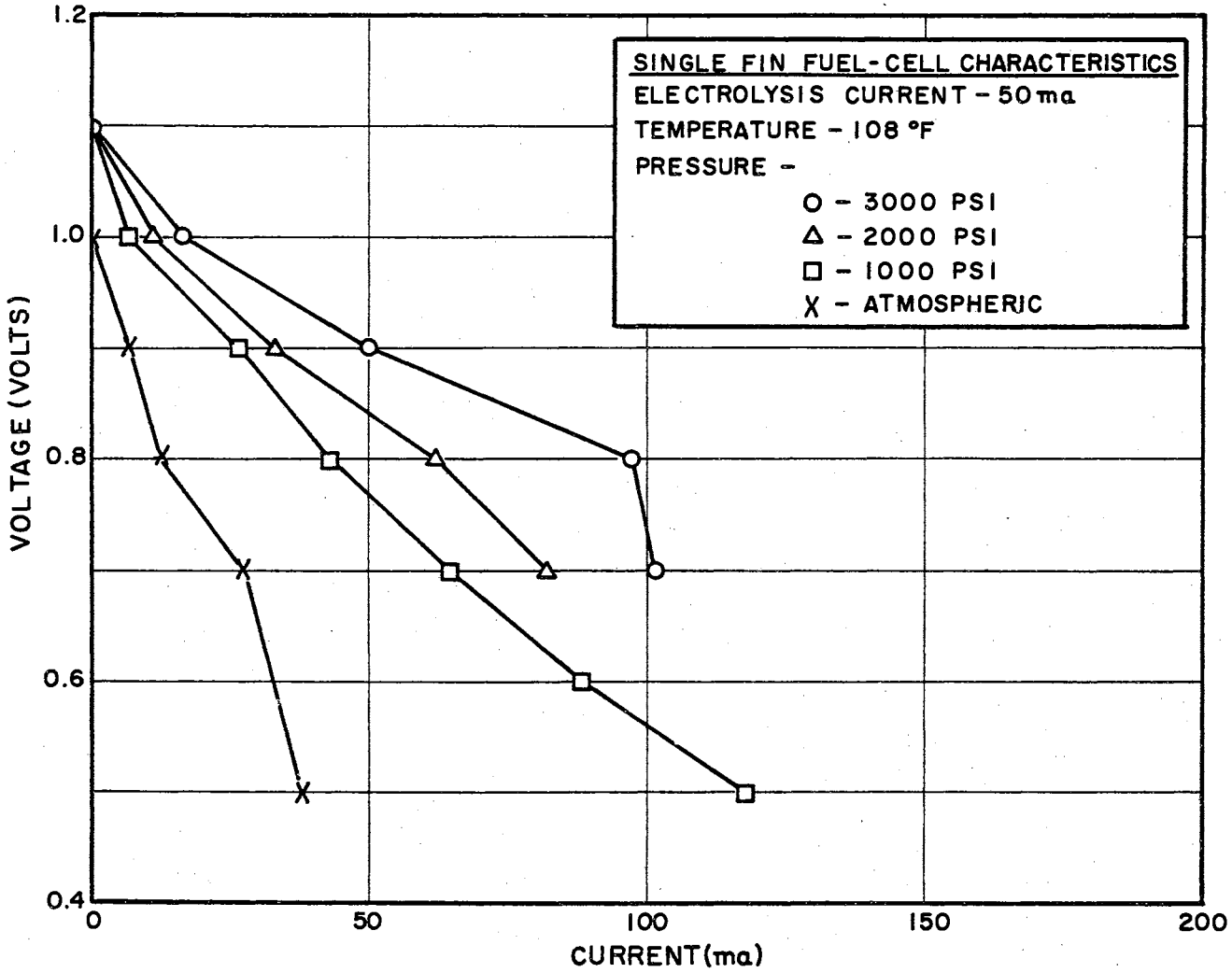

Figure 4.4.6. Effect of Pressure on the Fuel-Cell Characteristics of Activated-Nickel, Single-Fin Electrodes at 108°F

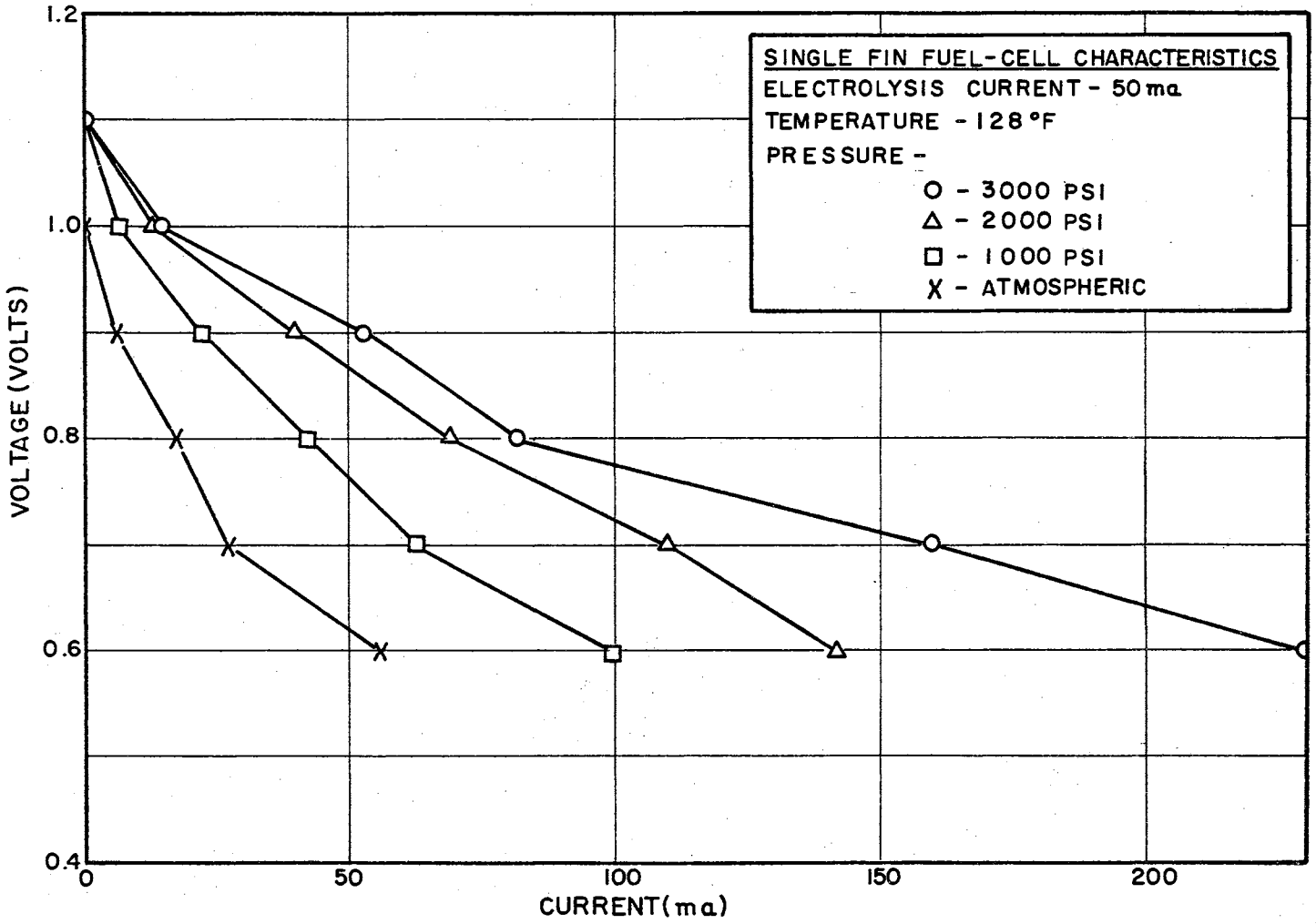

Figure 4.4.7. Effect of Pressure on the Fuel-Cell Characteristics of Activated-Nickel, Single-Fin Electrodes at 128°F

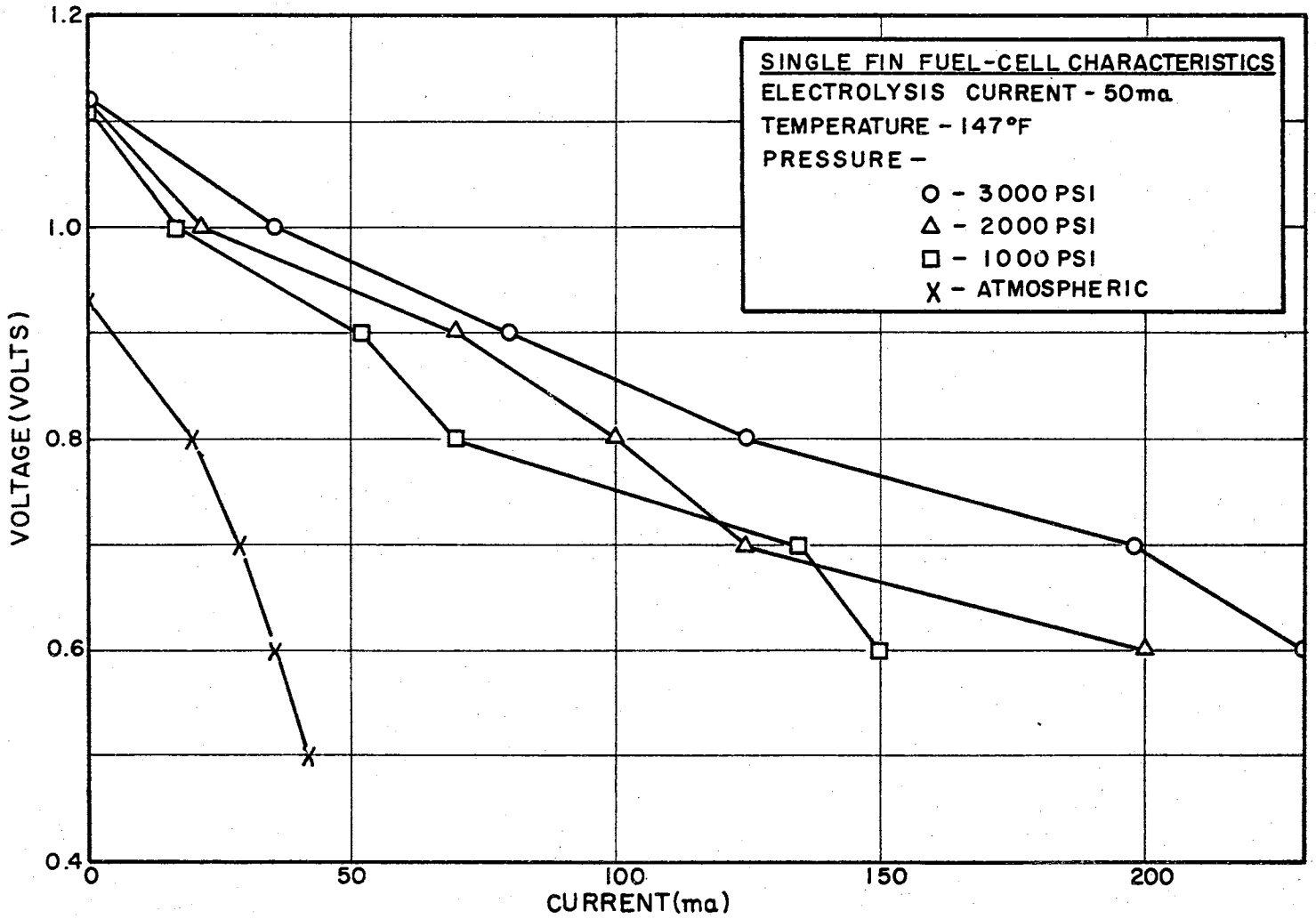

Figure 4.4.8. Effect of Pressure on the Fuel-Cell Characteristics of Activated-Nickel, Single-Fin Electrodes at 147°F

occurred above that temperature.

It is interesting to observe that the diamond-lattice approach to fuel-cell electrode design does not require porous electrodes to produce the desired reaction. The data plotted as Figure 4.4.9 indicates that a current density equivalent to 14 amperes per square foot at 0.7 volts is observed for this configuration when the electrode material is solid nickel which has been etched by concentrated nitric acid. The current density of 14 amperes can undoubtedly be increased by a refinement in the diamond-lattice structure. However, the use of porous material for the diamond-lattice electrode can give one the advantages of a porous electrode without the disadvantages discussed in Chapter III.

Justi (8) and others have noted that porous electrodes made from Raney Nickel contain large amounts of highly reactive hydrogen and oxygen, up to 1.1 protons per nickel-catalyst atom. Thus, in addition to the increased number of active sites made possible through the use of porous electrodes, one can also realize the advantage of having a cell which can continue for a relatively long time to supply electricity, even if the gas supply is temporarily interrupted.

A set of diamond-lattice electrodes fabricated from General Electric Foammetal--a type of porous nickel--was constructed to allow a comparison to be made between the solid and the porous electrodes. The Foammetal set of electrodes produced a current density equivalent to 140 amperes per square foot at 0.7 volts, as is shown in Figure 4.4.10. This figure is appreciably higher than the data previously quoted for the solid-nickel electrode. Further, the current output of the Foammetal electrodes persisted for as long as five minutes after the

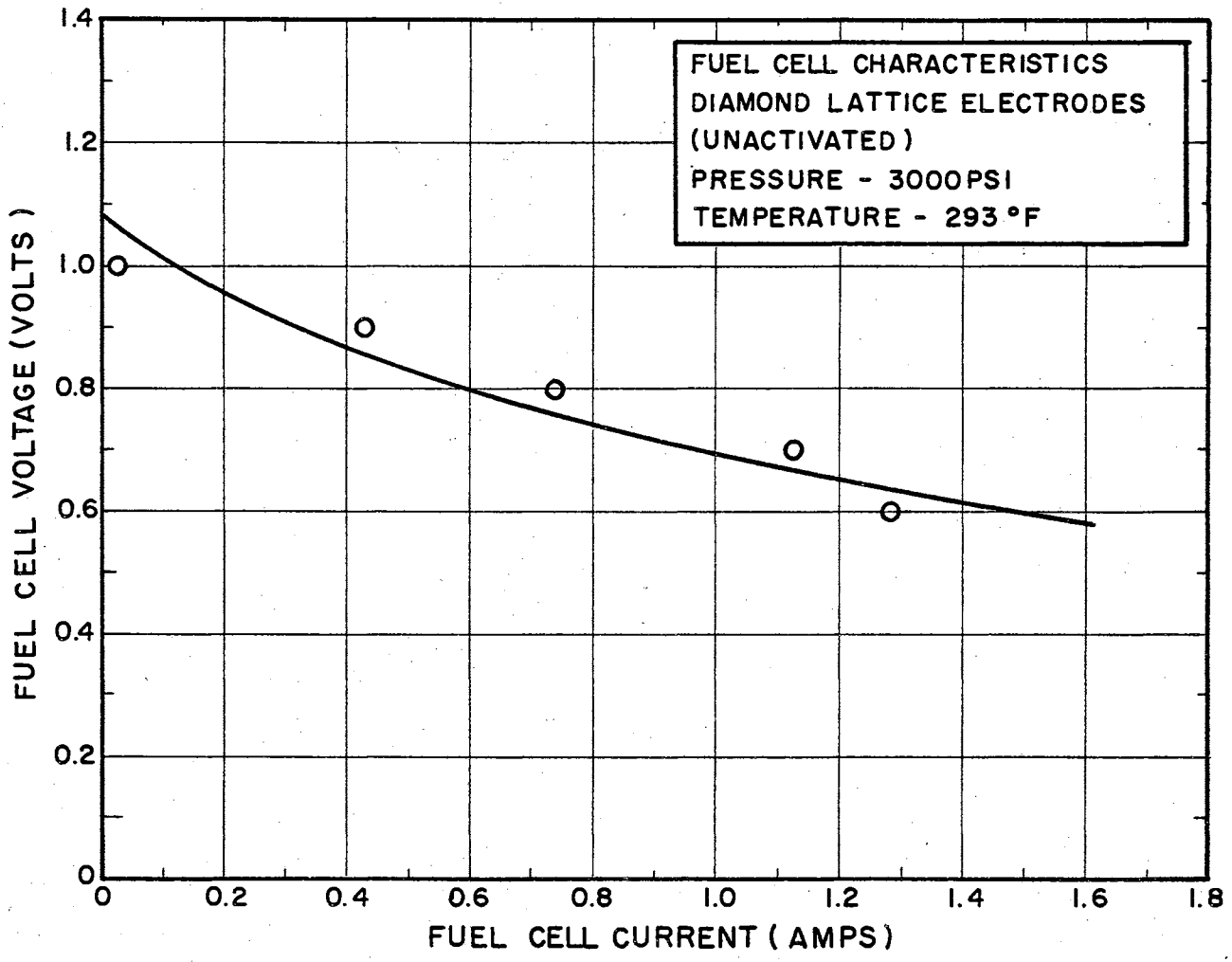

Figure 4.4.9. Fuel-Cell Characteristics of Unactivated, Solid-Nickel Electrodes With Diamond-Lattice Structure at 293°F and 3,000 psi

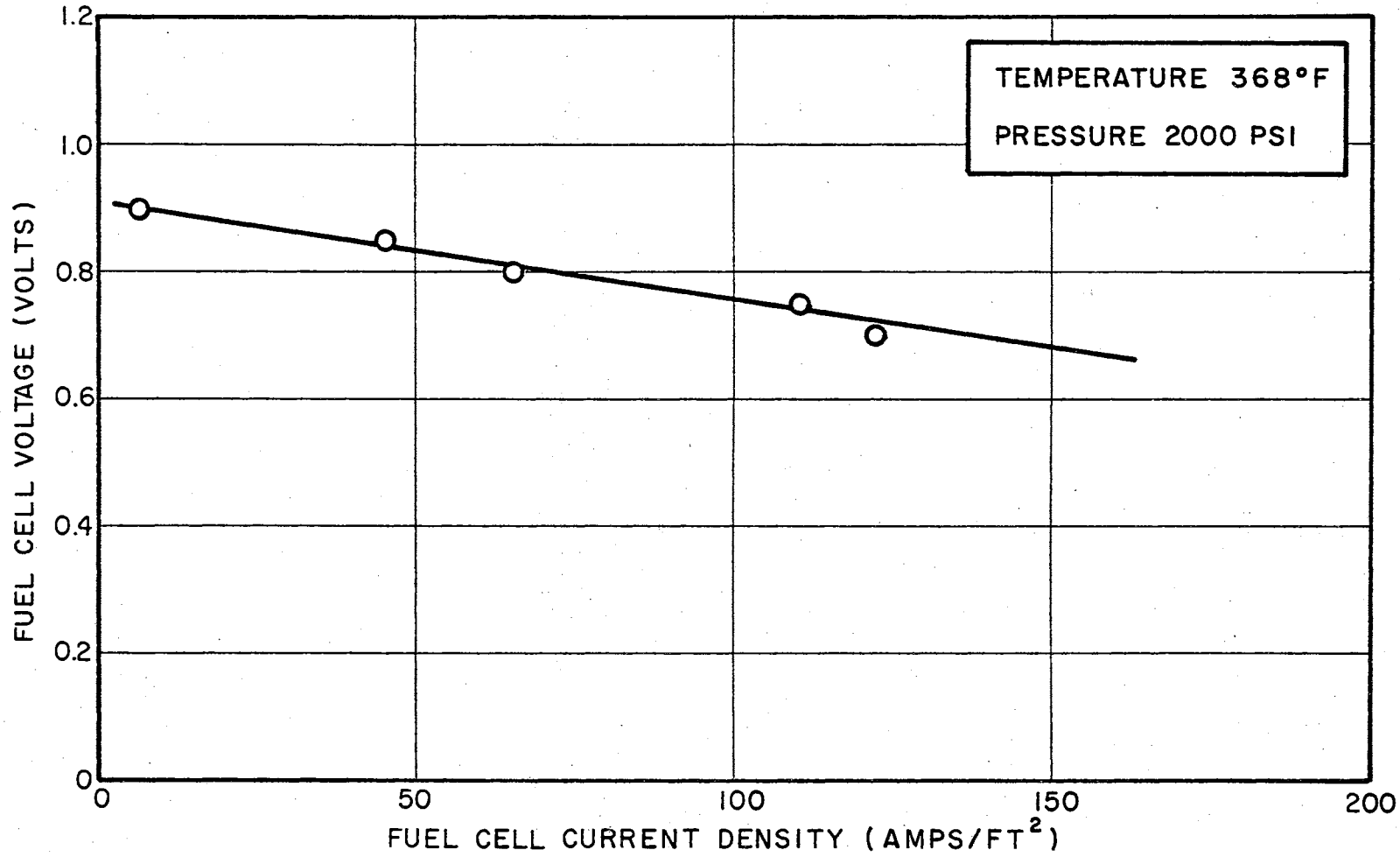

Figure 4.4.10. Fuel-Cell Characteristics of Foammetal-Nickel Electrodes With Diamond-Lattice Structure at 368°F and 2,000 psi

gas supply was interrupted. The current output of the solid electrodes, on the other hand, dropped in a few seconds following the interruption of the gas supply.

Voltage versus current curves for the Foammetal cell are plotted as a function of pressure and temperature in Figures 4.4.11 through 4.4.17 of this thesis. It is again apparent from these figures that the output characteristics of the cell are enhanced by both pressure and temperature.

As shown in the preceding figures, the diamond-lattice fuel-cell electrode structure is capable of producing appreciable values of current. Unfortunately, the Foammetal material proved to be unable to withstand the high-pressure, high-temperature environmental parameters of the fuel-cell system. The electrodes disintegrated very rapidly in the cell environment.

Two new types of porous electrode materials were obtained in an attempt to find an electrode with the corrosion-resistance characteristics of solid nickel and the current-density characteristics of porous materials. Each of the new electrode materials was fabricated from finely divided nickel powder which was sintered into plates one-eighth-inch thick. Material assigned the type number D differed from material type B in that material D contained a fine mesh nickel screen to give a degree of structural integrity to the electrodes.

Tests run on the electrodes made of these materials proved that both had excellent resistance to the corrosive aspects of the cell environment. However, each material exhibited an undesirable polarization characteristic which made them have voltage versus current characteristics which were inferior to the Foammetal electrodes. Data plotted

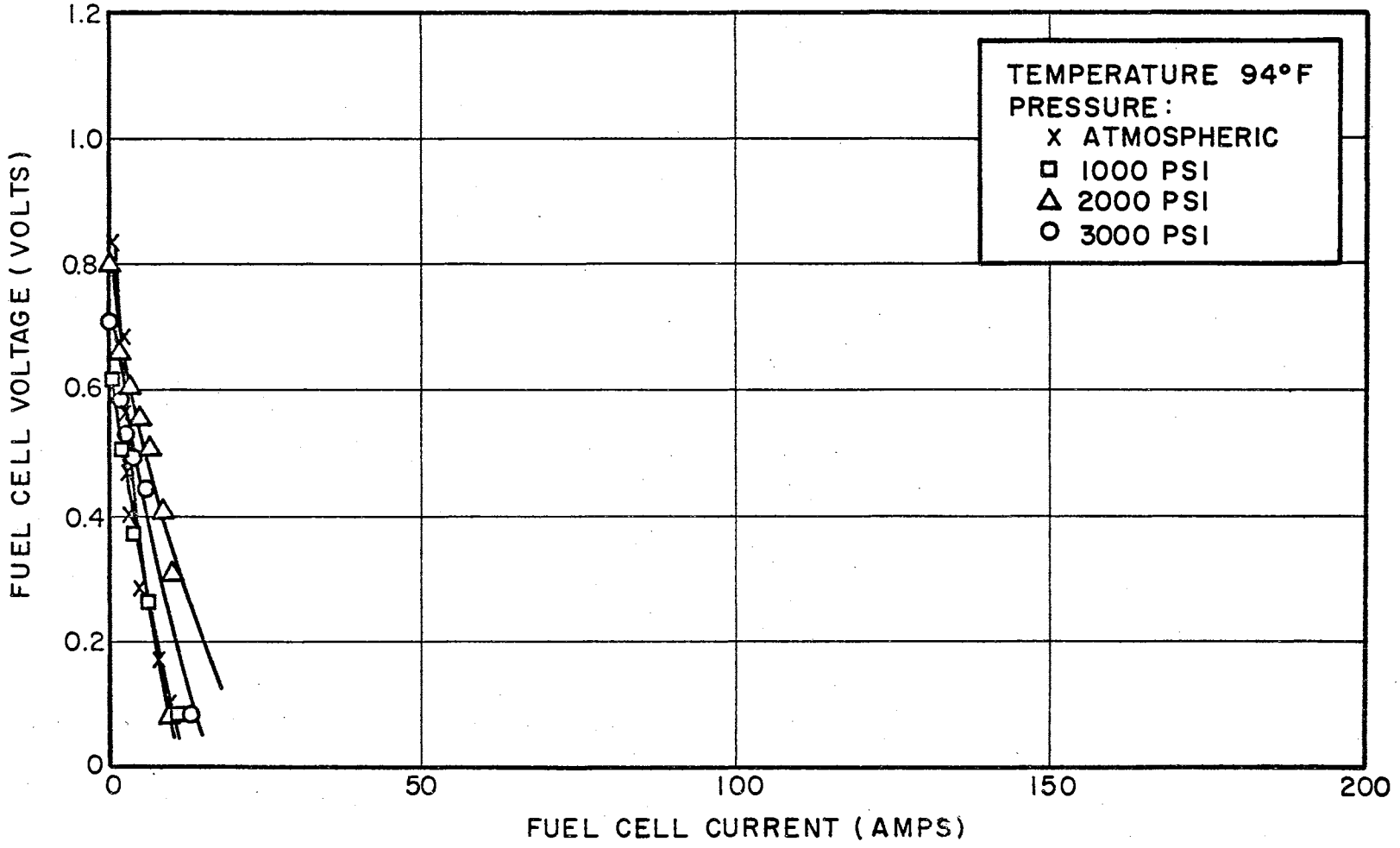

Figure 4.4.11. Effect of Pressure on the Fuel-Cell Characteristics of Foammetal-Nickel Electrodes With Diamond-Lattice Structure at 94°F

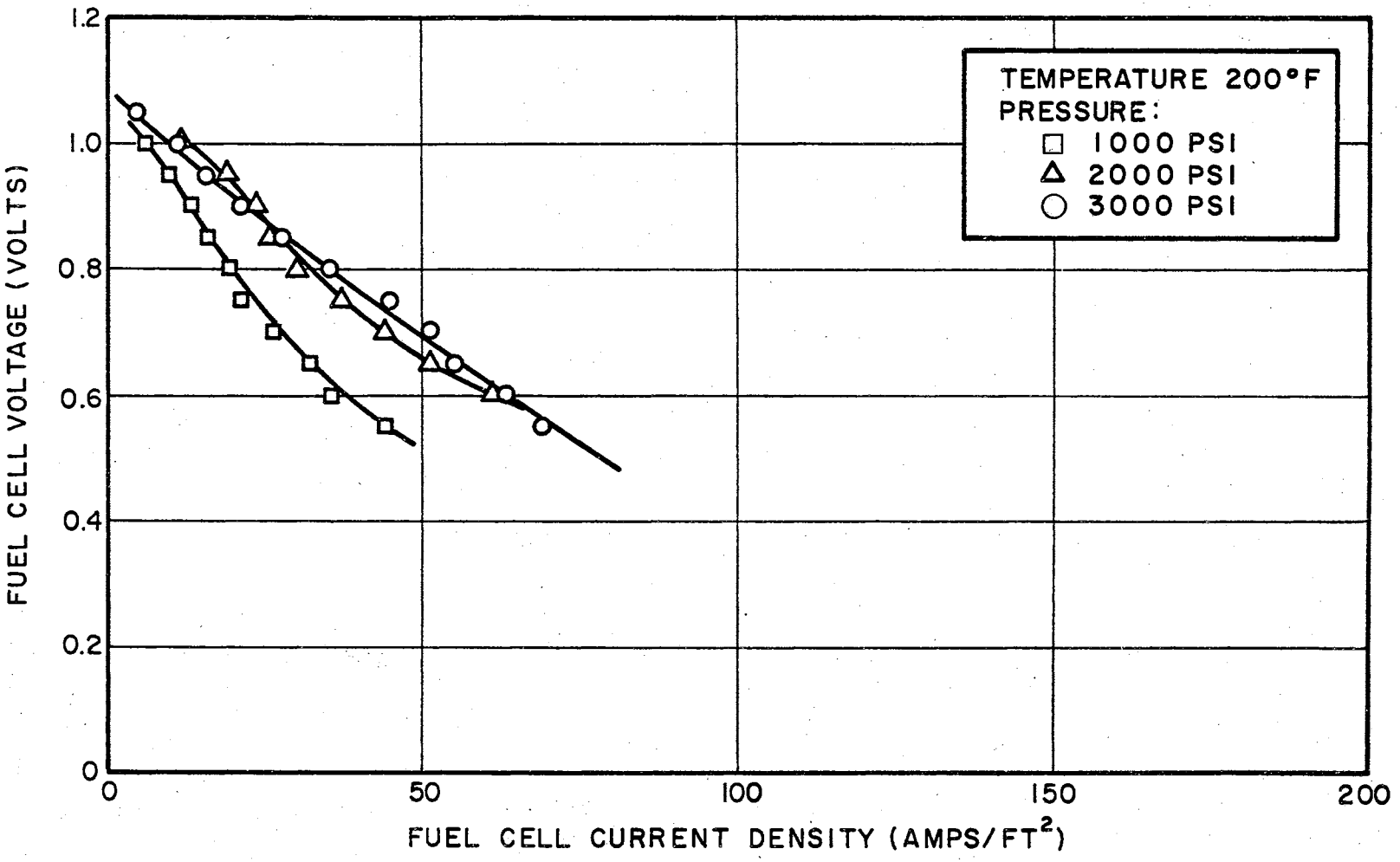

Figure 4.4.12. Effect of Pressure on the Fuel-Cell Characteristics of Foammetal-Nickel Electrodes With Diamond-Lattice Structure at 200°F

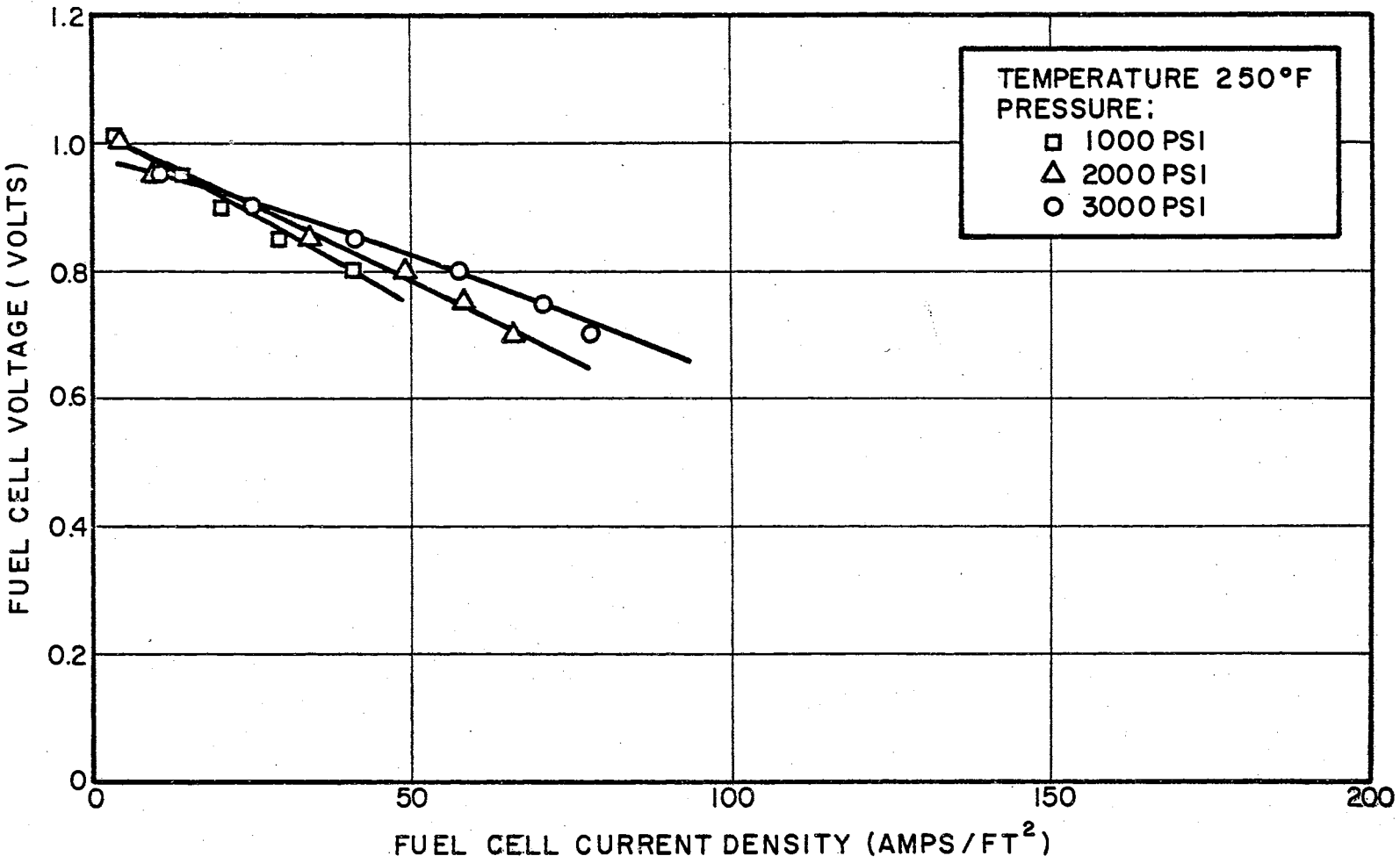

Figure 4.4.13. Effect of Pressure on the Fuel-Cell Characteristics of Foammetal-Nickel Electrode With Diamond-Lattice Structure at 250°F

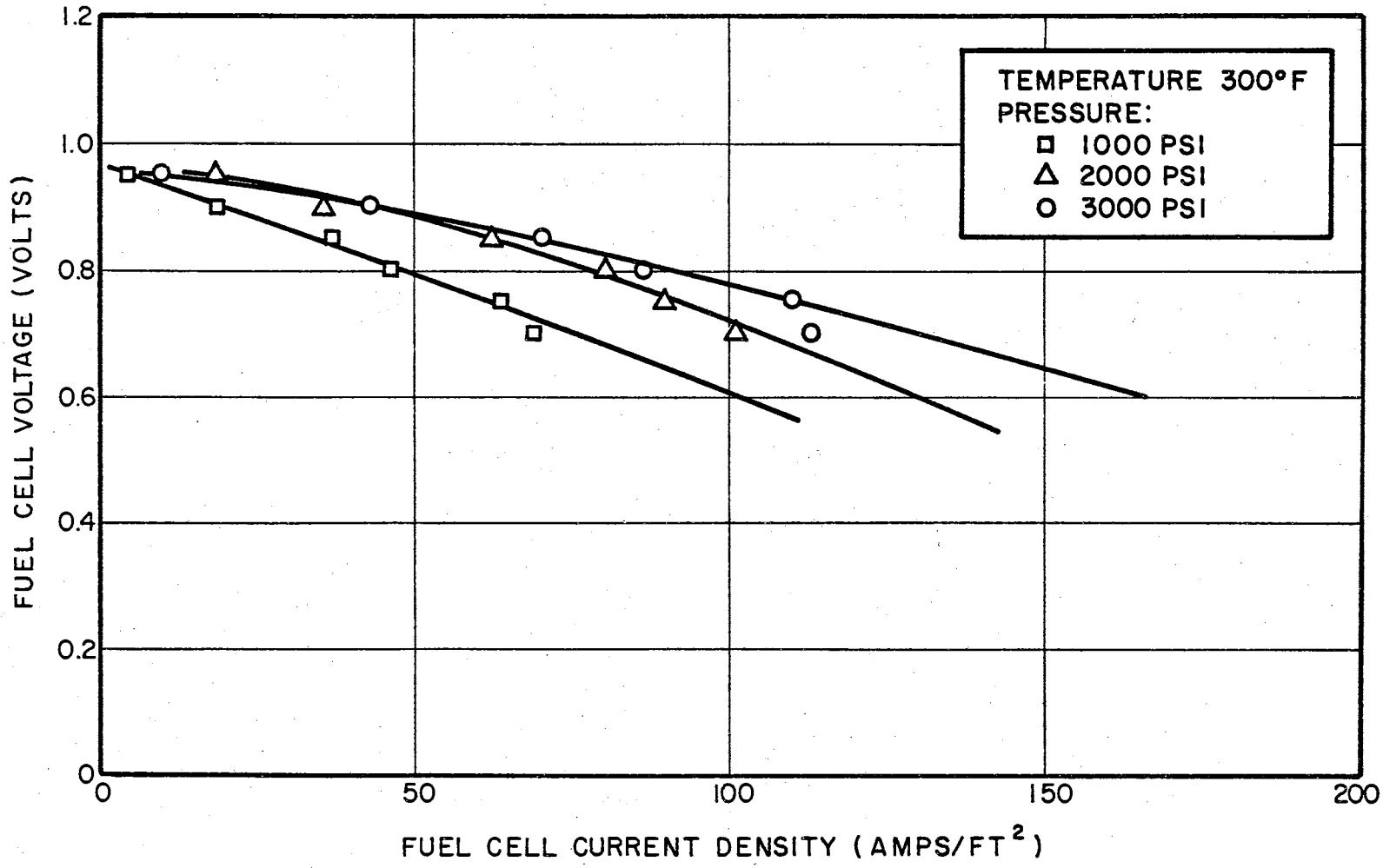

Figure 4.4.14. Effect of Pressure on the Fuel-Cell Characteristics of Foammetal-Nickel Electrodes With Diamond-Lattice Structure at 300°F

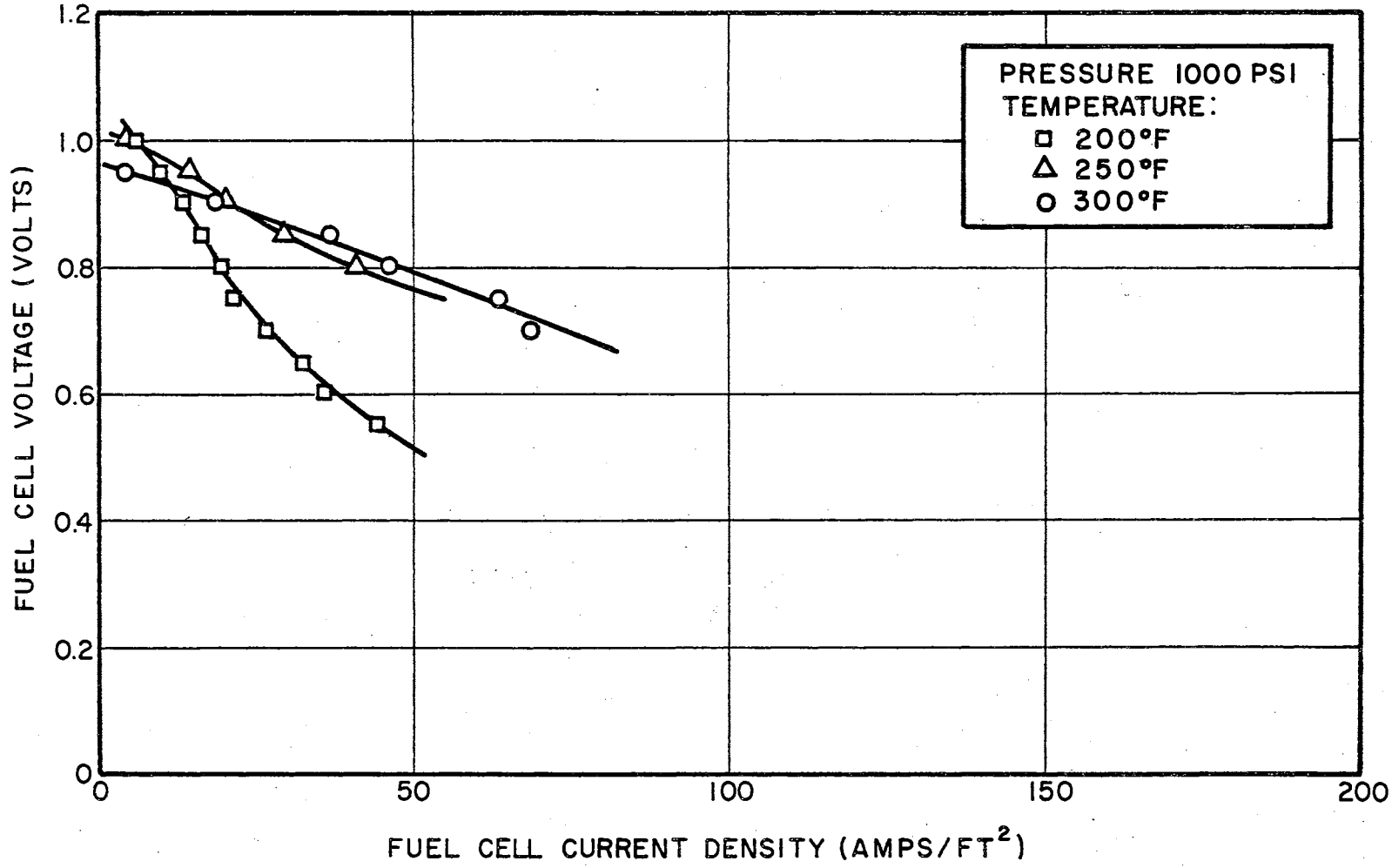

Figure 4.4.15. Effect of Temperature on the Fuel-Cell Characteristics of Foammetal-Nickel Electrodes With Diamond-Lattice Structure at 1,000 psi

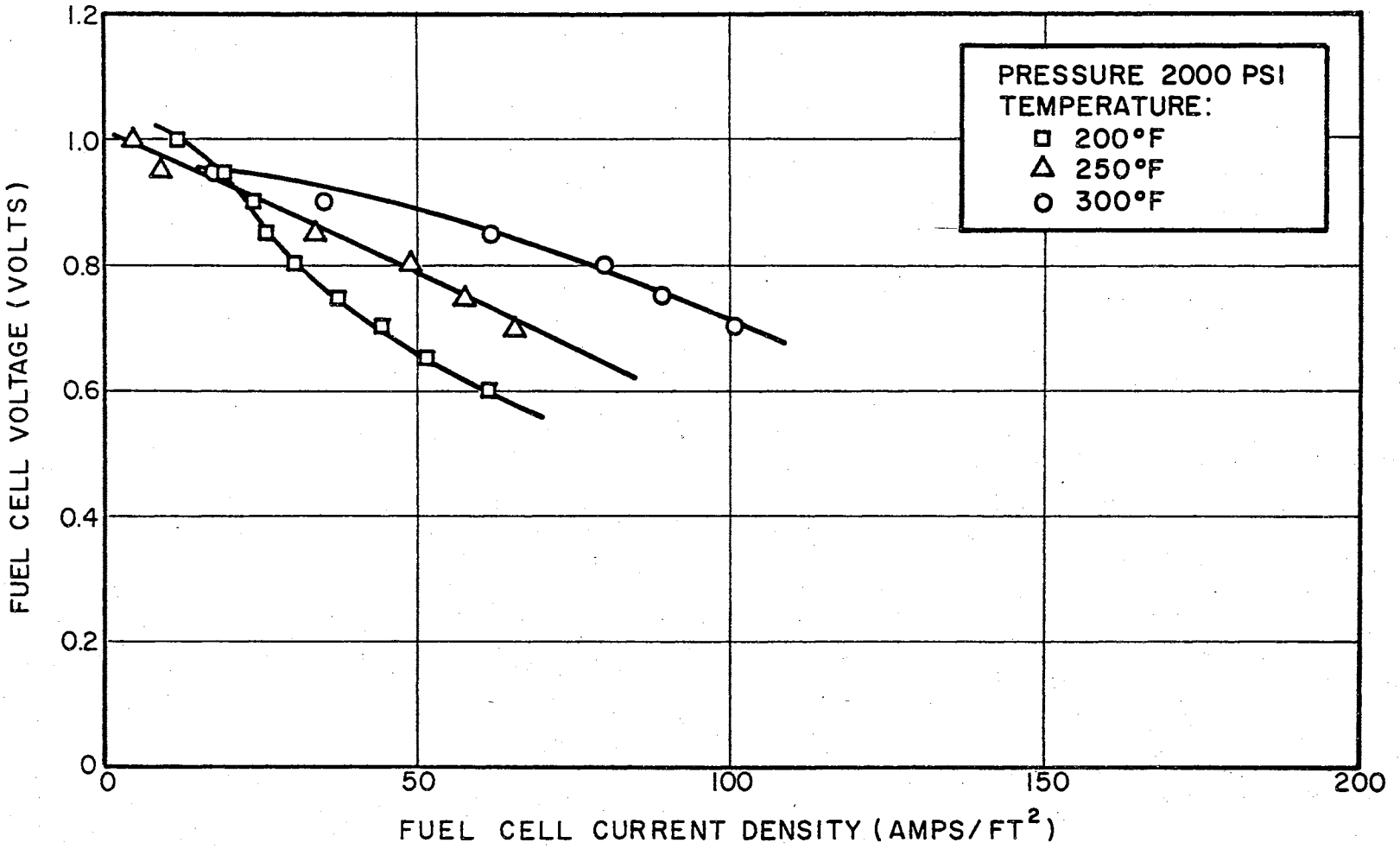

Figure 4.4.16. Effect of Temperature on the Fuel-Cell Characteristics of Foammetal-Nickel Electrodes With Diamond-Lattice Structure at 2,000 psi

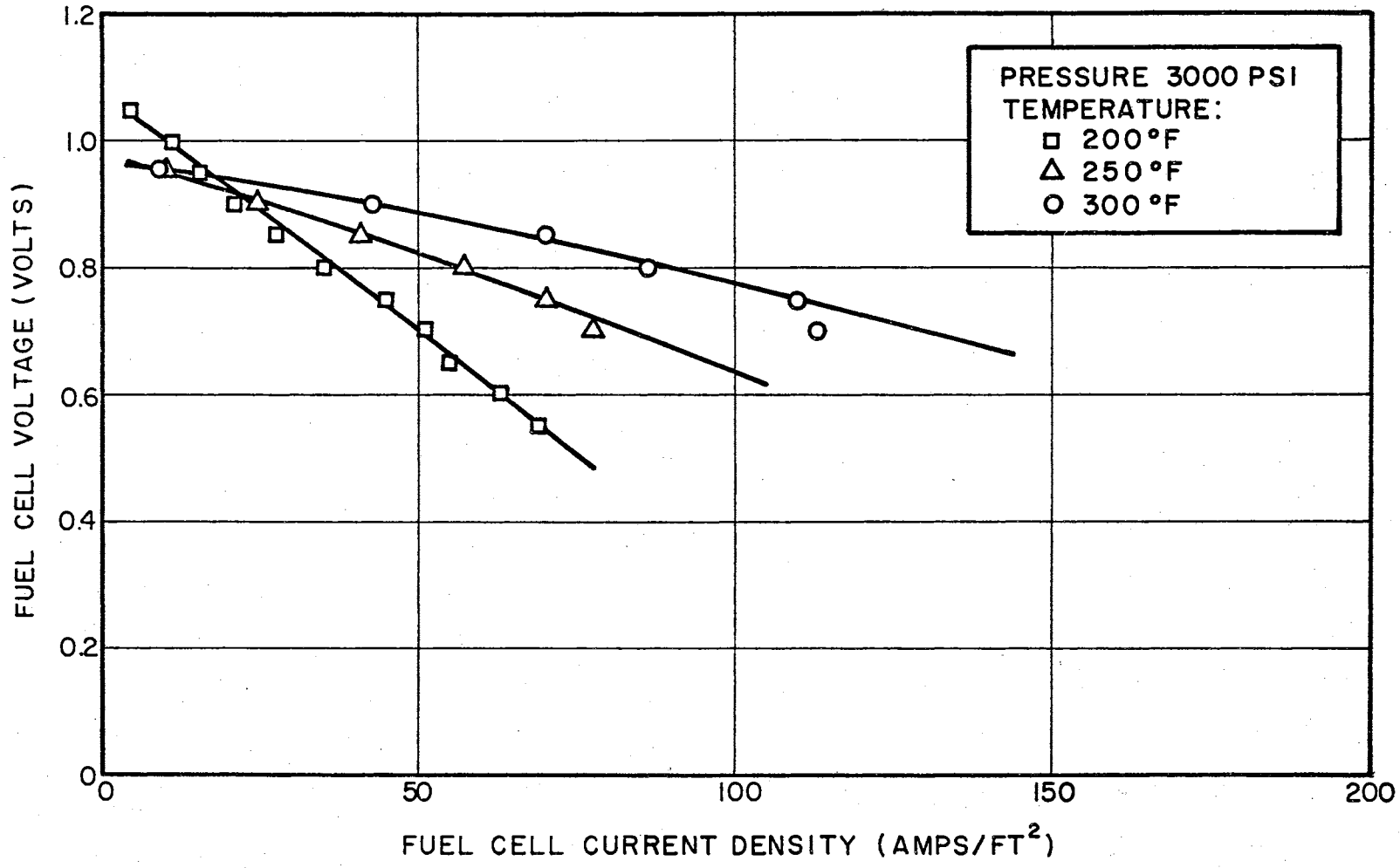

Figure 4.4.17. Effect of Temperature on the Fuel-Cell Characteristics of Foammetal-Nickel Electrodes With Diamond-Lattice Structure at 3,000 psi

in Figures 4.4.18 and 4.4.19 indicates that the electrodes fabricated from the new material exhibited a conventional voltage versus current relationship which was reduced in value by a 0.2 to 0.4 polarization voltage for a given value of current. Material B had a maximum current density of 26 amperes per square foot; and material D exhibited a maximum current density of 44 amperes per square foot, referred to a standard voltage of 0.7 volts per cell.

A modification of the diamond-lattice electrode configuration which might improve the manifold system of this type of structure and increase the number of active sites available for the cell reaction is the spiral electrode structure shown in Figure 3.3.4. Tests were run on the cell shown in the figure at an environmental pressure and temperature of 3,000 psi and 400°F, respectively. No catalyst was applied to the electrodes, which were fabricated from pure nickel cylinders then etched in a concentrated nitric acid solution.

The space between the electrodes was made extremely small so that a thin, porous teflon membrane could be used to keep the fuel and oxidizing gases separated. The data published by the manufacturer of these membranes indicated that they were markedly superior to the asbestos membrane used in most fuel cells in that the voltage drop in the teflon membranes was predicted to be less than ten percent of the drop associated with conventional asbestos membranes.

Unfortunately, the teflon membranes had a tendency to shrink when immersed in 25 percent potassium hydroxide and subjected to the high-pressure, high-temperature environment of the cell. A total of ten tests were run on the spiral electrode structure, utilizing three different types of teflon membrane. The result of each experiment was

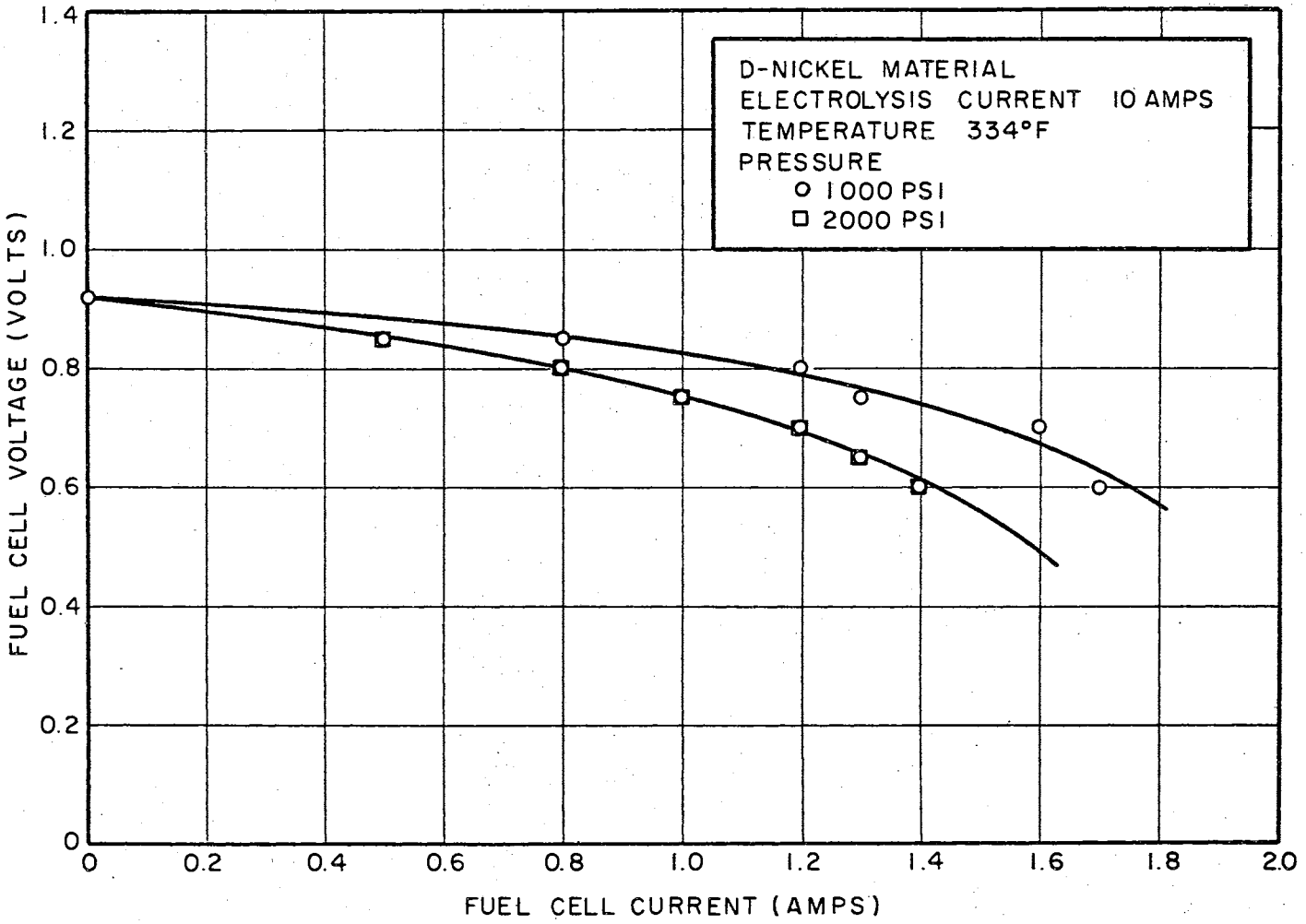

Figure 4.4.18. Fuel-Cell Characteristics of Diamond-Lattice Electrodes Using Sintered-Nickel Powder Containing a Fine Mesh Nickel Screen

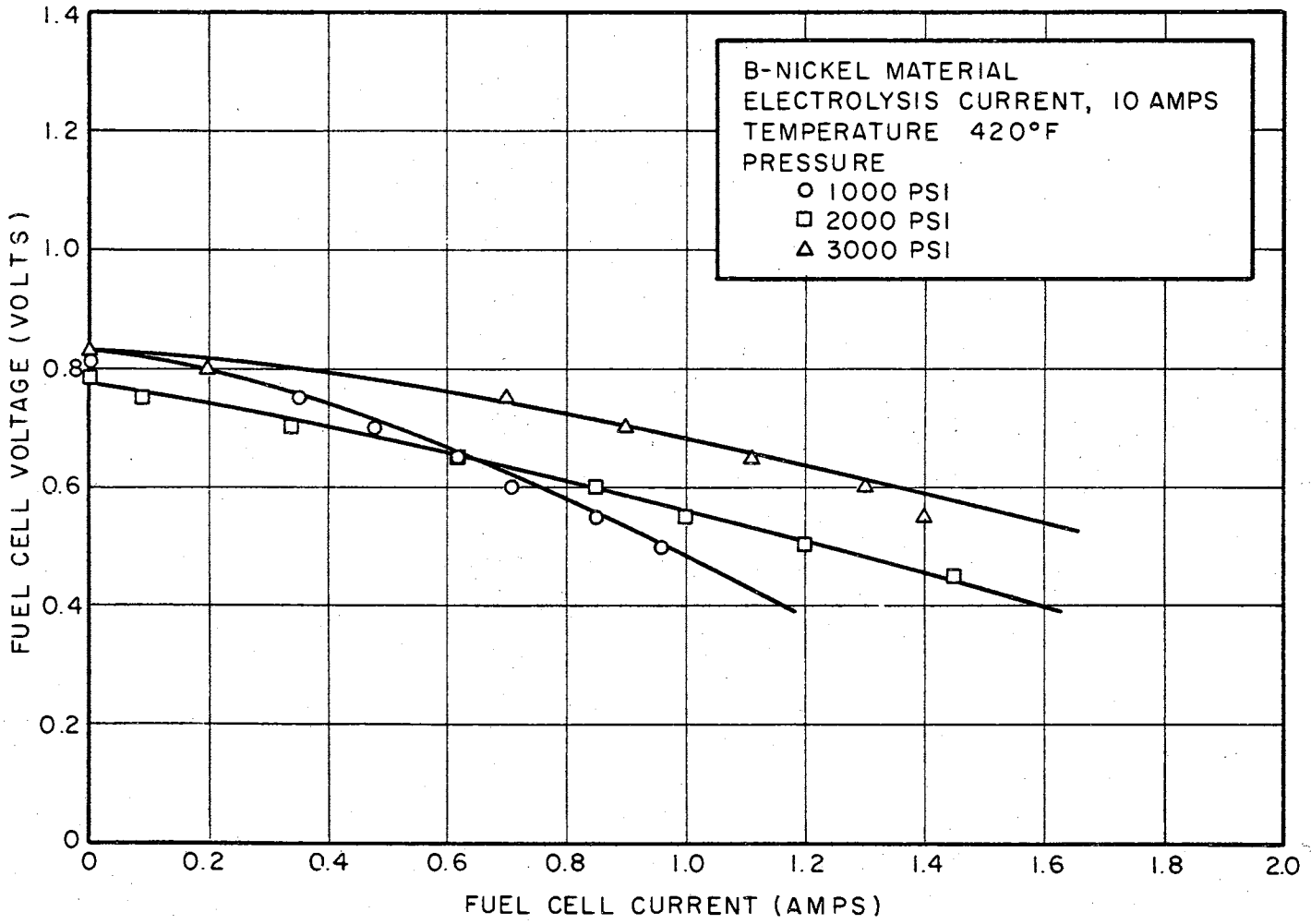

Figure 4.4.19. Fuel-Cell Characteristics of Diamond-Lattice Electrodes Fabricated From Sintered-Nickel Powder

the same--the membrane would tear and allow the fuel and oxidizing gases to mix before a complete set of data could be taken. The damaged membranes were sent to the manufacturer for further study.

The asbestos membrane used in the conventional fuel cells manufactured by Allis Chalmers was also found to be unsatisfactory in the spiral electrode fuel cell. Tests proved that this type of membrane swells when it absorbs potassium hydroxide. The expanding membrane filled the manifold of the spiral electrode cell and thus cut off the flow of gas to the active sites of the cell electrodes. In spite of the difficulties associated with the spiral electrode approach to fuel-cell design, information concerning such a cell is included in this thesis to show that the search for an optimum manifolding structure is not completed and that alternate structures should be examined.

CHAPTER V

SUMMARY AND CONCLUSIONS

5.1 Summary. This thesis consists of an analysis of the characteristics of high-pressure, high-temperature electrolysis cells and fuel cells. In Chapter II the basic theory of the hydrogen-oxygen reaction was summarized with emphasis given to the effects of pressure and temperature on cell performance, polarization characteristics of the cells, and the reversible voltage values associated with the reaction. In Chapter III the various problems related to the operation of fuel cells and electrolysis cells at high temperature and pressure are listed, and an alternate electrode structure is suggested as a possible means of surmounting these problems. The theoretical treatment, based on the technique of conformal transformations, which led to the "finned" electrode approach to cell design, is introduced in Chapter III and is documented in detail in Appendix B. In Chapter IV, experimental evidence supporting this new approach to hydrogen-oxygen fuel-cell and electrolysis-cell design is presented.

5.2 Conclusions. A fuel cell or an electrolysis cell which is operated at high pressures and temperatures is capable of having characteristics which are superior to similar cells which operate at lower pressures and temperatures. The various problems associated with operating such cells at high pressures and temperatures, however, must be

solved before they can be considered as economical and practical engineering devices.

The analysis presented in this thesis shows that a conformal transformation of parallel-plate electrodes can lead to a set of finned electrodes which have electrostatic characteristics mathematically related to the parallel-plate electrodes. Engineering modifications of the basic finned set has lead to the development of fuel-cell and electrolysis cell electrodes which have interesting engineering parameters. The electrolysis-cell electrodes which resulted from this analysis have energy density and efficiency characteristics which are superior to conventional electrolysis cells. The primary significance of the finned electrode approach to fuel-cell design is that it eliminates the interface problems associated with conventional high-pressure cells.

5.3 Recommendations for Further Study. The experimental facility which was used to accumulate data on the electrolysis-cell and fuel-cell electrodes developed in this study was limited to environmental pressures and temperatures of 3,000 psi and 450°F, respectively. This physical limitation confined the search for an optimum pressure and temperature environment for fuel-cell and electrolysis action to these upper limits. Environmental pressure and temperature facilities should be constructed which will allow the search for an optimum pressure and temperature environment to be extended to much higher ranges of pressures and temperatures. A further disadvantage of the environmental test facility used in this study is that it was the only facility of its kind available, and literally hundreds of tests had to be performed. This limitation of facilities made it impossible for extensive life

tests to be run on any of the electrolysis-cell or fuel-cell configurations which were examined. As a consequence, no information concerning the longevity of the electrodes in the extremely corrosive environmental conditions imposed by concentrated potassium hydroxide, high pressure, and high temperature. Such life tests must be run before any of the electrode structures can be given real engineering significance.

As a consequence of the lack of an environmental test facility which could be used to conduct life-test studies, the phenomena of hydrogen embrittlement, which other researchers have observed in high-pressure, high-temperature facilities which contain hydrogen, did not occur. Hydrogen embrittlement is believed to occur in fuel-cell and electrolysis-cell pressure chambers because of the highly reactive nature of the nascent hydrogen which is a part of the cell reaction. This nascent hydrogen can pass along the grain boundaries of the stainless steel environmental chamber until it reaches the oxides and sulfides in the steel, thus causing embrittlement to occur. As a consequence of hydrogen embrittlement, pressure chambers can weaken and lose their structural integrity. The obvious explosion hazard which then occurs is one which any researcher in high-pressure, high-temperature hydrogen-oxygen fuel-cell technology should examine.

The experimental results presented in Chapter IV of this thesis on the characteristics of the diamond-lattice electrode structure showed that this type of electrode can produce fuel-cell action. However, it was also clear that the materials used in the experimental examination were not optimum. Further, it was also observed that the manifolding character of the diamond-lattice electrodes was not optimized. More work should be devoted to the solution of these problems. The spiral,

cylindrical approach to cell design should also be subjected to further analysis.

The energy density characteristics and the polarization parameters of the fuel-cell electrodes examined in this study could undoubtedly be improved if the proper catalyst could be found. A concentrated effort should be devoted to this area of research. It should be noted here that the type of catalytic deposition technique used on the milled-fin electrodes developed in this study will differ greatly from the techniques employed on conventional fuel cells. The finned electrodes are essentially solid; therefore, electroplating techniques can be used to deposit catalysts on the electrode surfaces. Such techniques are not applicable to the conventional porous electrodes due to the high probability that the pores will be covered over by the plating action.

The design of the electrodes considered in this study was undertaken with the intent that they be used in an energy-storage system of the type shown in Figure 1.4.1. Such a system has not yet been constructed. Consequently, no information is available concerning the problems involved in constructing, controlling, or maintaining the various components of the system. A pilot system of the basic type shown in the system should be constructed so that these problems may be solved.

SELECTED BIBLIOGRAPHY

1. Grove, W. R. "On Voltaic Series in Combinations of Gases by Platinum." Phil. Mag. Volume 14. (1839) 127-130.

2. Grove, W. R. "On a Gaseous Voltaic Battery." Phil. Mag. Volume 21. (1842) 417-420.

3. Grove, W. R. Proc. Roy. Soc. Volume 4. (1843) 367-463.

4. Grove, W. R. Proc. Roy. Soc. Volume 5. (1845) 557-559.

5. Mond, L. L. and C. Langer. Proc. Roy. Soc. Ser. A. Volume 46. (1890) 296-304.

6. Ostwald, W. "Die Wissenschaftliche Elektrochemie der Gegenwart und the Technische Zunkunft." Z. Elektrochem. Volume 1. (1894) 122-125.

7. Baur, E. and J. Tobler. "Sammelreferat. Brennstoffketten." Z. Elektrochem. Volume 39. (1933) 169-180.

8. Justi, E. High Drain Hydrogen Diffusion Electrode Operating at Ambient Temperature and Low Pressure. Akademic der Wissenschaften and der Literature, Mainz, Abhandlungen der Mathematical-Natur-Wissenschaftlichen Klasse, No. 8. (1959); Translated by T. E. Burton, Research Information Services, Div. Personnel Int. Corp., 40 East 23 Street, New York 10, New York.

9. Grubb, W. T. and L. W. Niedrach. "Batteries With Solid Ion Exchange Membrane Electrolytes, II. Low Temperature Hydrogen-Oxygen Fuel Cells." Journal of the Electrochemical Society. Volume 107. (1960) 131-136.

10. Niedrach, L. W. "An Ion-Exchange Membrane Fuel Cell." Thirteenth Annual Battery Research and Development Conference, U. S. Army Signal Engineering Laboratories, Asbury Park, New Jersey, April, 1959.

11. "Gaseous Fuel Cell Provides Electric Power." Electrical Engineering. Volume 78. Allis Chalmers Research Division. (February, 1959) 195-196.

12. Kordesch, K. "The Hydrogen-Oxygen (Air) Fuel Cell With Carbon Electrodes." Fuel Cells. Ed. G. J. Young. New York: Reinhold, 1963.

13. Bacon, F. T. "The High-Pressure Hydrogen-Oxygen Fuel Cell." Fuel Cells. Ed. G. J. Young. New York: Reinhold, 1963.

14. Peattie, C. G. "A Summary of Practical Fuel-Cell Technology to 1963." Proc. I.E.E.E. Volume 51. (May, 1963) 795-806.

15. Liebhafsky, H. A. and L. W. Niedrach. "Fuel Cells." Journal of the Franklin Institute, 269, No. 4. (April, 1960) 257-267.

16. Young, G. J. Fuel Cells. New York: Reinhold, 1963.

17. Adams, D. R., et al. Fuel Cells. Cambridge, Massachusetts: Fuel Cell Research Associates, 1960.

18. MacInnes, D. A. The Principles of Electrochemistry. New York: Reinhold, 1939.

19. McMichael, P. Chem. and Met. Eng., 37 (1930) 484.

20. Koehler, W. A. Principles and Applications of Electrochemistry. Second Edition. New York: John Wiley and Sons, Inc., 1944.

21. Noegerrath, F. K. Zeits. Ver. deut. Ing. Volume 72. (1928) 373.

22. Sen, H. K. "Electrolytic Production of Pure Hydrogen and Oxygen Under Pressure." Transactions Institute of Chemical Engineering. Volume 13. (1935) 172-174.

23. Zdansky, A. Z. "Electrolytic Production of Hydrogen." Iron and Coal Trades Review. Volume 177, No. 4706. (August 1, 1958) 279-280.

24. James G. R. "Which Process Best for Producing Hydrogen?" Chem. Eng. Volume 67. (December, 1960) 161-166.

25. Morril, C. C. "Apollo Fuel Cell System." Proc. Nineteenth Annual Power Sources Conf. (1965) 38-41.

26. Hughes, W. L., C. M. Summers, and H. J. Allison. "An Energy System for the Future." I.R.E. Proceedings on Industrial Electronics. Volume IE-10. (May, 1963) 108-111.

27. Giacoletto, L. J. "Energy Storage and Conversion." I.E.E.E. Spectrum. Volume 2. (February, 1965) 95-103.

28. Podolny, W. H. "Regenerative Hydrogen-Oxygen Fuel-Cell System." Proc. Seventeenth Annual Power Sources Conf. (1963) 64-67.

29. Bruckner, A. and W. J. Fabrycky. "Economic Optimization of Energy Conversion." Proc. Third Annual Conference on Energy Conversion and Storage. School of Electrical Engineering, Oklahoma State University, October, 1965.

30. Hughes, W. L., C. M. Summers, and H. J. Allison. "Feasibility of Energy Storage by Water Electrolysis and High-Pressure Hydrogen Storage." Engineering Research Report, School of Electrical Engineering, Oklahoma State University, 1962.

31. Allison, H. J. "Fuel Cell Research at Oklahoma State University." Proceedings of the Second Annual Conference on Energy Conversion and Storage. School of Electrical Engineering, Oklahoma State University, October, 1964.

32. Liebhafsky, H. A. "The Fuel Cell and the Carnot Cycle." Journal of the Electrochemical Society. Volume 106. (1959) 1068.

33. Rossini, F. D. and D. D. Wagman. Selected Values of Chemical Thermodynamic Properties. Circular of the National Bureau of Standards, No. 500, Washington, D. C., 1952.

34. Plust, H. G. "Electrical Energy From Electrochemical Fuel Cells." The Brown Boveri Review. Volume 49. (January, 1962) 5.

35. Chang, S. S. L. Energy Conversion. Englewood Cliffs, New Jersey: Prentice-Hall, Inc., 1963.

36. Uligh, H. Physikalische Chemie. (1948) 323.

37. Angrist, S. W. Direct Energy Conversion. Boston: Allyn and Bacon, Inc., 1965.

38. Distefano, G. P., M. Ariet, L. L. Arice, and R. D. Walker, Jr. "Mass Transfer in Porous Gas Diffusion Electrodes." Contract DA-49-186-502-ORD-860, Harry Diamond Laboratory, Report 9, March, 1963.

39. Eisenberg, M. "Some Principles of Electrochemical Fuel-Cell Design." Electrochimica Acta. Volume 6. (1962) 93-112.

40. Mitchell, W. Fuel Cells. New York: Academic Press, 1963.

41. Rossini, F. D. Chemical Thermodynamics. New York: John Wiley and Sons, 1950.

42. Liebhafsky, H. A. and E. J. Cairns. "The Irreversible Fuel Cell." General Electric Report No. 64-RL-3679C, Schenectady, New York, June, 1964.

43. Cairns, E. J. and H. A. Liebhafsky. "The Thermodynamics of the Complete Fuel Cell." General Electric Report No. 63-RL-3399C, Schenectady, New York, September, 1963.

44. Alexander, L. R., A. M. Moos, R. L. Rapp, and R. C. Sommer. "Continuous Feed Fuel Cell Systems." Wright Air Development Center, Technical Report No. 57-605, ASTIA Document No. AD-142016, September, 1957.

45. Gorin, E. and H. L. Recht. "Fuel Cells." Mech. Eng. Volume 81. (March, 1959) 63-65.

46. Austin, L. G. "Mode of Operation of Porous Diffusion Electrodes." Contract DA-49-186-502-ORD-917, Diamond Ordnance Fuse Laboratory, Department 3, November, 1962.

47. Cairns, E. J., D. L. Douglas, and L. W. Niedrach. "Performance of Fractional Watt Ion Exchange Membrane Fuel Cells." A.I.Ch.E. Journal. Volume 4, No. 4. (December, 1961) 551-558.

48. "Stuart Electrolytic Hydrogen and Oxygen Plants and the Stuart Cell." The Electrolyser Corporation, Ltd., Bulletin.

49. Guth, E., C. G. Telschow, and H. G. Plust. "Electrical Energy From Electrochemical Fuel Cells. Part II. The H_2/O_2 Fuel Cell." Brown Boveri Review. Volume 49. (January, 1962) 20-34.

50. Lewis, G. N., M. Randall, K. S. Pitzer, and L. Brewer. Thermodynamics. Second Edition. New York: McGraw-Hill Book Company, 1961.

51. Churchill, R. W. Complex Variables and Applications. Second Edition. New York: McGraw-Hill Book Company, 1960.

52. Robinson, R. A. and R. H. Stokes. Electrolyte Solutions. Second Edition. London: Butterworth, 1959.

53. MacInnes, D. A. The Principles of Electrochemistry. New York: Reinhold, 1939.

APPENDIX A

FREE-ENERGY CONCEPTS RELEVANT TO THE HYDROGEN-OXYGEN FUEL-CELL REACTION

Basic to the analysis of the hydrogen-oxygen fuel cell is the concept of free energy, which is the factor that determines the amount of energy which can be derived from the reaction. The purpose of this appendix is to derive some of the fundamental relationships associated with this concept as they apply to the hydrogen-oxygen reaction.

The fundamental chemical reaction which occurs in hydrogen-oxygen fuel cells which utilize an alkaline electrolyte, written on a half-cell basis, is

$$H_2 + 2OH^- \rightarrow H_2O + e \quad \text{(Anode or Hydrogen Reaction)}$$

$$1/2\ O_2 + e + H_2O \rightarrow 2OH^- \quad \text{(Cathode or Oxygen Reaction)}$$

The overall cell reaction is

$$H_{2\,(g)} + 1/2\ O_{2\,(g)} \rightarrow H_2O_{(\ell)}\ , \tag{A.1}$$

where the hydrogen and oxygen are in a gaseous state; and the water by-product can be either a liquid or a gas, depending on environmental conditions.

In terms of the internal energy associated with the gas molecules involved in the reaction, the reaction is (49)

$$- \sum_i z_i U_i = Q - z \mathcal{F} E_{th} - W \ , \qquad (A.2)$$

where U_i is the internal energy associated with the i-th reactant. The term $z \mathcal{F} E_{th}$ is an electrical work (E_{th} = voltage, $\mathcal{F}$ is the Faraday, and z is the number of equivalents involved in the reaction). The term Q represents the heat added to the system, and W is a term representing the work done by the system. (The internal energy of the products of the reaction is neglected.)

For a constant pressure closed system, the expansion work of the system can be written as

$$W = \sum_i p \, \Delta V_i \ , \qquad (A.3)$$

where V is a change in volume of the system. Assuming that the volume of the water product of the reaction is negligible compared to the volume of the reactants associated with the reaction $\Delta V_i = -z_i V_i$, Equation A.3 then becomes

$$W = - \sum_i z_i \, p \, V_i \ , \qquad (A.4)$$

where V_i represents the change in volume of the i-th components. Subject to the above considerations, Equation A.2 may be written as

$$- \sum_i z_i \, (U_i + p \, V_i) = - z \mathcal{F} E_{th} + Q \qquad (A.5)$$

where the term $U_i + p \, V_i = H_i$, the enthalpy of the components of the system. It is to be noted that the right-hand side of Equation A.5 contains a heat term as well as an electrical term.

Let S_i denote the entropy of a substance i at some given operating pressure and temperature. Assuming all of i reactants are converted

from a gaseous to a liquid form, the entropy associated with i must decrease to a value corresponding to the entropy of the products of the reaction. An inspection of Table 2.3.1 shows that the entropy associated with the liquid water form is small compared to the entropy of the reactants. Correspondingly, the effective entropy change due to the conversion of the gaseous reactants into a liquid product is obtained by assuming that the entropy of the reactants disappears. This change in entropy causes an increase in the entropy of the system of

$$(\Delta S_1) = - \sum_i z_i S_i \ . \qquad (A.6)$$

Under these conditions, the second law of thermodynamics dictates that the increase in entropy of the system environment is

$$(\Delta S_2) = Q/T \ . \qquad (A.7)$$

The total entropy increase due to the chemical reaction is (for a reversible system)

$$(\Delta S_1) + (\Delta S_2) = - \sum_i z_i S_i + Q/T = 0 \ . \qquad (A.8)$$

Equation A.8 can also be written as

$$- T \sum_i z_i S_i + Q = 0 \ .$$

Solving Equation A.5 for Q and inserting this value into Equation A.8, one may conclude that (50)

$$- z \mathcal{F} E_{th} = \sum_i z_i (U_i + p V_i - TS_i) \ . \qquad (A.9)$$

Let the expression

$$U_i + p V_i - TS_i = G_i \ . \qquad (A.10)$$

It is apparent that the term $\sum_i z_i G_i$ represents a decrease of energy because of the reaction, and it is a free energy which may be converted into any other form. The term G is generally used to represent the Gibbs Free Energy of the reaction.

APPENDIX B

ELECTROSTATIC POTENTIAL DISTRIBUTIONS ABOUT FINNED ELECTRODE PAIRS

B.1 Introduction. Research at Oklahoma State University has indicated that there are many practical advantages in using finned-electrode structures for fuel cells and electrolysis cells. This thesis will examine the electrostatic potential distribution about such electrodes and compare this distribution pattern with that associated with a conventional set of parallel-plate electrodes. The analysis is divided into two parts. First, it is assumed that the medium between the electrodes is a charge-free space which satisfies Laplace's Equation. Lines of constant electrostatic potential will then be plotted for parallel-plate electrodes and for finned electrodes. Second, the case of a low mobility, concentrated plasma or electrolyte between the electrodes will be examined. In both cases it will be shown that the finned electrode structure does not drastically perturb the electrostatic potential characteristics of fuel cells or electrolysis cells. This analysis is included in this thesis because it documents the theoretical concept which led to the electrode configurations discussed in Chapter III.

B.2 Conformal Transformations of Cell Electrodes. The theory of conformal transformations is valid only for regions which satisfy

Laplace's Equation.

A conventional set of parallel-plate electrodes is shown in Figure B.2.1. For convenience, it will be assumed that the electrodes are semi-infinite in length and are separated by a distance of π units.

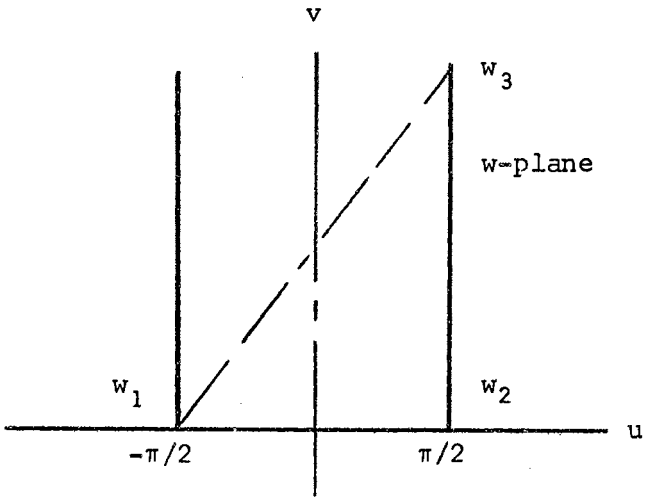

Figure B.2.1. Conventional Parallel-Plate Electrodes

The Schwarz-Christoffel transformation (51) can be used to transform the above set of electrodes into a single set of "finned" electrodes. The problem in such a case is simply to map the semi-infinite strip

$$-\pi/2 \leq u \leq \pi/2 \ , \quad v \geq 0$$

in the w-plane onto the half plane $y \geq 0$ in the z-plane. Consider that the strip in the w-plane is the limiting form of a triangle with vertices w_1, w_2, and w_3 (Figure B.2.1) as the imaginary part of w_3 approaches infinity. The limiting values of the exterior angles of w_1, w_2, and w_3 are $\pi k_1 = \pi k_2 = \pi/2$ for w_1 and w_2, respectively, and

$\pi k_3 = \pi$ for w_3.

Choose the points $x_1 = -1$, $x_2 = 1$, and $x_3 = \infty$ as the images of the vertices in the z-plane, as shown in Figure B.2.2. Then the derivative of the mapping function can be written as

$$\frac{dw}{dz} = A\,(z + 1)^{-1/2}\,(z - 1)^{-1/2}$$

$$= A\,(z^2 - 1)^{-1/2} \qquad \text{(B.2.1)}$$

$$= A'\,(1 - z^2)^{-1/2}$$

thus

$$w = A' \sin^{-1} z + B$$

Let

$$A' = 1/a \quad \text{and} \quad B = b/a \ ,$$

then

$$w = (1/a) \sin^{-1} z + (b/a)$$

or

$$aw = \sin^{-1} z + b$$

or

$$aw - b = \sin^{-1} z \ . \qquad \text{(B.2.2)}$$

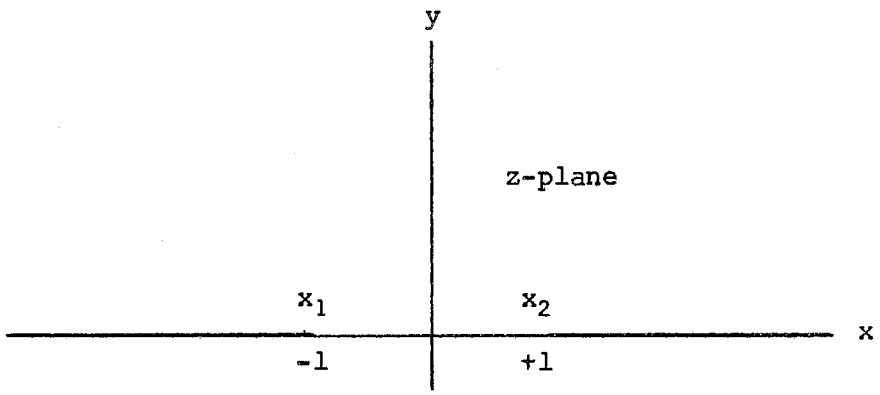

Figure B.2.2. Single-Fin Electrode Configuration

It follows from the above that $z = \sin (aw - b)$, a convenient form with which to satisfy the boundary conditions. Now, if

$$w = - (\pi/2) \ , \ z = - 1$$

and

$$w = \pi/2 \ , \ z = 1$$

so the equations

$$- 1 = \sin \left(- (\pi/2) \ a - b\right)$$

and

$$1 = \sin \left((\pi/2) \ a - b\right)$$

can be used to solve for the constants a and b. Thus, $a = 1$ and $b = 0$. The transformation equation is, therefore,

$$z = \sin w \ . \qquad \text{(B.2.3)}$$

If fringing effects are neglected at the bottom of the semi-infinite strip, the equipotential lines and the flux lines will be straight lines parallel to the electrodes and perpendicular to the electrodes, respectively. It is desirable that these lines be transformed into the z-plane so that an idea of the field configuration about a set of finned electrodes can be realized.

The following identity will be useful:

$$\sin w = \sin u \cosh v + i \cos u \sinh v \ .$$

With the above identity, the transformation $z = \sin w$ can be written as

$$u = \sin x \cosh y \ , \ v = \cos x \sinh y \ .$$

Equipotential lines in the w-plane are characterized by

$$u = c \ , \quad -\pi/2 \leq u \leq \pi/2 \ .$$

In the z-plane they become characterized by the parametric equations

$$x = \sin c \cosh v \ , \ y = \sinh v \cos c \ .$$

These parametric curves represent the right-hand half of the hyperbola

$$\frac{x^2}{\sin^2 c} - \frac{x^2}{\cos^2 c} = 1 \ , \qquad (B.2.4)$$

if c is greater than zero and the left-hand half if c is less than zero.

Lines of constant flux in the w-plane are characterized by

$$v = c \ , \ -\pi/2 \leq u \leq \pi/2 \ ,$$

and in the z-plane they become characterized by the parametric equations

$$x = \cosh c \sin u \ , \ y = \sinh c \cos u \ .$$

If c is greater than zero, then y is greater than or equal to zero; and these equations represent the upper half of the ellipse

$$\frac{x^2}{\cosh^2 c} + \frac{y^2}{\sinh^2 c} = 1 \ . \qquad (B.2.5)$$

If c is less than zero, they represent the lower half of the ellipse. Lines of constant flux will not be considered further in this thesis. Constant potential lines in the z-plane, based on the conformal transformation developed in this appendix, are shown in Figure B.2.3. Each point of a constant potential line in the w-plane maps into one point of the hyperbola and, conversely, according to the given parametric equations. The points $z = \pm 1$ are the foci of the hyperbolas. Since

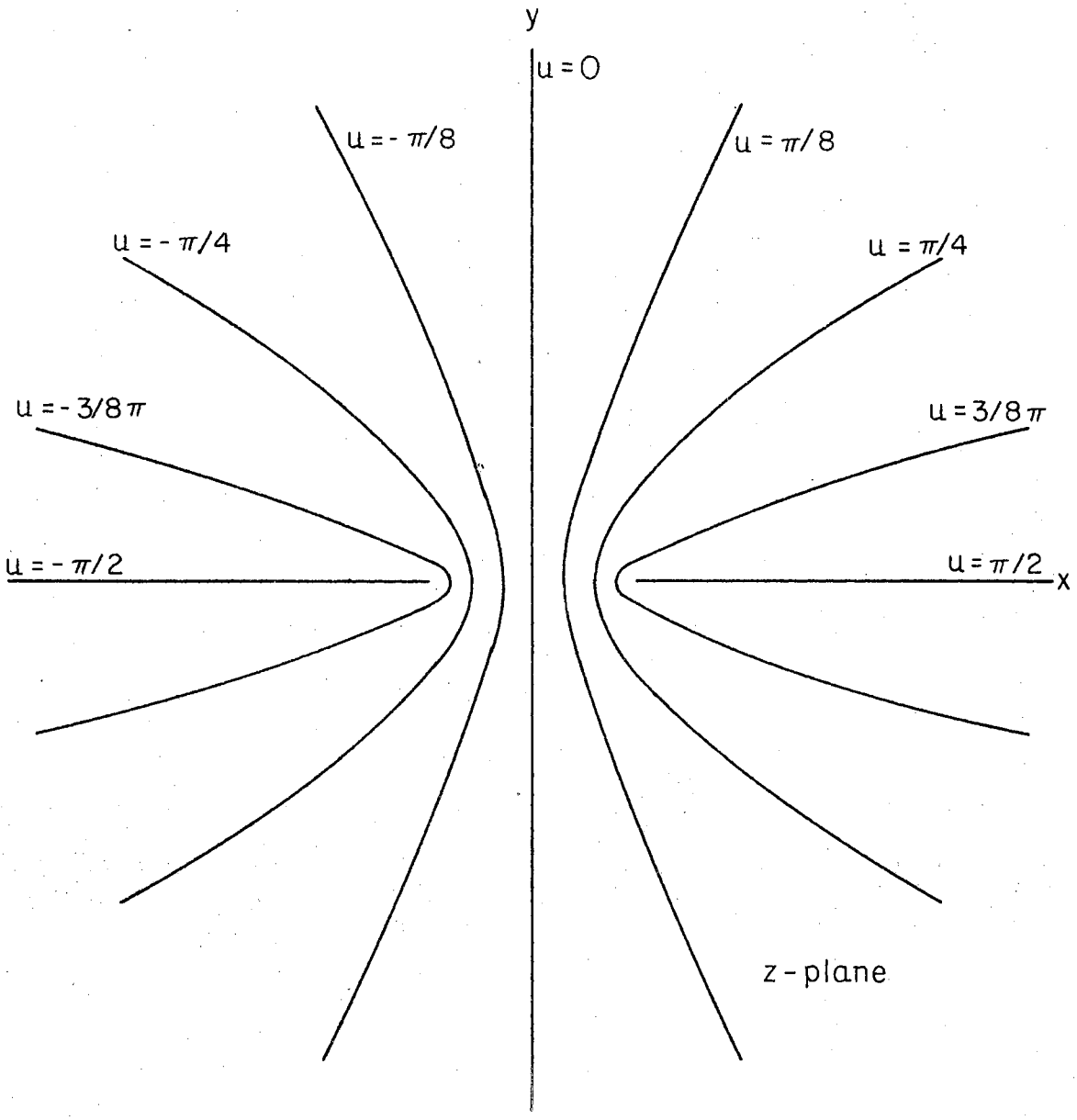

Figure B.2.3. Equipotential Lines Associated With a Single-Fin Cell Configuration

the mapping is conformal, it is a one-to-one mapping.

The preceding discussion has shown that the field configuration about a set of finned electrodes differs greatly from that of a set of parallel-plate electrodes. A single set of fins is of no real value in a practical fuel cell or electrolysis cell, however. Many sets of fins, arranged as in Figure B.2.4, would be more desirable in an actual application.

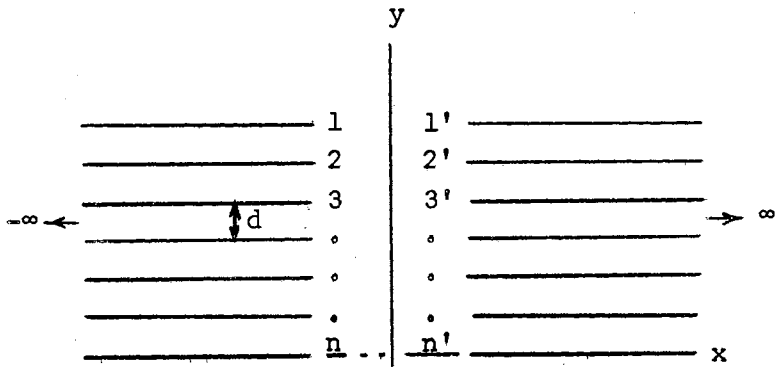

Figure B.2.4. N-Finned Electrode Set

The electrodes 1, 2, 3, ..., n are parallel, semi-infinite plates; and they all are assumed to have the same potential. Electrodes 1', 2', 3', ..., n' are parallel, semi-infinite plates and are here assumed to be at a potential of +V with respect to the electrodes 1, 2, 3, ..., n. Since the system under discussion is assumed to be linear, the principle of superposition applies; and the potential distribution pattern for the n-finned set of electrodes shown in Figure B.2.4 can, therefore, be determined from that of a single set of fins using this principle.

For convenience, let the z-plane for the n-finned configuration be

oriented as shown in Figure B.2.4. From the discussion of the preceding section, then, the potential pattern set up by each electrode is as follows:

$$\text{Single-Fin Set 1-1'} \quad \frac{x^2}{\sin^2 c} - \frac{y^2}{\cos^2 c} = 1$$

$$\text{Single-Fin Set 2-2'} \quad \frac{x^2}{\sin^2 c} - \frac{(y - d)^2}{\cos^2 c} = 1$$

$$\text{Single-Fin Set p-p'} \quad \frac{x^2}{\sin^2 c} - \frac{(y - pd)^2}{\cos^2 c} = 1 \qquad \text{(B.2.6)}$$

where p goes from 0, 1, 2, ... as n goes from 1, 2, 3, ...

Suppose now that it is desirable to determine the potential at some arbitrary point x,y not on the electrodes. The potential at this point will be given by an infinite series of terms--one term for each fin on that side of the y-axis where the point x,y is located. The contribution of the i-th fin to the potential at x,y is determined by c_i in the equation

$$\frac{x^2}{\sin^2 c_i} - \frac{(y - p_i d)^2}{\cos^2 c_i} = 1 \, . \qquad \text{(B.2.7)}$$

Thus

$$V_{xy} = \sum_{i=1} c_i \, ,$$

where $-\pi/2 < c_i < \pi/2$.

It is apparent that plotting lines of constant potential utilizing the above equation represents a tedious undertaking. However, a graphical approach can be used which will indicate the general shape of these equipotential lines. Figure B.2.5 shows the superimposed lines of

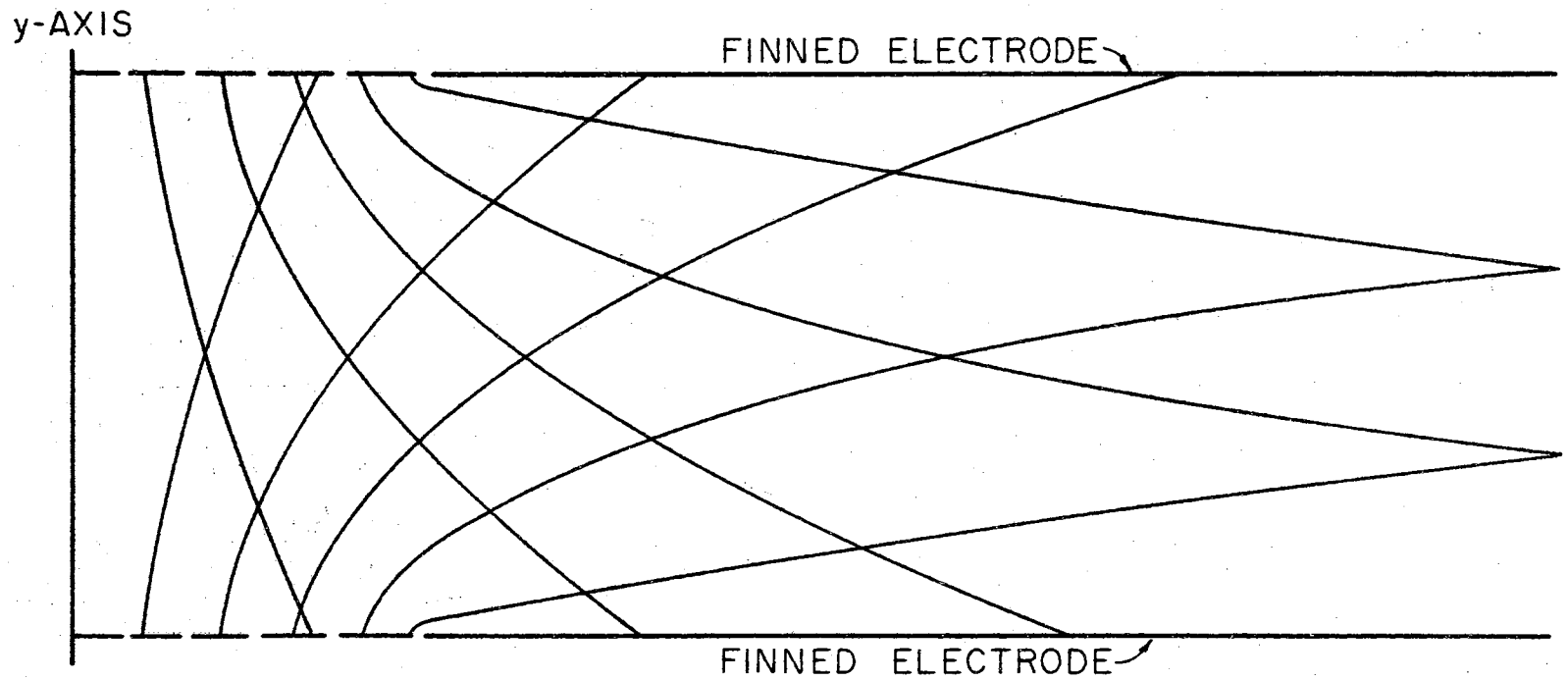

Figure B.2.5. Superimposed Equipotential Lines for a Two-Fin Set (Electrodes Widely Spaced)

constant potential associated with a two-finned set of electrodes. The lef-hand electrode will have a symmetrical potential distribution and is not shown in the figure. For the case shown, the potential between the fins is known only at the intersection points of the curves. Figure B.2.6 and Figure B.2.7 indicate how the intersection points vary with changes in the spacing between the fins. The fact that a pattern of the constant potential lines which exist in the "two-fins" case has been established is shown in Figure B.2.8, which shows the locus of the lines of constant potential established by the intersection of the superimposed potential lines shown in Figure B.2.5.

For the case of n-fins, the potential distribution shown will be essentially as is shown in Figure B.2.8. For small values of x in a neighborhood about x = 1 (i.e., close to the tips of the fins), it is evident that the potential distribution will be dominated by the adjacent fins; and the contribution of the other fins will be slight. However, for values of x much greater than one, the potential will be determined by the contributions of many of the fins. It is apparent that a potential surface will be formed for $x \gg 1$ which will be equal to the electrode potential.

B.3 Potential Distribution in a Concentrated Electrolyte. The preceding analysis has indicated the potential distribution associated with finned electrodes where the environment surrounding the electrodes was a charge-free space. In an actual fuel cell or electrolysis cell, however, the environment around such electrodes is a concentrated electrolyte which consists primarily of charged particles. Laplace's equation is obviously invalid in such an environment. It is necessary

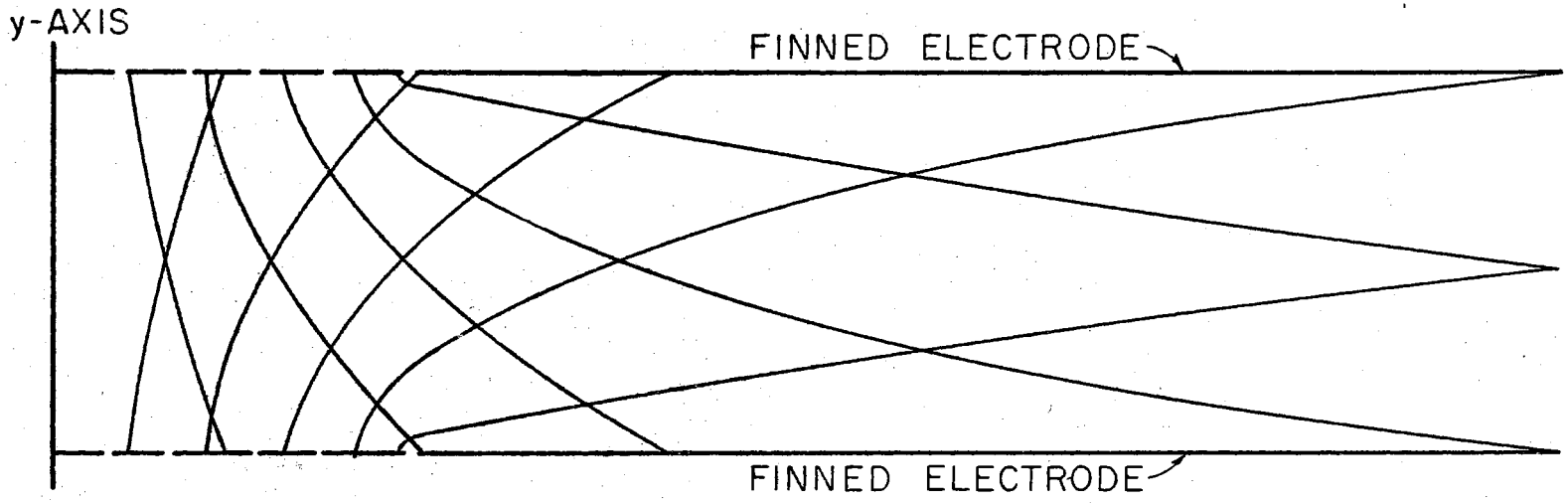

Figure B.2.6. Superimposed Equipotential Lines for a Two-Fin Set (Moderate Spacing Between Electrodes)

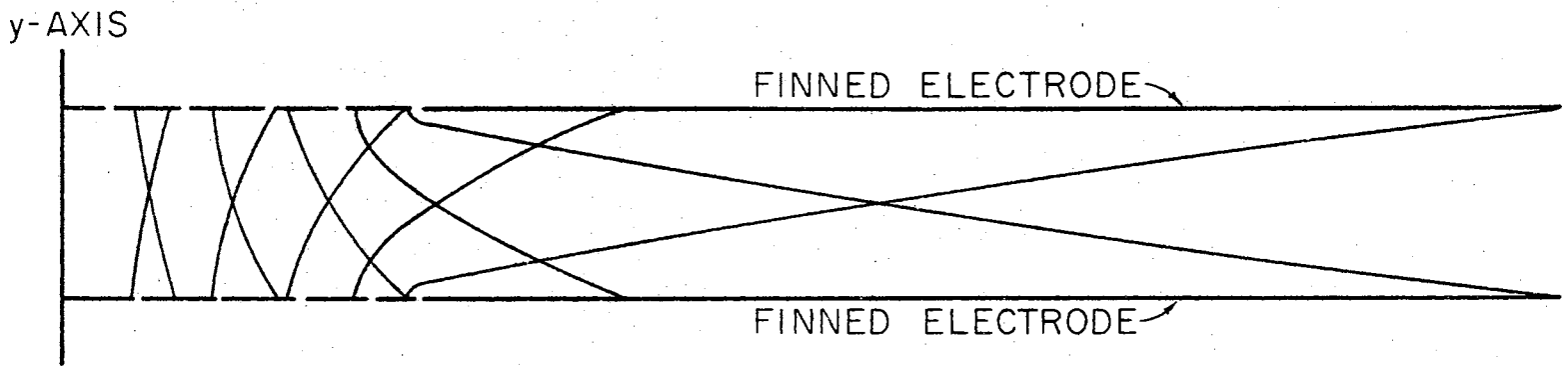

Figure B.2.7. Superimposed Equipotential Lines for a Two-Fin Set (Electrode Fins are Closely Spaced)

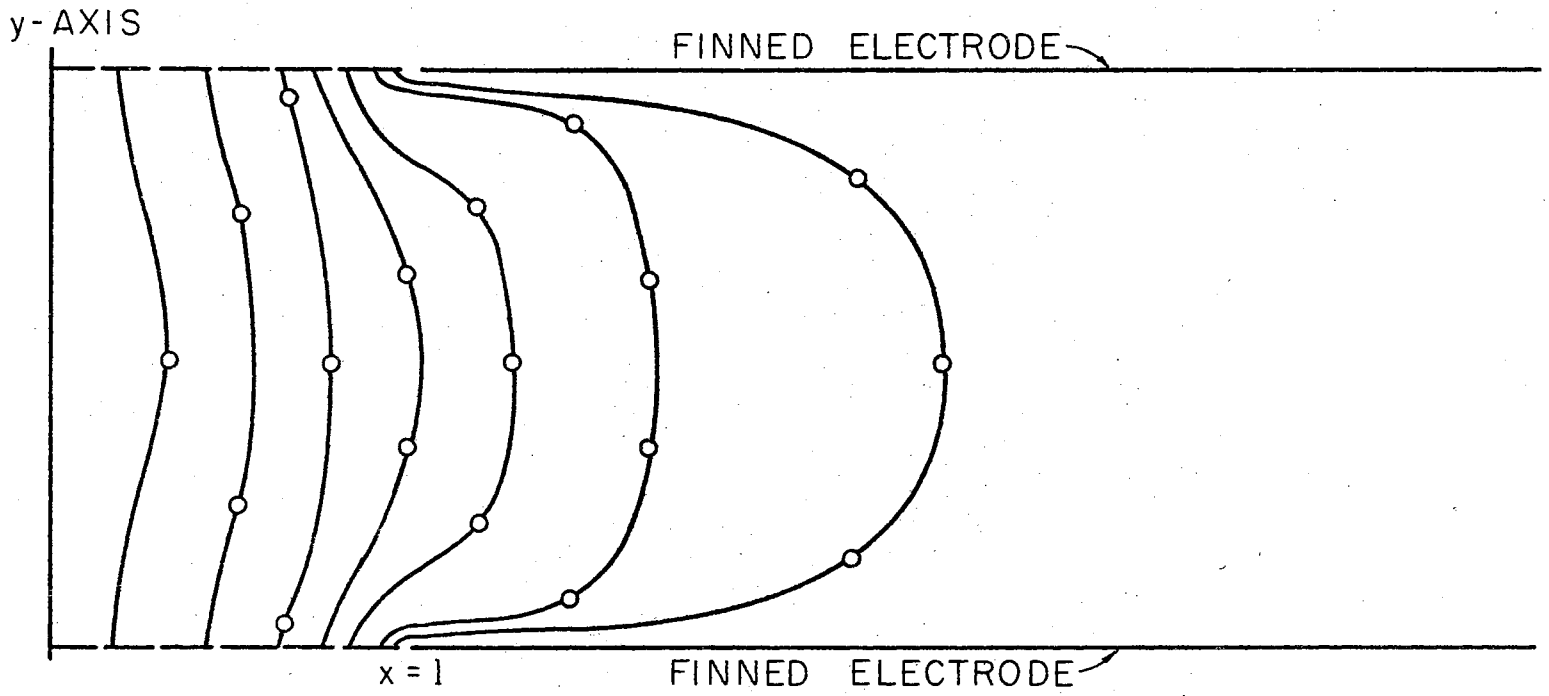

Figure B.2.8. Potential Distribution Between Fins

in the case of an actual cell to utilize Poisson's equation in conjunction with a charge distribution function to determine the potential distribution about an electrode in this case.

A concentrated electrolyte such as 25 percent KOH consists essentially of potassium ions and hydroxyl ions. In such an environment, the ions are subject to forces which vary inversely as the square of the distance between them; and the relationship between charge density in the electrolyte and the potential is given by Poisson's equation

$$\nabla^2 \psi = - \rho/\varepsilon \ . \qquad \text{(B.3.1)}$$

The equation states that at any point in the electrolyte determined by three-space coordinates $(x, y, z; r, \theta, \phi)$, the divergence of the gradient of the potential or the total outward flux of the force at this point is proportional to the charge density at this point. In an electrolytic medium, the charge density at a distance r from the j ions is

$$\sum_{i=1}^{s} n_{ji} e_i \ , \qquad \text{(B.3.2)}$$

where the summation is over all the ions (+ and -) in the solution. Therefore, in general (52),

$$\nabla^2 \psi_j (r_1, r_2) = - \frac{1}{\varepsilon} \sum_{i=1}^{s} n_{ji} e_i \ , \qquad \text{(B.3.3)}$$

where r_1 and r_2 are general vector distances. For a stationary system, the motion of ions is determined essentially by thermal consideration so that the statistical distribution of the ions is established by Maxwell-Boltzmann statistics, with the result that the distribution function for the ions in the electrolyte has the form

$$n_{ji} = n_i \, e^{-U_{ji}/kT} \qquad (B.3.4)$$

where U_{ji} is the potential energy of the i ion in the vicinity of the j ion and kT is its kinetic energy. It follows from Debye (53) that the solution for ψ_j is

$$\psi_j = \frac{-z_j \, q \, \kappa}{\varepsilon} , \qquad (B.3.5)$$

where z_j is the valence of the j-th ion, q is the electronic charge, and

$$\kappa = \frac{q^2}{kT \, \varepsilon} \sum_{n=1}^{s} n_i \, Z_i , \qquad (B.3.6)$$

or, inserting various constants and inverting, obtain

$$1/\kappa = 7.924 \times 10^{-11} \sqrt{\frac{\varepsilon T}{\Gamma}} \qquad (B.3.7)$$

which is the ionic radius of the j-th ion. T in the equation is temperature in absolute units, and Γ is the ional concentration. At 25°C the value of $1/\kappa$ for potassium in a 25 percent solution of potassium hydroxide is 1.33 angstroms; and for hydroxyl ions, the figure is 2.70 angstroms.

The above values of the ionic radii of the ions in the electrolyte are significant in that they represent the distance of closest approach of the ions in the electrolyte to the charged plates which comprise the electrodes. The hydrogen electrode in a fuel cell will be negative and will, therefore, attract a cloud of potassium ions, which will be oriented approximately 1.33 angstroms from the surface of the electrode. Correspondingly, the oxygen electrode will accumulate a cloud of

hydroxyl ions. This cloud of ions serves to insulate the electrolyte from the effects of the charge distribution associated with the electrodes. The result is that charges which are several $1/\kappa$ units away from a given electrode are completely unaffected by the existence of the electrode. Therefore, the fact that the electrodes are finned or parallel plates makes no difference to the operation of the cell, insofar as the potential distribution associated with the electrodes is concerned.

VITA

Hansell Jack Allison

Candidate for the Degree of

Doctor of Philosophy

Thesis: A NEW APPROACH TO HIGH-PRESSURE, HIGH-TEMPERATURE HYDROGEN-OXYGEN FUEL-CELL AND ELECTROLYSIS-CELL DESIGN

Major Field: Electrical Engineering

Biographical:

Personal Data: Born in Baton Rouge, Louisiana, January 16, 1938, the son of Hansell J. and Nonnie Y. Allison.

Education: Graduated from Istrouma High School in Baton Rouge, Louisiana, in 1955; received the Bachelor of Science degree in Electrical Engineering from Louisiana State University in June, 1959; received the Master of Science degree in Electrical Engineering from Louisiana State University in June, 1961; completed requirements for the Doctor of Philosophy degree in May, 1967.

Professional Experience: Industrial experience includes one and one-half years as a design engineer with General Dynamics in Fort Worth, Texas, and one year as an applications engineer with Texas Instruments, Inc., in Dallas, Texas; was a member of the staff of Louisiana State University from 1959 to 1961; employed by the School of Electrical Engineering of Oklahoma State University as an instructor from September, 1961, to September, 1966; since September, 1966, employed as Assistant Professor in the School of Electrical Engineering at Oklahoma State University.

Professional Organizations: Member of the Institute of Electrical and Electronics Engineers, Sigma Tau, Eta Kappa Nu, Sigma Xi, Triangle, Pi Mu Epsilon, Tau Beta Pi, Phi Kappa Phi, and Phi Eta Sigma.